ADDIS ABABA INSTITUTE OF TECHNOLOGY

SCHOOL OF MECHANICAL AND INDUSTRIAL ENGINEERING

A Thesis submitted in partial fulfillment of the Degree of Masters of Science in Mechanical Engineering (Manufacturing Engineering)

Investigation of Physical, Mechanical, and Thermal Properties on Hybrid Carbon Nanotubes with Flax Fibers and Eggshell Composites for Disk Brake Pad Application

By: Iliyas Ketsela

ID:GSE/2013/12

Advisor: Mesfin Gizaw (PhD)

June, 2024

Addis Ababa, Ethiopia

ADDIS ABABA UNIVERSITY

ADDIS ABABA INSTITUTE OF TECHNOLOGY

SCHOOL OF MECHANICAL AND INDUSTRIAL ENGINEERING

Investigation of Physical, Mechanical, and Thermal Properties of Hybrid Carbon Nanomaterials With Flax Fibers and Eggshell Composites for Disk Brake Pad Application

By: Iliyas Ketsela

Submitted by the requirements for the degree

Master of Science (M.Sc.)

Approved by: Board of Examiners

Dr. Mesfin Gizaw(PhD)	----------	----------
Advisor	Signature	Date
Dr. Desalegn Wogaso(PhD)	----------	----------
Internal Examiner	Signature	Date
Mr. Henock Zewdu (PhD Candidate)	----------	----------
External Examiner	Signature	Date
Dr. Araya Abera(PhD)	----------	----------
Chairman of the School	Signature	Date

Declaration

I declare that the work entitled, "Investigation of Physical, Mechanical and Thermal Properties on Hybrid Carbon Nanotubes with Flax Fibers and Eggshell Composites for Disc Brake Pad Application," is the original work that I have completed entirely by myself. It was written under the supervision of Dr. Mesfin Gizaw during my MSc studies at the Addis Ababa Institute of Technology. This work has not been proposed for a degree at this University or any other University.

---------- ----------

Iliyas Ketsela Date

(Candidate)

This is to certify the above declaration provided by the candidate is correct to the best of my knowledge.

---------- ----------

Dr. Mesfin Gizaw Date

(Thesis Advisor)

Acknowledgment

Throughout the process of writing my thesis, I have faced several difficulties, but I have persisted. For this reason, I would like to begin by thanking the Almighty Allah for all of his blessings and experiences learned during my life. My advisor, Dr. Mesfin Gizaw, is greatly appreciated for his help with my thesis. My wife, Mrs. Cleopatra Seyoum, has my deepest gratitude for her constant love, understanding, and support. I am very grateful for all the late nights you shared with me. Finally, I just wanted to thank all of my classmates, especially Ms. Paulos Girma, for always being there for me and constantly encouraging me. Throughout the entire process, you have served as my motivation.

Thank you all.

Dedicated to Cleopatra, Hibba, and Mekiya

Abstract

Friaction materials are used to make brake pads, and these materials are forced up against the braking rotor, to slow down or stop a vehicle. Now days Metallic and semi-metallic compounds have replaced asbestos-based in commercial brake pads. Consequently, problems such as; excessive wear rates, noises, and vibration persist. Therefore, this research is required to improve the current performance of the brake pads in terms of wear rate, and coefficient of friction (COF). Naturally extracted fibers and fillers (flax fibers and eggshells) are required as a component for structural strength and polyester resin as a binding material in brake pad applications to overcome such problems. As a result, Hybrid nanomaterial constituents like (MWCNTs) and additional friction modifier (Al_2O_3) composites can replace asbestos-based ones which can cause lung cancer. Also, to guarantee long-term performance and to reduce environmental pollution, a higher level of care must be taken in the selection of good friction materials, to convert these materials a literature review is conducted on natural fibers and friction modifiers to obstacle this problem Also, the effects of particle size and volume fraction distributions are discussed the methodology section has the design of experiments, material preparation, and testing procedures for formulated materials. Nine samples were created for the comparison of (flax fiber, eggshell, MWCNTs, and Al_2O_3) reinforced with polyester resin composite in detail with variable fractions using the compression molding technique. The physical, mechanical, and thermal properties of the samples are evaluated and analyzed using the FEM analysis technique. Finally, The well-dispersed Flax fiber, eggshell, alumina particles, and polyester resin of sample SE with a 6wt.%, 21wt.%, 3wt.%, 8wt.%, and 62wt.% respectively created a larger contact surface. Consequently, the composite's surface hardness rose, reducing the specific wear rate of the brake linings and raising the coefficient of friction, also with improved absorption capabilities.

Keywords: Flax Fiber, MWCNTs, Alumina (Al_2O_3), Polyester Resin, Brake Pads

List of Abbreviation

EG: Egg Shells

FF: Flax Fiber

CS: Coconut Shell

CSP: Coconut Shell Powder

COF: Coefficient of friction

CNTs: Carbon nanotubes

CNCs: Carbon Nanocomposites

MMCs: Metal Matrix Composites

FRC: Fiber-reinforced composites

HNC: Hybrid Nanocomposites

ROM: Rule of Mixture

TA: Taguchi Analysis

DOE: Design of Experiments

NAO: Non asbestos organic

MWCNTs: Multi-walled carbon nanotubes

PKF: Palm Kernel Fiber

PKS: Palm Kernel Shell

SEM: Scanning electron microscopy

ASTM: America Society for Testing and Material

WHO: World Health Organization

SWR: Specific Wear Rate

IARC: International Agency for Research On Cancer

IJERT: International Journal of Engineering Research & Technology

IJMET: International Journal of Mechanical Engineering and Technology

Table of Content

List of Tables

List of Figures

Chapter One

1. Introduction

1.2 Background of the Study

All disk brake assemblies have brake pads (Friction lining materials) which cause the vehicle's kinetic energy to be converted into thermal energy, the heat energy produced is transferred to the components in contact through conduction, which causes the material to deteriorate and overheat seals and brake fluid. Then a high thermal loading may result in judder (changes in disc thickness), surface cracking, and severe wear. A vehicle possesses an amount of kinetic energy depending on the weight and speed of the car. Therefore, a braking system is a crucial part of reducing the velocity of a vehicle. Thus, this energy must be dissipated to slow down or stop the car [1]. The brake linings used in automotive braking systems are disc and drum brake linings. While disc brakes function similarly but are not protected, drum brakes are contained inside drums, the brake lining is drawn outward and forced against the drum [2]. Asbestos, non-asbestos organic (NAO), semi-metallic, low-steel, and low-carbon materials are typically used to make brake pads [3]. An exploded view of a sliding disc brake is shown in Figure 1.1 below.

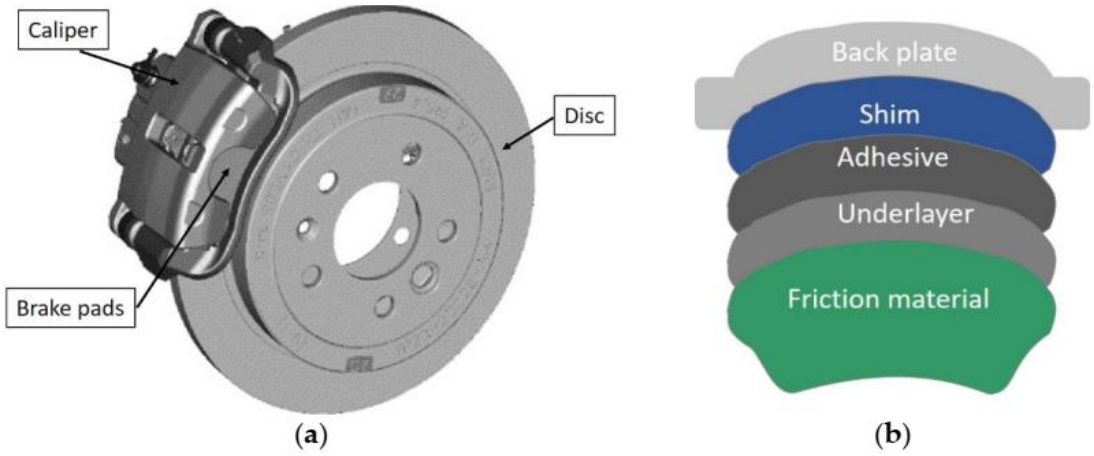

Figure 1.1 (A) Sliding disc brake (B) Brake pad structure *[4]*

The Four main components that makeup brake pads are binders, fillers, frictional modifiers, and reinforcements. The reinforcements provide strength to the composite matrix. The frictional modifiers comprise a combination of abrasives and lubricants; abrasives enhance the frictional characteristics, and stabilize the coefficient of friction and wear rate; solid lubricants provide thermal stability. The

fillers make up the brake lining's free volume and reduce the cost. The binder links the components to maintain the brake lining's structural integrity under varied mechanical and thermal stresses [5]. Ceramic, Fully-Metallic, Semi-Metallic, and Non-Asbestos Organics (NAO) are the four main divisions of brake pad materials. Fully and semi-metallic friction materials outperform non-asbestos organics in terms of wear and thermal stability, but they also generate more noise and quickly degrade the disk material. In contrast, ceramic materials have a much greater temperature tolerance, generate little noise, and are suited for fast cars. Depending on their components, they are categorized as shown in Figure 1.2 below [4].

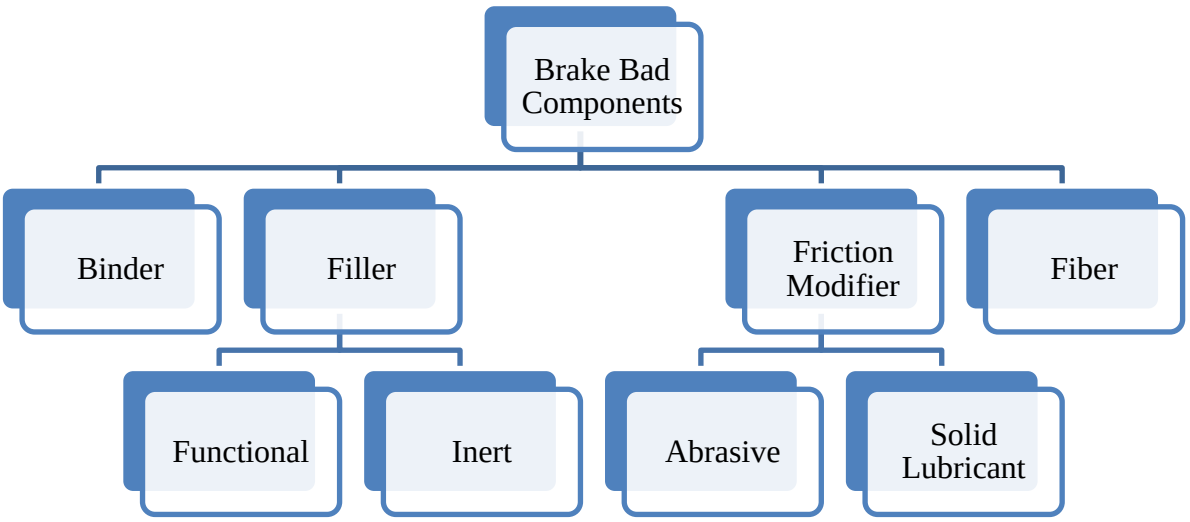

Figure 1.2 Grouping of the components of friction material *[4]*

Additionally, friction materials must satisfy several critical parameters such as uniform friction, high wear resistance, low noise, and damping capabilities over a wide temperature, pressure, and velocity range [6]. In terms of collisions, a car's brake pad performance has an impact on passenger safety. Thus, greater care and precision must be employed in the selection of brake pad materials. This is greatly impacted by the selection of particle size, type of fiber, filler, binder, and optimum volume of fractions. It also affects their mechanical and thermal characteristics [3]. Fibers are composed of many filaments with widths ranging from 5-15 mm [7]. Natural fibers perform better than synthetic fibers in terms of specific strength and modulus. With advancements in technology, they will be able to compete with some of the synthetic fibers in brake pad applications [8].

In this regard, prospective Flax Fiber as reinforcements, and eggshell as filler are examined. The final goal was to determine whether flax fiber and eggshell-based particles might be used as fiber and fillers in structural material, MWCNTs as a solid lubricant, and polyester resin as a binding agent by analyzing their morphology, hardness values, water and oil absorption capacities, and frictional properties of the brake pad composites. SEM was used to analyze the surface micro-structure, pin-on-disc measurement was used to determine wear rate, and Rockwell hardness (HRH-scale) was used to measure hardness values. FEA techniques were developed to assess its characteristics in terms of static structural, transient structural, and transient thermal impacts on the developed friction lining brake pad materials by simulating using ANSYS software. Finally, the hybridization process with compression molding manufacturing technique and post-curing in an oven may play a significant role in examining the physical, mechanical, and thermal qualities of the brake pad composites.

1.3 Problem Statement

The most widely used kind of brake in automotive applications is the brake pad [3]. According to specific publications, a comparable material for brake pads should have a higher friction coefficient, be more ecologically friendly, and have good wear resistance [9]. The ban on asbestos as friction materials for brake pads is addressed in several articles.To replace asbestos, NAO, metallic and semi-metallic ceramic compounds are used [1]. The use and management of asbestos remain issues worldwide, particularly in lower-income nations where regulations prohibiting their use have not been implemented [10]. Commercially available brake pad materials have produced several issues, including excessive noise while working, poor heat dissipation capacity, and durability [11]. Continuous wear and thermal cracks due to High temperatures and material selections lead to problems with disc brakes Therefore, the development of a reliable, durable brake pad will benefit not only the environment but also the entire nation. The ultimate objective of the research was to create a brake pad that is safe for human use, easily accessible, and free of asbestos while simultaneously enhancing, abrasion, and wear resistance. Finally, using flax fiber (FF), eggshells ($CaCO_3$) as a reinforcement and filler, multi-walled carbon nanotubes (MWCNTs), alumina (Al_2O_3), as friction modifiers, and polyester resin, as a binding agent enhanced the current issues of the brake pad. a description of Physical, and mechanical characteristics, as well as their thermal impact on the evaluation results, were analyzed by FEA technique using ANSYS 2024 software version.

1.4 Objectives

1.4.1 General Objective

These studies investigate the Physical, mechanical, and thermal properties of hybrid carbon nanotubes with the effects of flax fiber, eggshell, alumina, and polyester resin, significantly influencing the friction material's properties.

1.4.2 Specific Objectives

- ✓ To determine the optimal volume fraction of the Flax Fiber, eggshell, MWCNTs, and Al_2O_3-reinforced polyester resin composite
- ✓ To assess the physical and mechanical characteristics, such as:water and oil absorption, hardness, impact strength, wear rate, and coefficient of friction.
- ✓ To analyze their thermal results on the optimized friction lining material using FEA by developing a simulation on ANSYS software.

1.5 Research Questions

- ✓ What was the optimum volume fraction of Flax Fiber/eggshell with MWCNTs and Al2O3-reinforced polyester resin composite brake pads?
- ✓ What were the wear rate and coefficient of friction of Flax Fiber/eggshell with MWCNTs, Al_2O_3 reinforcement, and polyester resin as a matrix composite for brake pad application?
- ✓ What thermal results were obtained for the FEA simulation parameters to be analyzed?

1.6 Scope of the Study

To identify natural fibers with carbon nanotube composite as a possible friction material for brake pad applications. It examined (MWCNTs) as solid lubricants and alumina (Al_2O_3) as an abrasive or friction modifier. Also, Eggshell ($CaCO_3$) as a filler and Flax Fiber as structural materials by incorporating polyester resin as a binding agent. In this regard, a description of physical mechanical, and thermal characteristics, as well as their impact on the evaluation results, were analyzed using the FEA technique using ANSYS software.

1.7 Motivation Statement

The manufacturing sector produce products locally to import substitutes.The need for advanced materials and manufacturing techniques is one among several to produce friction materials locally. Therefore, Hybrid natural fibers (flax fiber and eggshells) with Nanomaterial addition with polyester resin are the best with lower costs and environmentally freindly uses.

1.8 Structure of the Thesis

Chapter One: This section explores the development of new brake pad materials that address the limitations of current commercially available options. It examines the use of hybrid natural fibers, nanocomposites, and eco-friendly fillers to create a durable, high-performing, and environmentally-friendly brake pad solution. The research aims to identify the optimal composition and manufacturing techniques to enhance the physical, mechanical, and frictional properties of the brake pads.

Chapter Two: This section provides a detailed literature review of the key components and manufacturing processes of composite brake pads. It covers the role of binders, fillers, friction modifiers, and fibers in achieving the desired mechanical, thermal, and tribological properties. It also discusses the environmental impact of brake pad materials and the potential of natural fibers as sustainable alternatives. Overall, this comprehensive analysis aims to guide the development of high-performance and eco-friendly brake pad formulations.

Chapter Three: This section outlines the research methods and materials used to investigate the characteristics and impacts of natural-based hybrid nanomaterials on brake pad performance. It covers the design of experiments, material preparation, testing procedures, and modeling approaches employed in this study.

Chapter Four: This section presents the experimental results and discussion of a study on hybrid nanocomposite brake pads, including hardness, impact strength, coefficient of friction, wear rate, and surface morphology. The results are compared to existing formulations using different natural fibers and fillers. Finite element analysis was also conducted to understand the structural and thermal behavior of the brake pad system. Displays various findings from the experimental tests using graphs and tabulated data and a detailed discussion of the findings. Additionally, the obtained result is used to generate an ANSYS simulation brake pad model, and the results are extensively confirmed using ANSYS software.

Chapter Five: This chapter presents the conclusions of the research on the development of natural fiber-based brake pads. The influence of MWCNTs and Al2O3 on the mechanical properties of flax fiber with eggshell as a filler in the composite is investigated. The results show that the flax fiber and eggshell polyester resin composite with MWCNTs and alumina exhibits superior mechanical qualities compared to other natural brake pad composite materials. Further recommendations and future work are discussed, including the need for additional testing and analysis to fully characterize the natural fiber hybrid nanocomposite materials.

Chapter Two

2. Literature Review

2.1 Introduction

The composite brake pad is the most important component for vehicle safety measures. It is a heterogeneous material with more than 10 different elements combined to reduce porosity and durability, by increasing strength and stiffness and lowering noise. It is possible to create different formulations by changing the ingredients' weight ratios. A careful evaluation of the friction and wear qualities is necessary when choosing a novel formulation [3]. Factors that influence friction and wear, include the microstructure, metallic counter face, rotating speed, pressure, and temperature of the contact surface [12]. The binder is fortified with rubbers to enhance its dampening properties, and binders must also be extremely thermally stable. Abrasives keep the brake pads stable during braking and help control the frictional properties. Solid lubricants provide the best sliding conditions by stabilizing and maintaining a steady coefficient of friction within the required range even in the face of high loads, temperatures, and velocities at the contact surfaces. Generally, solid lubricant concentrations are less than 10% vol. [13]. Fillers make up more than 85% Wt. of commercial brake pads [14].

In braking situations, the friction generates tremendous heat, which causes the binder, (thermosetting phenolic resin) to lose its binding capacity [15]. A build-up of cumulative wear particles due to periodic heat dissipation and accumulation may stop further wear [16].

The main difficulty in manufacturing brake pads is balancing the material composition to ensure that there is a certain and adequate amount of third-body (wear-related by-product) material which is primarily made up of a few more brake pad components and iron oxide from the disk brake. It can cause unpredictable, damaging surface erosion, which can either increase or decrease the effectiveness of the brakes. To have the best braking functionality and efficiency, more extensive brake pad ingredients must be converted into the nano-crystalline third body [13].

The third body typically performs two functions: It uses a thin covering with nanostructure to shield the surface areas of contact and it forms secondary contacts to increase the surface area of contact. The primary objective of brake pad design is to maximize brake pad performance while maintaining modest surface area and mechanical integrity [17].

Polymers are designed to have strong mechanical strength, lightweight, ease of processing, thermal properties, and resistance to chemicals, wear, and abrasion for tribological reasons, and are the main

materials used to create brake pads [3]. The Archard formula is used to determine the pad's wearing strain [3].

$S = C * D * L$, ---------- *(1)*

Where "L" indicates the applied load,

"S" indicates strain wear,

"D" indicates sliding distance, and

"C" indicates the coefficient of wear.

2.2 An Overview of the Friction Materials

Friction is mainly caused by adhesion and abrasion, and it typically arises from the formation and peeling of the friction layer, which retains the contact load and modifies friction behavior [4]. Friction materials are primarily used to adjust the friction coefficient, enhance fade resistance, lower noise and porosity, also, be resistant to heat and moisture, and are ideal for decreasing vibration during braking [18]. It was found that when sliding speed and temperature increased, the specific wear rate increased, Meanwhile, the excessive roughness (asperities) in the brake pad surfaces increased the rate of repeated impact loads. As a result, it increased frictional thrust, delamination, and fiber fracture caused by local vibrations and crackling at the sliding surface contact, which will affect how well the brake pads wear. Composite materials with great wear resistance are effectively created by the combination of natural fibers and resin. Additionally, the optimal material ratio, bonding qualities, and wear can all be enhanced by decreasing the size of the filler's particles [1]

Macías et al. employed iron sulfide to look for indications of dispersed oxygen. The oxygen diffusion damages the brake pad since it might lead to instability. As a result, COF is more stable at high temperatures. The abrasion-based wear mechanism was improved by the iron-based pads, making it appropriate for braking applications [3].

2.3 Main components of brake pads

2.3.1 Binder

The function of the binder is to maintain the cohesiveness of the constituents of the friction material under mechanical and thermal loads while preserving other important characteristics. To improve damping properties and make the resin extremely thermally stable, rubbers are added to the friction lining material, the binder typically varies from 20 to 40% by Weight [19]. The temperature required for thermal decomposition increases with resin heat resistance, lowering oxidation and decomposition. As a result, the brake pads' frictional characteristics will be stable or Heat-resistant binder resins can lower the rate of wear and particle emission of the brake pad [1].

Epoxy was primarily utilized as a matrix in the research on flax composite materials; however, a small number of tests using polyester as a resin were performed [20]. By securely joining the other three components, the binders reduce the wear rate and friction of the brake pads, which in turn reduces the component shear rate [21].

Table 2.1 Physical, Mechanical, and Thermal Characteristics *[22]*

Properties	**Polyester Resin**	**Hardener**
Density (g/cm^3)	1.09	0.97
Specific gravity	1.14±0.1	1.02±0.1
Color	Clear or Blue	Clear or Brown
Viscosity at 25°c (MPa)	550	600
Mixing proportions	10	2
Poisons ratio	0.3	0.3
Melting temperature (°c)	280	280
Coefficient of thermal expansion (1/°c)	$90.4*10^{-6}$	$90.4x10^{-6}$
Thermal conductivity (λ)$Wm^{-1}K^{-1}$	0.22	0.22

2.3.2 Filler

Materials that have little effect on friction performance are called fillers. Inert and functional are two categories of fillers. The inert is only employed to fill space and to cut production expenses. The functional kind has a specific utility, like providing thermal resistance. Fillers help to reduce cost by 85% weights or higher Therefore, it is common practice to add harder particles, like Al_2O_3 to enhance or optimize performance, to raise the COF (μ) created by the scraping of the material's surface against the disc [21]. Regarding Nano clay, there was a drop in friction performance and an improvement in wear qualities [23]. The spread of the fracture and delamination may have been inhibited by the use of filler material but, it has the advantages of reducing the amount of resin required and the overall cost of the composites. Composites with 5 wt. % eggshell powder can withstand greater bending stresses, but 10wt.% deflects less. According to the flexural strength experiment, stiffness can be increased with 5% of eggshell filler and declines with increasing filler quantity. With each subsequent increase of up to 10%, flexural strength increases by 5% and remains largely stable. Hardness is decreased by using eggshell filler material. However, using different compositions to increase hardness can be done. In the future, wear testing must be conducted on samples of the same composition to prevent cracks and delamination [24].

Lee and Filip claim that reducing material wear will probably lessen any adverse effects on the environment, emphasizing the need to exhibit strong thermal stability and recovery from moisture or high temperatures. According to Suddell et al, flax fiber composites are frequently employed in place of asbestos in car disk brakes, and are now replacing other automotive components that were formerly made with glass fibers [25]. EggShell particles are composed of organic components similar to those found in ceramics. It increases hardness and will boost the wear rate and coefficient stability of the composite surface. Additionally, research by Ray et al. demonstrated that as ES particle loading increased, mechanical strength fell while density, voids, and wear resistance increased [26]. Epoxy composites bonded with sisal fibers and ES particles can have their wear index increased by calcination treatment [27]. It is new to use ES particles as filler or reinforcing material to improve the mechanical, thermal, and tribological properties of polymer-based composites. However, the role of ES particles in brake linings has not received much attention. The wear rate and coefficient of stability of the composite surface are predicted to increase with hardness. The polymer (polymethyl methacrylate) composite may last longer if 5% wt. of ES is added as a long-lasting, deterioration-resistant filler. By combining ES particles, bamboo particles, and fibers to form a hybrid material, it can control the friction coefficient and improve mechanical properties. In fiber-reinforced polyester composites, the addition of 10% by weight of iron filler can reduce flammability and improve heat stability [10]. ES particles can take the role of metal particles [28]. Egg shells are readily available as trash in large quantities in the food sector. About 95% of eggshells are composed of calcium carbonate ($CaCO_3$), or calcite, while 5% are made up of organic substances such as type X collagen, sulfated polysaccharides, and other proteins. Because eggshell waste improves the mechanical and heat stability qualities of reinforced biopolymeric composites, it may be a good option for an environmentally friendly filler material [29]. For example, Edokpia et al. used Eggshells ($CaCO_3$), which are biodegradable and environmentally friendly as a fiber in place of asbestos to create brake pad samples with gum Arabic (GA) in place of formaldehyde resin, The best bonding performance is provided by GA with a weight of 15% to 18% [30].

Challa Ramesh and colleagues researched the characteristics of eggshell powder as reinforcement and polyamide as the matrix material. Consequently, mechanical qualities increased along with the amount of eggshell powder. Similarly, Senthil J, et al. investigated the mechanical characteristics and water absorption of polymer composites strengthened with calcium carbonate or eggshell powder. The outcomes demonstrated that the hardness and tensile qualities increased along with the amount of eggshell [31]. Increasing the amount of ES nanoparticles in the mixture improves water absorption and causes the thickness of the composite to expand [10].

Table 2.2 Physical, mechanical, and thermal properties of eggshell *[32]*

Properties	**Eggshells**
Bulk density (g/cm^3)	0.8
Moisture content	1.18
Poissons ratio	0.3
Surface area (g/m^2)	21.2
Shear modulus (GPA)	9.4
Melting temperature (^oc)	825
Coefficient of thermal expansion ($1/^oc$)	$5.4x10^{-6}$
Thermal conductivity (λ)$Wm^{-1}K^{-1}$	0.45

2.3.3 Friction Modifier

Solid lubricants lower and stabilize the friction coefficient level throughout a broad temperature range, and abrasives help to reduce the friction material's wear resistance. Lubricants also can cover the rotor surface with a thin layer at high temperatures, which shields it from noise and vibration yet excessive lubrication and abrasive can lead to significant fluctuations in the friction coefficient and can also deteriorate the composite material, abrasives, and lubricants typically make up to 10% and 52.9 % of the weight respectively [33]. Ceramic materials are formed in a variety of shapes, including filaments, long fibers, and short (whisker) fibers. Because of their isotropic qualities, particulate composites are superior to other types of composites. To construct MMCs, reinforcement was added by using alumina (Al2O3), silicon carbide (SiC), boron carbide (B4C), graphite (Gr), carbon nanotubes (CNTs), carbon (C), silicon oxide (SiO2), fly ash (FA), eggshells (ESs), and other ceramic particles. ES has the characteristics of ceramic particles, such as low density, renewability, environmentally friendly, and thermal resilience at high temperatures [34]. Alumina (Al2O3) is the toughest and hardest particle than other ceramic particles and has lower particles than diamond, silicon carbide, and boron carbide. The presence of alumina always improves the composite material's hardness and tensile strength. Furthermore, the interfacial reaction layer and wettability of alumina were consistently superior. However, occasionally, after the solidification process, porosity was created inside the composite material due to low particle size and high weight percentage of alumina [35].

Table 2.3 Mechanical and thermal properties of Alumina (www.accuratus.com)

Mechanical properties	**Al_2O_3**
Density (g/cm^3)	3.69
Flexural Strength (MPa)	330
Poisson's Ratio	0.21
Hardness Kg/mm^2	1175
Maximum use temp. ^oc	1700
Coefficient of thermal expansion ($1/^oc$)	$8.1x10^{-6}$
Thermal conductivity (λ)$Wm^{-1}K^{-1}$	18

Table 2.4 Principal friction modifiers employed in friction materials *[33]*

Abrasive	Zircon, zirconium silicate, quartz, alumina, zirconia, silicon carbide, chromium oxide, silica, mullite.
Lubricant	Antimony trisulphide, graphite, molybdenum disulfide, tin sulfide, petroleum coke, lead sulfide.

2.3.4 Fibers

The primary functions of fiber in friction materials are to improve mechanical qualities, as well as to offer structural integrity and thermal stability. Additionally, it lessens thermal and shear stress, which might influence friction instability and thermal fading [36]. The use of natural fibers is growing due to their better strength and stiffness, affordability, and lightweight nature over glass fiber. They require less energy (low processing equipment needed) to produce than synthetic fibers, offer safe working conditions, and can be utilized as a biodegradable reinforcing material. Natural fibers' physical and mechanical properties are greatly influenced by their physical characteristics, which include their cross-section, moisture content, cellulose content, and fiber structure. Furthermore, the physical and mechanical properties of hybrid composites are determined by the fiber volume fraction [37].

Table 2.5 Mechanical and thermal properties of Natural Flax Fiber *[38]*

Properties	**Flax Fiber**
Density (g/cm^3)	1.5
E-Modulus (GPa)	50
Elongation to Fracture(%)	2.7-3.2
Young's Modulus (GPa)	27.6
Melting temperature(^{o}c)	220
Coefficient of thermal expansion (1/ ^{o}c)	-8x10^{-6}
Thermal conductivity (λ)Wm^{-1}K^{-1}	0.11

2.4 Natural Fibers in Brake Pads

A material for the production of brake pads is Biomass fibers derived from agricultural processes, as it is both ecologically beneficial and commercially viable. Based on their source (steam), Natural Fibers can be subdivided into three groups: Animal, Mineral, and Plant. These fibers have a variety of mechanical and physical characteristics; for example, plant fibers are excellent for strength and stiffness due to their high cellulose content [38]. Natural fibers can only be used for a limited number of applications due to their inherent qualities such as poorer wettability and incompatibility with various polymeric matrices than synthetic fibers and less regular and homogeneous. As a result of the need for chemical treatments to enhance mechanical qualities, it is challenging to determine the best candidates for usage in friction materials. The most promising fibers are those made from palm kernel, flax, agave, aloe, etc. [4]. Table 2.6 below shows the mechanical and chemical properties of a few agricultural waste sources for composites [1].

Table 2.6 The mechanical and chemical characteristics of agricultural waste *[1]*

Chemical Properties					**Physical and Mechanical Properties**			
Agr-Waste Type	**Cellulose (%)**	**Hemi-cellulose (%)**	**Lignin (%)**	**Wax (%)**	**Density (g/cm3)**	**Elong. (%)**	**Tensile Strength (MPa)**	**Young's Modulus (GPa)**
Jute	45–71	13–21	12–26	0.5	1.3–1.4	1.5–1.8	393–800	10–30
Flax	71	18–20	2.2	-	1.4–1.5	1.2–3.2	345–1500	27.6–80
Bamboo	73	12	10	-	0.6–1.1	4–7	360–590	22–54
Bagasse	55–57	23–24	24.–26	-	0.3–1.2	6.2–8.2	257–290	15–18
PKS	31.33	17.94	48.83	-	0.9–2.3	2.1–5.0	227–278	2.7–3.2

2.5 Flax fiber as Brake Lining components

Flax fiber (Linum usitatissimum as its scientific name) as a brake lining ingredient is the most significant member of the non-wood natural fibers produced either manually or mechanically and is undamaged from the top to the root. Due to their distinct features like durative, sustainable, bio-degradable, flammable, and economically feasible, they are excellent for strength and stiffness due to their high cellulose content [38].Each flax fiber is composed of multiple layers, in these layers, cellulose and hemicellulose can be found in a thin main wall, and a secondary wall, which contains microfibrils formed of a mixture of 30 to 100 cellulose molecules, strengthens the fiber. Condensed lamellae made up of roughly 3% pectin and 14% hemicellulose are implanted with cellulose fibrils that have a diameter between 0.2 and 0.25 µm, which causes water absorption (moisture content ~8.95 wt.%) and thermal fiber breakdown. The flax plant has a 90 –125-day life cycle, (times for vegetation, flowering, and maturation) and can grow in a temperate area when there is enough humidity [39]. The rising emphasis on flax fiber, to make composites is due to a variety of factors, including oil consumption capacity, environmental regulations, as well as sustainability concerns. Moreover, flax fibers are competitive with glass fibers and can be used as a reasonable replacement. In some instances, One important advantage is that flax fibers may be thermally recycled by burning them with leftover slag, which produces energy without producing a lot of waste. [40]. The fibrous bundles seen in a plant stem's inner bark are where Bast fibers are gathered as shown in Figure 2.1 below [38].

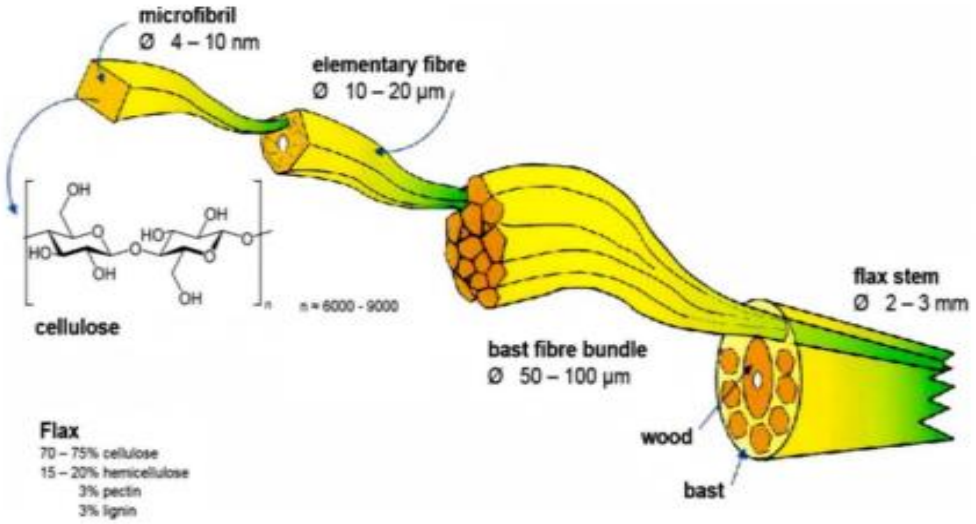

Figure 2.1 Flax fiber Architecture *[38]*

2.5.1 Flax fiber parameters

The properties of flax fiber include its orientation, length, thickness, adhesion to the matrix, treatment, and so forth. When compared to raw flax fibers, the interfacial strength of the finished composites was much higher after surface pretreatment. In the longitudinal direction, the fibers are stiff and robust due to the secondary cell wall's highly crystalline structure. However, the presence of amorphous zones between the crystallites. Variables like harvesting, extraction, growth phase, the orientation of the cellulose microfibrils, and the hollow core of the lumen give flax fiber its extraordinary and unique properties. As fiber orientation increases, strength and modulus decrease, and the interfacial strength of the final composites is greatly increased by the stress of the flax fibers [38]. The Young's moduli and Poisson ratio of the composite are influenced by the fibers' longitudinal and transverse directions. Due to an increase in the stress difference between the tensile and compressive modes, micro buckling happens as the volume fraction rises [41].

2.5.2 Flax Fiber's Mechanical and Physical Properties

The longest elementary fibers and the lowest microfibril orientation are found in flax fiber, which has the highest tensile strength. With a diameter of 35 to 50 μm, the modulus of elementary fibers ranges from 39 to 78 GPa. The difference in fiber lumen size and the presence of more cellulose in microfibrils are the causes of this variation in tensile strength [38]. Flax is 2-3 times more durable against wear and abrasion When compared to cotton fiber. It is incredibly breathable and effectively absorbs moisture. The automobile industry has seen a sharp rise in the use of flax fibers in recent years [42]. The mechanical characteristics of composites made of natural fibers are significantly impacted by moisture absorption. Poor contact between the fibers and matrix may result from their differing affinity for water. To solve this issue, covalent connections between the fibers and matrix are formed during the polymerization phase by using hydroxyl groups [43].

Dhakal et al., claim using different wt.% of flax fibers as reinforcement resulted in a considerable increase in tensile modulus (higher than epoxy resin). However, the flexural modulus is unaffected by moisture absorption, therefore the flexural failure stress is lower than the tensile failure mode. This is a result of the flexural samples failing in the modes of tension, shear, and compression. [44]. In terms of mechanical parameters (maximum tensile strength of 280 MPa) and (specific modulus of 29 GPa g/cm^3), Arctic flax/epoxy composites performed better than glass/epoxy composites [45].

Liang et, al Glass fiber/epoxy and flax fiber/epoxy composite fatigue behaviors; they claimed that flax composites had the advantage of constant modulus under cycle stress [46]. Yuan et al. used the hot compression technique method to test the mechanical properties of flax/PLA composites. The ideal processing parameters are determined to be 5% silane-treated flax fiber concentration for 40% fiber

volume fraction, with 190 °C molding temperature, and 3 minutes of heating [47]. The addition of more Al_2O_3 with flax fiber and resin has less ability to carry the impact energy, reduced interfacial bonding, and energy absorption capacity. It also disturbs the matrix continuity leading to stress concentration which can act as a crack initiator and propagator; Due to the formation of voids during the compression molding method [48]. It has been extensively studied how well flax composites made of epoxy function mechanically [40] Table 2.7 below displays the common mechanical characteristics of the significant bast fibers.

Table 2.7 Typical properties of some bast fibers compared to E-glass *[40]*.

Fibers	**Density (kg/m3)**	**E-modulus (GPa)**	**Elongation at break (%)**
E-glass	2550	71	3.4
Flax	1530	58 ± 15	3.27
Jute	1520	60	2

2.5.3 Surface Treatment on Flax Fibers

High-quality fibers are typically made via a process known as mercerization, sometimes known as Alkali treatment. Due to the removal of cementing agents like lignin and hemicellulose during the mercerization process, the chemical composition, degree of polymerization, and molecular orientation of the cellulose crystallites are all affected. Investigations into the mechanical characteristics of polystyrene composites supplemented with chemically treated flax fiber revealed that mercerization enhanced the mechanical characteristics of polystyrene composites. On the other hand, the shape and chemical makeup of the surface, mercerization, and other factors all have a significant impact on how quickly flax fibers degrade thermally and how hot they process [40].In comparison to other natural and synthetic fibers, flax fiber has exceptional strength and stiffness. It has been demonstrated that alkali treatments improve flexural properties when combined with NaOH solutions of 5%, 6%, and 10% strength [49].

2.5.5 Factors affecting the properties of Flax Fiber Reinforced Composites

The development of natural fiber reinforced composite (FRC) requires the chemical makeup and surface adhesive bonding of natural fiber. Among the ingredients that make up natural fibers are cellulose, hemicelluloses, lignin, pectin, waxes, and water-soluble materials [50]. Flax fiber has several drawbacks such as fiber's hydrophobicity and environmental variables (humidity and temperature), which reduce their mechanical capabilities due to matrix aging and fiber swelling. Humidity can harm composites in the form of interfacial fiber and matrix microcracks which appear randomly and without warning [51].

Compression molding and foam stacking circumstances cause hydrophilic flax fibers in composites to expand and water molecules might travel through the many capillaries. The linkages between the binder and the fibers will subsequently break, weak thermosetting glue (like epoxy) will develop microcracks, and the water absorption value will increase. Due to the presence of the OH group, lignocellulose natural fibers have a high hydrophilicity. By creating a hydrogen connection between the cellulose, hemicellulose, and lignin's water-hydroxyl groups, it improves the composites' ability to absorb water. Flax fibers are an affordable material with unique mechanical properties that have the potential to take the place of synthetic fibers in composites. Variation in their qualities is their greatest disadvantage [52]. Pucci et al., studied to improve the wetting and swelling Properties and the impact of thermal treatment of flax fibers, as a result, it has been demonstrated to become less hydrophilic after heat treatment [53].

2.5.6 Thermal Properties of Flax Fiber Reinforced Composites

Thermodynamic stability has a significant impact on composite performance. Temperature, heating rate, and chemical composition are some of the factors that can affect how quickly plant fibers degrade thermally. Flax fiber can withstand heat up to 170 °C for 120 minutes and up to 2000 °C for 30 minutes without losing any of its strength. The increased polymer mobility caused by a rise in temperature causes a reduction in the storage modulus. In a hybrid composite, the addition of other fibers, such as basalt fiber, can improve the storage modulus while simultaneously making the composite stiffer. To ascertain the competitive potential of these fibers for automotive applications, flax fibers reinforced thermoset, vinyl ester, and polyester resin composites were investigated [38].

The degradation of flax fibers affects the curing temperature in thermosets. As cellulose makes up the majority of natural fibers, it also regulates the degrading behavior. Bledzki et al., baked the untreated flax fibers in a lab oven set between 170-210 °C For 120 minutes, as a result, below 170 °C, and over 170 °C the tenacity and polymerization degree decreased. Similarly, Bledzki et al. studied flax fiber treated with 34% acetylation by raising the breakdown temperature from 319 °C to 360 °C. Moreover, it was asserted that the composition of flax fibers was changed by the elimination of lignin and hemicellulose, improving their thermal stability [40].

2.6 Carbon Nanomaterials in Brake Pads

Carbon Nanocomposites (CNCs) are ideal for brake pad applications because of their high rigidity, excellent tribological characteristics, and low wear rate. CNTs are an additive of choice for the production of brake pads and as an alternative filler in friction materials due to their effectiveness in enhancing a variety of Nano composites' qualities [54].

MWCNTs are the primary friction modifiers utilized for their frictional qualities because of their high stiffness, heat resistance, exceptional damping factors, and low density [55]. Singh et al. used CNTs to enhance the brake pad's tribological characteristics, as a result, it increases its strength and wear resistance while lowering its thermal conductivity and density. In other investigations, the inclusion of about 5–25 vol. % of friction formulations of MWCNTs improves friction stability, fade, and recovery behaviors [56]. Hwang et al. investigated the impacts of CNT on the material compositions by substituting 1.7%, 4.7%, and 8.5% of CNT for barite. The outcomes demonstrated that it might enhance the materials' thermal friction stability and cause a simultaneous decrease in the specific wear rate and COF. The undispersed bundles of CNT on the contact surface may have contributed to the increase in CNT concentration. [57]. Lee et al. studied MWCNTs which has shown numerous improvements in tribological characteristics of brake lining materials. This result could be attributed to CNTs' strong toughness and high ratios with low density [58].

Gbayan and Kanny created a hybrid polymer-based Nano composite brake pad, and MWCNT was used as a friction modifier to control the pad's frictional performance. It is demonstrated that a 90% reduction in stopping distance and wear rates was recorded [59]. The primary rationale for utilizing carbon nanomaterials as a friction modifier is their large surface area, which allows for the addition of modest amounts of material while improving the frictional properties. High rigidity, excellent tribological characteristics, and low wear. The frictional qualities of composites are controlled and enhanced through the application of multi-walled carbon nanotubes (MWCNTs) as friction modifiers [3].

Table 2.8 Mechanical and thermal properties of MWCNTs *[60]*

Properties	**MWCNTs**
Density (g/cm^3)	2.1
Melting temperature (^oc)	1300
Coefficient of thermal expansion ($1/k$)	$2*10^{-5}$
Thermal conductivity ($Wm^{-1}K^{-1}$)	3000

2.6.1 Environmental Impacts of Nanomaterials

Nanomaterials are becoming a solution to many of the technological issues that industries are currently facing. However regular usage of these materials causes large accumulations, which may accumulate swiftly into biological systems. Many molecules can be found in a tiny region because nanomaterials have a very large surface area-to-volume ratio. As the number of molecules grows, the substance's cumulative inherent toxicity rises noticeably [61].

Due to the considerable mass of airborne particles that brake pads produce, it's critical to determine how hazardous the wear debris is and to understand how it interacts with the environment [12]. CNTs can also affect human systems by entering our bodies through the windpipes, and if they remain in the lungs for a long time, they can lead to inflammation and malignancies. Some CNTs have characteristics that are comparable to those of asbestos and may actively promote the development of lung cancer. MWCNT is a special kind of toxin that can prevent cells from repairing their DNA. It is crucial to conduct a study on the long-term effects of CNT buildup on the environment. There are currently insufficient studies on the wear debris produced by carbon nanocomposite brake pads and its effects on the environment. The range of carbon nanoparticles produced by tribological methods makes evaluating the whole environmental impact of these materials difficult [3].

The mechanism by which particles disperse, react, and accumulate is illustrated in Figure 2.2 below, along with the potential consequences of the widespread use of carbon nanomaterials. Research has shown that this leads to a decline in the fertility of the soil [62].

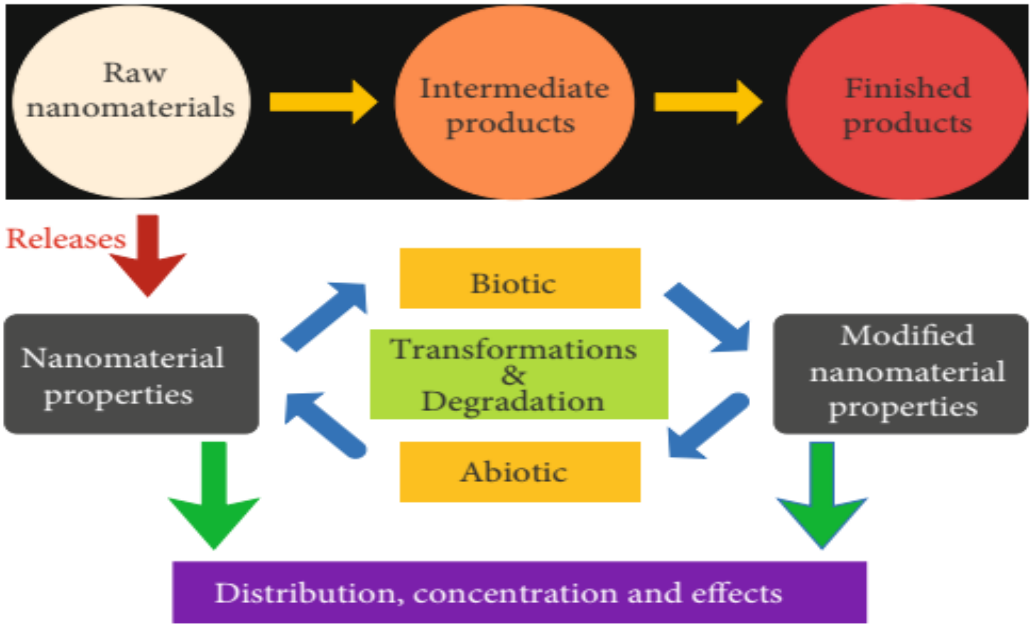

Figure 2.2 The dispersal, accumulation, and impact of nanoengineered particles *[62]*.

2.7. Pollution from brake systems

Particulate matter (PM) is comprised of submicron-sized liquid and solid particles dispersed in the atmosphere. In the human respiratory system, particle behavior varies over a broad size range (100 nm to 10 µm). PM with a diameter of less than 10 µm may pose a threat to the tracheobronchial and alveolar areas. PM, constituents consist of organic carbon, nitrates, sulfates, organic molecules (such as polycyclic aromatic hydrocarbons), and biological components [4].

Moreover, the braking process also produces a significant number of airborne particles, which are nearly indistinguishable from other atmospheric particles when released into the environment by the pads rubbing against the disk rotors. When we come to the disc material Grey cast iron is the most popular and it offers great thermal properties, wear resistance, and mechanical strength [3].

A measurement of 4.7 g/km was made for electric vehicles (EVs) and $\sum CO_{adds}$ 133.9 g/km for passenger automobiles fuelled by gasoline. One of the main causes, contributing as much as 21% of all emissions associated with driving, is brake wear. The production of friction materials could also generate volatile organic molecules like (formaldehyde) phenolic resin. Furthermore, braking events can result in the production of dangerous chemical compounds with a high melting point. [4].

The total $\sum CO_{add}$ emissions from the participants were compared using Equation 2 below [4].

$$\sum CO_{add} = \sum_{i=1}^{n} m(i) * R_t(i) \text{ ----------(2)}$$

Where: R(t) denotes the pollutant's relative toxicity with carbon monoxide,

m(i) denotes the pollutant's mass emissions, and

n denotes the total number of pollutant types taken into consideration.

Friction materials must have 0.5% of copper components by 2025, as opposed to 5% beginning in 2021. Despite being classified as dangerous metals, Antimony (Sb), zinc (Zn), and Nickel (Ni) are usable today without restrictions. Sb may cause cell hypoxia since it can enter the human body by inhalation, the food chain, and skin contact [63]. During braking, high temperatures can cause some Sb_2S_3 to oxidize into Sb_2O_3, which has the potential to cause cancer [64]. When fossil fuels are refined for the production of composites, dangerous gases including CO_2, methane, and nitrous oxide are released. These pollutants can damage processing machinery and cause deadly illnesses (cancer) [65].

2.8 Hybridization of Natural and Synthetic Fiber-Reinforced Composites

Natural fibers derived from plants are a superior alternative to commonly used synthetic and mineral fibers due to their renewability, availability, biodegradability, and environmentally friendly behavior. In general, a hybrid composite is described as the blending of two or more fillers into a single matrix. Natural and synthetic fibers reinforced hybrid polymer composites have been utilized to improve the performance of the composites. Some of the advantages are high specific stiffness and strength, good fatigue strength and damage tolerance, corrosion resistance, low density and thermal expansions, non-magnetic properties, low energy consumption during fabrication, and lower production costs. Hybridization provides an alternative to chemical treatment by merging organic and artificial hydrophobic fibers. This method reduces the material's absorption of water while also enhancing its properties [66].

The hybrid composite's shape, surface finish, and environmental tolerance are all determined by the resin type. Depending on the processing method, two types of resins (thermoplastic and thermoset) are frequently bonded with various fillers.

Emad Omrani et al. discovered that a highly ordered fiber allows for improved wear and friction, therefore processing and alignment of the fiber affect the tribological characteristics [20]. According to Fu et al., 5.6 vol.% flax fibers produced the best tribological characteristics [67]. Three primary factors, the materials (matrix and filler), the technique of preparation, and the interaction between the fillers and the matrix, substantially impact the final hybrid composite product's attributes [65]. The manufacturing process and sequential procedures of friction materials are broken down into distinct steps, as shown in Figure 2.3 and Table 2.9 below.

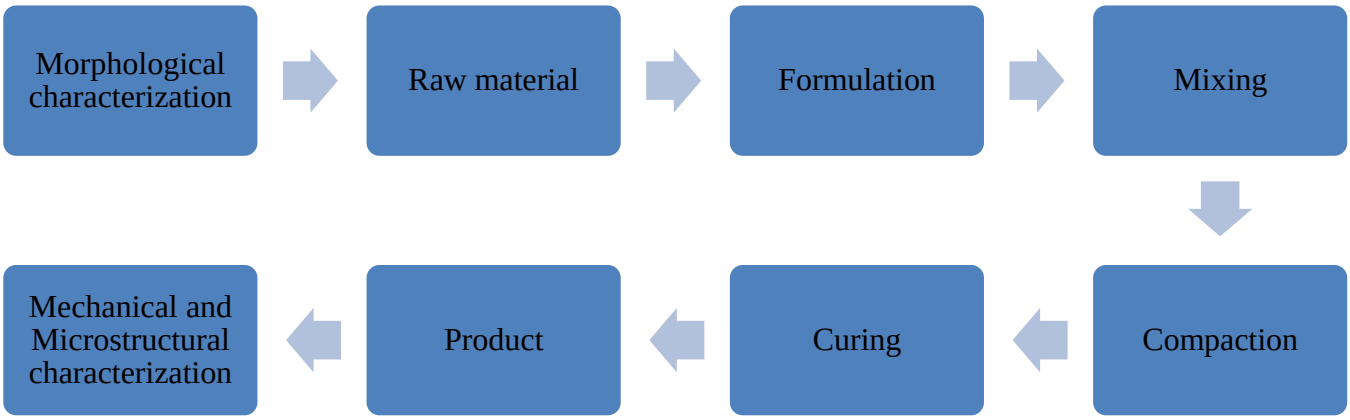

Figure 2.3 Brake pad manufacturing process overview. *[4]*

Table 2.9 Sequential procedure followed in developing composites *[68]*.

Procedure	**Conditions**
Sequential mixing in shear mixer	Shovel and chopper speeds: 140 and 2800 rpm; total time: 20 minutes. Fibers (10 min), fillers and friction modifiers (6 min), and binders (4 min) are the order of mixing.
Curing in hydraulic cure press	Compression Molding Machine: the die temperature was adjusted to 145 °C and the compression pressure to 13 MPa. During curing, (7 min to cure) breathing techniques for eliminating volatile gasses developed.
Post curing	5.5 h at 160 °C in a hot air oven
Finishing	Grinding of the baked pad in the belt grinder

2.9 Mechanical properties of hybrid polymer reinforced composites

Fiber volume fraction substantially impacts the final mechanical characteristics of composites. Poor bonding between the reinforcement and matrix was seen with increasing fiber volume fractions. Further investigation showed that smaller fiber volume percentages resulted in a degradation of mechanical properties. The prediction of the mechanical behavior of hybrid materials depends on material parameters, such as the reinforcements (fibers or particles) and matrix mechanical properties, the distribution and dispersion of reinforcements, volume fractions of the reinforcements, and test conditions. The rule of mixture (ROM) is often applied to predict the mechanical behaviors of hybrid materials. There are several models to predict these theoretical models including Voigt, Reuss, Hirsch, and Tsai–Pagano [69].

The tensile and thermal characteristics of hybrid composites made of glass/epoxy, banana/epoxy, and flax/epoxy composites were assessed by Srinivasan et al. with the aid of a compression molding machine. Mechanical qualities such as tensile strength, flexural strength, and impact strength as well as (SEM), structural morphology have been examined. The results showed that the mechanical properties had higher values [70].

Achebe et al. investigated the use of palm kernel fiber (PKF) as a filler and epoxy as a binder the specific gravity and hardness increased with the amount of filler. Similarly, Ikpambese et al. investigated various proportions of 100µm PKFs in combination with epoxy, Al_2O_3, and $CaCO_3$ (eggshell). Aigbodion et al. used phenolic resin and bagasse with a composition of 30% and 70%, respectively, on a 100µm sieve. As a result, the wear rate rises along with a decrease in hardness, density, and compressive strength as sieve grade size increases as a filler [54].

For vehicle brakes, friction linings need to have a relatively high friction coefficient (usually between 0.40 and 0.47), which is stable throughout a wide range of pressure and temperature fluctuations. In addition, they ought to have sufficient mechanical strength, little shrinkage, low moisture sensitivity, low wear rates, and strong bonding to the back plate. Bashar and Darlington combined coconut shells (CS) and coconut shell powder (CSP) with polyester and epoxy. The findings indicated that adding CS powder increased the brittleness (hardness) but lowered breaking, impact, and compressive strength [71].

Assarar et al discussed the effects of water on the aging characteristics of epoxy composites, After the initial 1-day immersion in water, the failure stress fell by around 13%. The reduction in failure stress between 1 -20 days of immersion was only an additional 2% or 15%. According to the Figure below, a 30% drop in the flax/epoxy composite's normalized Young's modulus within the first 10 days indicated a substantially worse outcome from water aging than glass fiber composites [72].

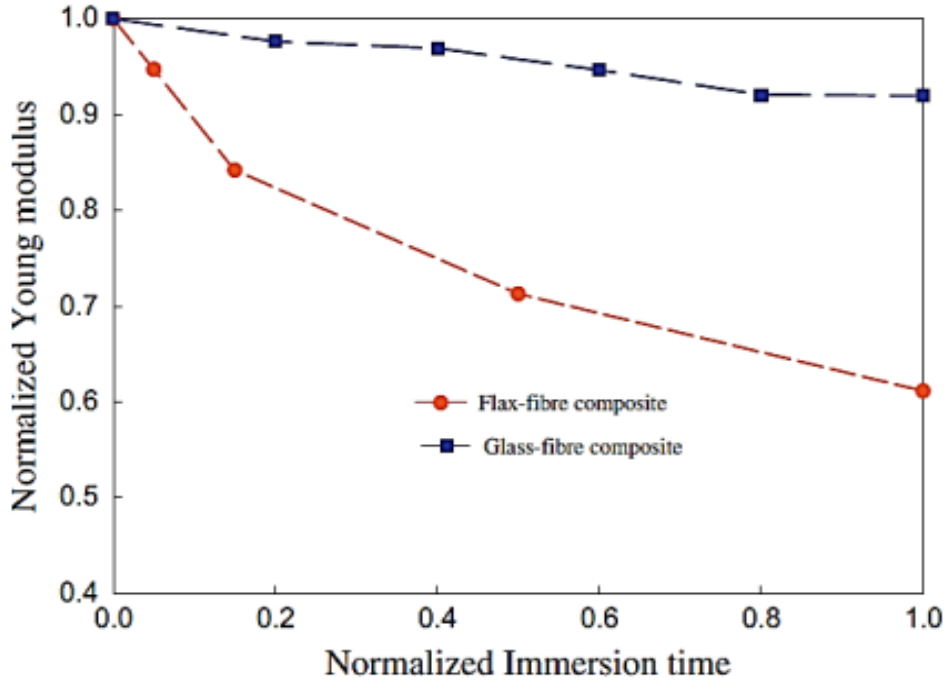

Figure 2.4 Normalized Young's modulus(t = 0) vs normalized immersion time *[72]*

2.10 Design Parameters For Brake Lining Material Compositions

The design parameters were optimized to reduce variance before the design was optimized to achieve mean goal values for output parameters. Special orthogonal arrays are used in the Taguchi method to analyze every design factor with the least amount of experiments. Factorial optimization can be accomplished with fewer tests by using the Taguchi technique, which can lead to lower experimental expenses, better optimization quality, and suitable design solutions [73]. Yilma et al. also used the Taguchi technique to evaluate the brake lining composition. This study found that a combination of 22% epoxy resin, 16% graphite particles, 15% steel particles, 11% basalt particles, and 3% wheat straw fiber produced the best water absorption capacities [74].

2.11 Summary of the Literature

Table 2.10 Findings and gaps identified in the Literature's

S.N	Authors	Findings From Literature	Gaps Identified From Literature
1	(S.kumaran,2021) (K.J. Lee,2009)	Frictional qualities are controlled and enhanced by applying MWCNTs as friction modifiers due to their high toughness and low-density ratios. High rigidity, excellent tribological characteristics, and low wear rate are some of the characteristics of carbon nanocomposite.	insufficient studies on the wear debris produced by CNC brake pads and its effects on the environment and MWCNTs volumetric ratio gives the desired frictional properties still limited. CNTs can affect human systems but how severely is unknown.
2	(W.Österle,,2011)	It is crucial to convert brake pad ingredients into a nano-crystalline third body to achieve the best braking efficiency and functionality, Solid lubricants are applied in amounts less than 10% of the total volume portion.	How much brake pad ingredients must be converted into the nano-crystalline third body is not fixed in amount.
3	(M.Assarar,2011)	Adding (CSP) increased the brittleness (hardness) but lower breaking, impact, and compressive strengths.	Hardness and specific gravity increased as the filler increased in what %wt stable is still unknown.
4	(K.Venkastesh,2019)	Fillers help to reduce cost by 85% weights or higher, it is common practice to add harder particles, like Al2O3 to enhance or optimize performance, to raise the COF.	COF (μ) is created by the scraping of the material's surface against the disc, but the percentage of filler (harder particle) is not indicated in the finding.

5	(S. Pujari, 2019,) (S.Ray,2022)	In fiber-reinforced polyester composites, the addition of 10% by weight of iron filler can reduce flammability and improve heat stability And also ES particles can take the role of metal particles, By improving the thermal stability.	Both ES and iron filler in brake linings improve thermal stability but which one is more advantageous is not clear regarding their pros and cons.
6	(M. Pavan,2018)	composites with 5 wt. % ES powder can withstand greater bending stresses, but 10wt.% deflects less. According to the flexural strength experiment, stiffness can be increased with 5% of ES filler and declines with increasing filler quantity.	The spread of the fracture and delamination may have been inhibited by the use of filler material but additional tests (wear) are recommended on samples of the same composition.
7	(D.V. Lucio,2018)	ES improves the mechanical and heat stability qualities of reinforced biopolymeric composites, it may be a good option for an environmentally friendly filler material.	Although ES is readily available as trash in large quantities in the food sector it's not very well-known as a filler material.
8	(R.H. Mohamed,2019)	the properties of ES powder as reinforcement and polyamide as the matrix material were investigated. As a result, with an increase in ES powder, it was found that the mechanical properties increased as well.	the hardness and tensile qualities also increased along with the amount of ES powder in what proportion or amount the the properties increased is yet Un-known.
9	(S.Sunardi,2023)	If 5 wt.% of ES is added, the polymethyl methacrylate composite might wear less. Enhancing the mixture's ES	Increasing the amount of ES nanoparticles in the mixture improves water absorption and causes the

		nanoparticle content increases the composite's ability to absorb water and expand in thickness combining fibers, bamboo particles, and ES particles to form a hybrid material.	thickness of the composite to expand in more contradicting terms and how the COF is adjusted is not clear yet. the COF may be adjusted and mechanical qualities can be enhanced.
10	(G. S.Manoharan,2019)	While too much abrasive can cause abrasion and degrade the composite, Excessive fluctuations in the COF can result from using too much lubricant. Generally, lubricants have a 5.29%wt., while abrasives have up to 10%wt.	To achieve the appropriate COF and WR the fluctuations in the COF are still inconsistent with %wt. of lubricant and abrasives.
11	(Manoharan,2019)	Alumina (Al2O3), is utilized extensively in composites. It is harder than other ceramic particles and less than diamond, silicon carbide, and boron carbide. Furthermore, the interfacial reaction layer and wettability of alumina were consistently superior.	Even if the presence of alumina always improves the composite material's hardness and tensile strength after the solidification process, porosity was created inside the composite material due to low particle size and high %wt. Of alumina.
12	(D. Shrawan,2020)	the physical and mechanical properties of hybrid composites are determined by the fiber volume fraction. And also the cross-section, moisture content, cellulose content, and fiber structures.	In the case of Natural fibers' how the physical and mechanical properties are greatly influenced by their physical characteristics is not very well known.
13	(Ghosh P.2020)	The flax fiber modulus, which depends on the fiber diameter	The study focused on thermoset, vinyl ester, and

		(35–50 µm), varies from 39 to 78 GPa. Also, Flax fiber can withstand heat to 170 °C for 120 minutes and up to 2000 °C for 30 minutes without losing any of its strength. As fiber orientation increases, strength and modulus decrease, and the interfacial strength of the final composites is greatly increased by the stress of the flax fibers.	polyester resin composites reinforced with flax fiber but the increased polymer mobility caused by a rise in temperature causes a reduction in the storage modulus which is not very well known.
14	(A.P.Irawan,2022)	The temperature required for thermal decomposition increases with resin heat resistance, lowering oxidation and decomposition. As a result, the brake pads' frictional characteristics will be stable or can lower the rate of wear.	COF, WR, and particle emission of the brake pad using polyester resin as a binder are not investigated well. However, a few tests using polyester as a resin were performed.
15	(K.Oksman,2001)	Maximum tensile strength of 280 MPa and 29 GPa g/cm^3 modulus was obtained for arctic flax/epoxy when compared to glass/epoxy composite for fatigue behaviors.	What is the result for impact strength for flax composites that have constant modulus under cycle stress,
16	(Y.Yuan,2011)	The ideal processing parameter for flax/PLA is determined to be 40% fiber vol.,5% silane-treated flax fiber concentration at 190°C molding temperature for 3 minutes of heating.	if the parameters are changed with different molding temperatures and time What will be the result for Volume fraction, is not discussed well.
17	(S. Alix,2011)	It has been proven that alkali treatments boost flexural characteristics when paired with	What is the influence of Chemical fiber treatments on impact strength,

		5%, 6%, and 10% strength NaOH solutions.	hardness, and wear resistance characteristics is not discussed.
18	(U. Huner,2015)	Flax fibers are an affordable material with unique mechanical properties that have the potential to take the place of synthetic fibers in composites. Due to the presence of the OH group, lignocellulose natural fibers have a high hydrophilicity.	Variation in their qualities is their greatest disadvantage due to their hydrophilic nature which is not addressed appropriately.
19	(P.Singh,2022)	Untreated flax fiber was baked in a lab oven set between 170-210°C for 120 minutes as a result below and over 170°C the tenacity and polymerization degree decreased. Similarly, flax fiber treated with 34% Acetylation was studied by raising the temperature to 319-360°C.	The finding didn't address the shape and chemical makeup of the surface mercerization, and other factors that all have a significant impact on how quickly flax fibers degrade thermally and how hot they process well.
20	(A.Patnaik,2011) (J. Hwang,2010)	In terms of CNT, the inclusion of about 5%-25% MWCNTs improves friction stability and fade recovery. 1.7%, 4.7%, and 8.5% of CNT for barite might enhance the materials' thermal stability. friction stability causing a simultaneous decrease in the SWR and COF.	The impacts of CNT on the material compositions by substituting the optimal %wt. might enhance the brake pad's tribological and other characteristics.
21	(S.Sunardi,2023) (S.Kabir,2018)	Many molecules can be found in a tiny region because nanomaterials have a very large surface area-to-	As the number of molecules grows, the substance's cumulative

		volume ratio a considerable mass of airborne particles is produced in brake pads, to the surrounding environment.	inherent toxicity rises noticeably.thus it's critical to determine how hazardous the wear debris is and how it interacts with the environment.
22	(G.C.Giovanna,2022)	One of the main causes is brake wear, which can contribute up to 21% of all emissions from traffic or air pollution caused by harmful components of brake pads. A ∑CO add of 133.9 g/km was measured for passenger automobiles fueled by gasoline, and 4.7 g/km for electric vehicles (EVs).	Knowing a significant number of airborne particles, which are nearly indistinguishable from other atmospheric particles when released into the environment by the pads rubbing against the disk rotors is a major concern.
23	(S. Binoj,2017)	Water aging characteristics of flax/ epoxy have 30% drops in Young's modulus within the first 10 days of the immersion period from water aging than glass fiber composites. The reduction in failure stress between 1 -20 days of immersion was only an additional 2% or 15%.	The failure stress fell by around 13% After the initial 1-day immersion in water. The variations failure stress are not adequately elaborated.
24	(L.Pickering,2016)	The Young's moduli and Poisson ratio of the composite are influenced by the fibers' longitudinal and transverse directions.	Due to the increased stress difference between the tensile and compressive modes micro buckling happens as the volume fraction rises and how the buckling will occure is still unknown.

25	(S. Alix,2011)	The addition of Al2O3 with flax fiber and resin has less ability to carry the impact energy, reduced interfacial bonding, and energy absorption capacity. The volume fraction of fiber is the factor that influences the mechanical and physical properties of hybrid composites.	Due to the formation of voids during the compression molding method, it's unknown for the addition of Al2O3 with flax fiber regarding volumetric ratio.
26	(N.Dhakal,2006)	Using different wt.% of flax fibers as reinforcement resulted in a considerable increase in tensile modulus (it exceeds the amount of epoxy resin). However, the flexural modulus is unaffected by moisture absorption.	The flexural failure stress is lower than the tensile failure mode. The result of the flexural samples failing in the modes of tension, shear, and compression is not justified.
27	(L. Pickering,2016)	Poor contact between the fibers and matrix may result from their differing affinity for water. To solve this issue, covalent connections between the fibers and matrix are formed during the polymerization phase by using hydroxyl groups.	The hydroxyl (OH) group is formed during the polymerization phase. How much moisture absorption impacts the mechanical properties needs to be justified.
28	(M.Zhang,2019) (A.Iijima,2007)	During braking high temperatures can cause some Sb2S3 to oxidize into Sb2O3 which has the potential to cause cancer.	Sb may cause cell hypoxia since it can enter the human body by inhalation, and skin contact.
29	(Safri S.N.,2017)	Hybridization provides an alternative to chemical treatment by merging organic and artificial hydrophobic fibers. This method reduces the material's absorption	The process and alignment of the fiber affect the tribological characteristics of the hybrid composite

		of water while enhancing its properties. For improved wear and friction.	therefore additional research is needed.
30	(M. Mochane,2019)	Three primary factors, the materials (matrix and filler), the technique of preparation, and the interaction between the fillers and the matrix, substantially impact the final hybrid composite product's attributes.	Three factors are identified as basic parameters for the hybridization process but there is a need for volumetric fractions reinforcements, and test conditions to be determined for their attributes.
31	(R. Srinivasan,2014)	With the aid of a compression molding machine, the mechanical qualities such as, flexural, and impact strength as well as structural morphology have been examined for glass/epoxy, banana/epoxy, and flax/epoxy, and the mechanical properties had higher values.	There is not enough analysis done for the glass/epoxy, banana/epoxy, and flax/epoxy composite properties it needs some tests need to be conducted.
32	(M. P.Hirematha,2018) ((OluwafemiE.Ige,2019)	The mechanical strength decreased as the quantity of ES particle content increased, whereas the density, voids, and wear resistance increased. The type of Epoxy composites bonded is the major concern in the case of ES particles.	The wear index of epoxy composites bound with ES particles and sisal fibers can be raised with calcination treatment therefore using polyester resin as a matrix should be investigated thoroughly.

33	(A. Belhocine,2014)	The SWR on temperature, sliding velocity, pressure, and sliding distance parameters during the experiment were calculated using the Taguchi technique.	Which parameter was shown to have the most effect, followed by other variables was not discussed well.

2.12 Summary of Gaps Identified from the Literature

- Brake pads with a full or semi-metal component deteriorated disks more quickly and produced excessive noise. Thus, The primary challenge is maintaining a specific and sufficient amount of third-body material, at the brake pad-disk brake interfaces which is composed of the required nanostructure gained by balancing the material composition.
- Carbon nanoparticles are softer than NAO pads. However, their high surface area and excessive wear particles can alter the frictional properties of composites when introduced in tiny quantities. These particles are also very hazardous to the environment causing lung cancer.
- natural fibers can be applied to a restricted number of uses. Due to their intrinsic characteristics, also show inferior wettability and incompatibility with different polymeric matrices Evaluating which candidates are best suited for use in friction materials is difficult because chemical treatments are required to improve mechanical properties.
- A resin with high-loading fillers often has less ability to transfer the impact energy, which increases the fracture propagation due to the voids formed during the compression molding process. Therefore, When more Al_2O_3 was added to the flax fiber, the composite's impact strength was reduced.
- Increased loadings of Al_2O_3 fillers break the continuity of the matrix, causing stress concentration that can initiate cracks, weaken the link between the fiber and resin at the interfacial area, and lower the composites' ability to absorb energy.
- The production of friction materials, is becoming more and more concerned with climate change. The function of nano additives and nanofillers, which are expected to aid in the creation of nanostructured friction layers or friction films functioning at the braking interface, has not received adequate investigation.
- Investigating the effects of MWCNTs on temperature-sensitive friction properties, such as wear response to friction materials and friction fade, is crucial.
- The amount of research on the wear debris and environmental consequences of carbon Nano composite brake pads is still limited.

- Determining the severity of these materials' environmental consequences requires a detailed analysis of the many types of carbon nanoparticles generated by tribological processes.
- Automotive brake pad friction linings need to have a relatively high friction coefficient, usually between 0.40-0.47, that remains constant throughout a broad temperature and pressure range.
- To improve the mechanical and physical qualities of brake pads made from agricultural waste, a detailed evaluation of the type, amount, and particle size is required. And also, influenced by the kind and quantity of resin used.
- Cellulosic fibers are both polar and hydrophilic, which causes limited bonding compatibility with hydrophobic polymer matrixes and a loss of mechanical characteristics from moisture content uptake, which restricts the development of natural fiber-reinforced hybrids.

Chapter Three

3. Research Methods and Materials

3.1 Methods

The general methods employed to achieve the objectives of this thesis are displayed in Figure 3.1 below. All of the steps that are involved in the investigation of natural-based hybrid nanomaterial characteristics and their impacts on brake pads are discussed.

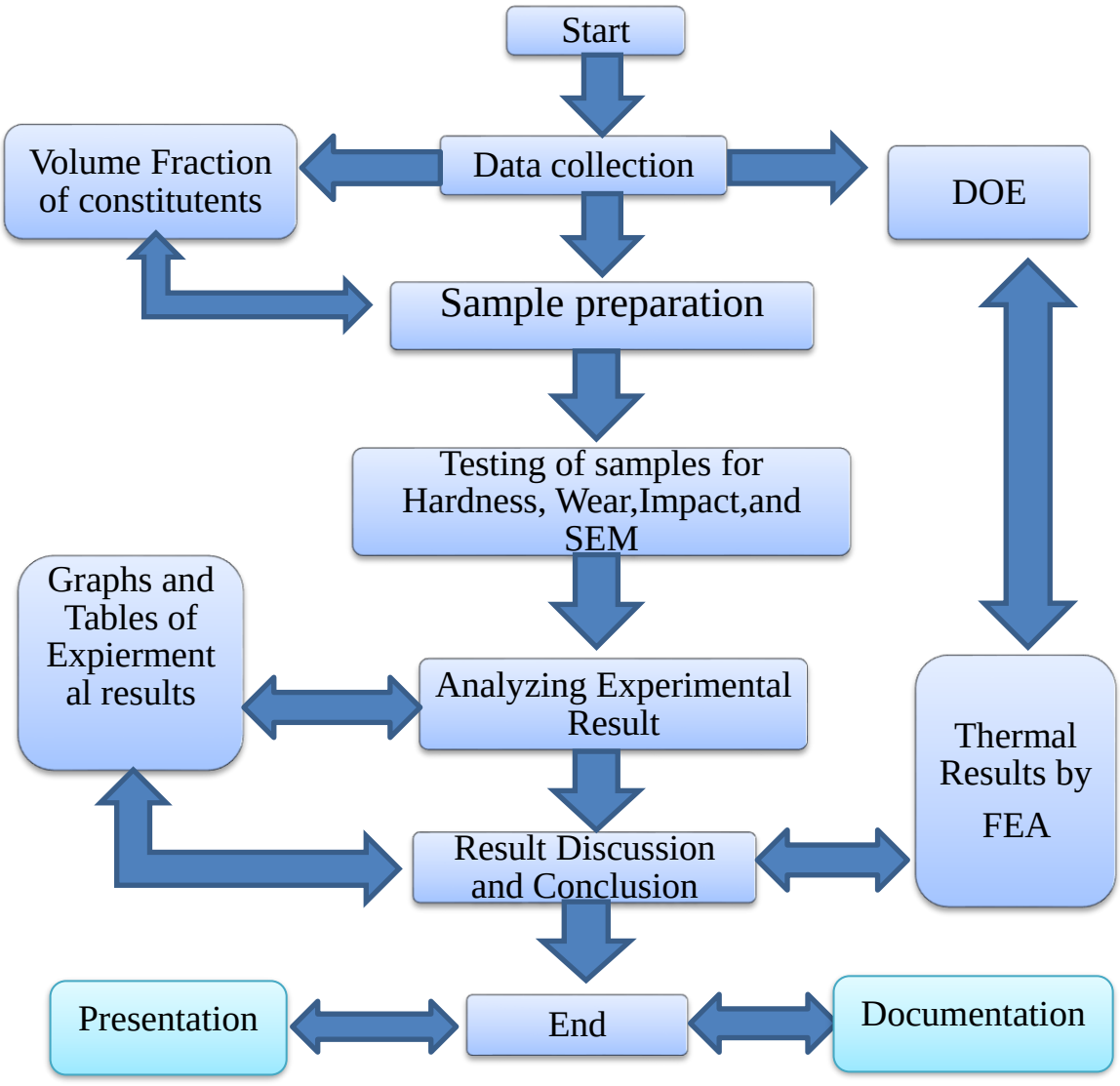

Figure 3.1 The general strategies used to accomplish this thesis's goals

3.1.1 Design of Experiment

The experiments were conducted using the design of experiments (DOE) techniques, and it is used for combining the 3 factors and 3 levels by using Minitab 21 version software. The Taguchi L9 method was used to determine the combination of process parameters for each trial. The detailed composition used is given in Table 3.1 below shows Nine mixtures that were produced with variable amounts of FlaxFiber as reinforcement, Eggshell as fillers, polyester resin as binding, and constant amounts of MWCNTs as a lubricant and Al_2O_3 as a abrasive material based on the Taguchi L9 methods. The three friction lining material characteristics that were selected as input parameters for the experimental technique are weight fractions of the Binder Resin (Polyester), Flax Fiber Treated with (%5 NaOH), and Eggshell particles of the composites. As indicated in Table 3.1, it was found that each parameter had three levels. Nine experiments were included in the experimental matrix, as shown in Table 3.2 below.

Table 3.1 Factors and levels of brake pad experiments

DOE Parameters	**Units (g)**	**Values at levels**		
		1	**2**	**3**
A. Flax Fiber Treated with (%5 NaOH)	Wt.%	6	11	21
B. Eggshell Particle	Wt.%	6	11	21
C. Binder (Polyster Resin)	Wt.%	57	62	72

Table 3 2 Material composition of brake pad linings

Sample Code	**Flax Fiber (%)**	**Eggshell (%)**	**Polyester Resin (%)**	**Al_2O_3 (%)**	**MWCNTs (%)**	**Total (%)**
SA,SE,SI	6	21	62	8	3	100
SB,SF,SG	11	6	72	8	3	100
SC,SD,SH	21	11	57	8	3	100

3.1.2 The Mixture Rule

The optimal and mean volume percentages of Flax fiber, Eggshell, MWCNTs, Al_2O_3, and polyester resin (Resin+Hardner) are 6wt.%, 21wt.%, and 3wt.%, 8wt.%, and 62wt.% respectively. The values obtained from the pycnometer reading measure the densities as shown in Figure 3.2 below and the other previously calculated data and known results are shown;

Figure 3.2 Measuring the densities of flax fiber using a pycnometer

- Density of Flax (ρ_F) = 0.6571g/cm^3
- Density of Al_3O_2, (ρ_{Al2O3}) = 3.69 g/cm^3
- Density of MWCNTs (ρ_{MWCNTs}) = 2.21 g/cm^3
- Density of Eggshell (ρ_{ES}) = 0.80 g/cm^3
- Density of polyester (ρ_p) = 1.09 g/cm^3
- Volume of Composite (V_C) = 200mm x 100mm x 5mm=1

3.1.3 The density of the composite

The density of composites (ρc) can be calculated based on the volume proportions of the particle (Vp) and matrix (Vm). Calculating the composite density at various reinforcement volume percentage fractions was done using Equation 3 below.

$$\rho_c = \rho_r V_r + \rho_m V_m \quad \text{.....(3)}$$

Where: ρ_m-ρ_c - Density of composite, and matrix respectively.

V_m-ρ_r - Densities of the matrix and reinforcement, respectively.

3.1.4 Reinforcement and matrix mass fraction

The weight % fraction of the matrix (Wm) and reinforcing particles (Wr) is defined by Equation 4 below. Assuming that the densities of the reinforcement particles (ρr) and matrix (ρm) are known. Furthermore, Composite, reinforcement, and matrix are denoted by the subscripts c, r, and m, respectively.

$$W_r=\frac{\rho r}{\rho c} * V_r;\ W_m=\frac{\rho m}{\rho c} * V_m \quad \ldots\ldots\ldots\ldots\ldots\ldots(4)$$

Where: W_r -W_m weight of the reinforcement and matrix respectively.

ρ_r -ρ_m Density of reinforcement, matrix respectively

Equation 5 defines the volume percentage of the matrix and reinforcing particle as illustrated:

$$\%\ Vr_f=\frac{Vr}{Vc};\ \%\ Vm_f=\frac{Vm}{Vc} \quad \ldots\ldots\ldots\ldots\ldots\ldots\ldots..(5)$$

Where: %Vmf= vol. mass fraction of matrix, and

%Vrf = vol. mass fraction of reinforcement

Equation 6 specifies the volume of the composite for a system consisting of reinforcement particles and matrix. Every component's volume fraction in a composite must equal to one:

$$VC = Vr + Vm = 1 \quad \ldots\ldots\ldots\ldots\ldots\ldots\ldots(6)$$

Where: Vc = vol. of composite,

Vr-Vm -Volume of reinforcement, matrix respectively

Table 3.1 The calculated outputs for densities, weights, and volumes of the composites

S.C	Density of Composite (g/cm^3)	Volume of Composite (g/cm3)	Volume of Matrix (g/cm^3)	Volume of Reinf. (g/cm^3)	Weight of matrix (g)	Weight of Reinf. (g)
SA	1.1237	112.37	69.669	42.700	78.287	47.981
SB	1.3172	131.72	94.838	36.882	124.92	48.580
SC	1.1622	116.22	66.245	49.975	76.989	58.080
SD	1.2035	120.35	68.599	51.751	82.558	62.282
SE	1.2991	129.91	80.544	49.366	104.634	64.131
SF	1.1225	112.25	80.821	31.43	90.721	35.280
SG	1.1573	115.73	83.325	32.404	96.432	37.501
SH	1.1605	116.05	66.148	49.901	76.764	57.910
SI	1.2609	126.09	78.175	47.914	98.570	60.414

Notice:Wc=ρc*Vc,Wm=ρm*Vm,Wr=ρr*Vr,Vm=Vc*%Vmf,Vr=Vc*%Vrf,ρc=ρr Vr+ρmVm

3.2 Material selections

A brake pad lining material is generally classified as reinforcements, frictional modifiers, fillers, and binders its function is also tabulated as shown in table 3.2 below.

Table 3.2 Classification of the elements of brake lining

Classification	**Functions**	**Ingredients**
Fiber	Enhances mechanical strength	Flax fiber
Filler	Enhances particular characteristics, lowers manufacturing costs, and fills voids	Eggshell particles powder
Friction modifier	Establishes the appropriate friction properties	Al_2O_3, and MWCNTs
Binder	Binds the components of all brake linings.	Polyester resin

In this study, flax fibers, eggshell (ES) particles, carbon nanotubes (MWCNTs), aluminum oxide (Al2O3), and polyester resin served as the main raw ingredients for the brake linings. The natural raw materials used in this investigation are flax fiber and ESs, as shown in Figure 3.3 (a) and (b). The source of the flax fiber was Holleta in the west of Oromia. ESs were gathered from the trash in homes. In this study, brown country chicken eggs were the type of ES used.

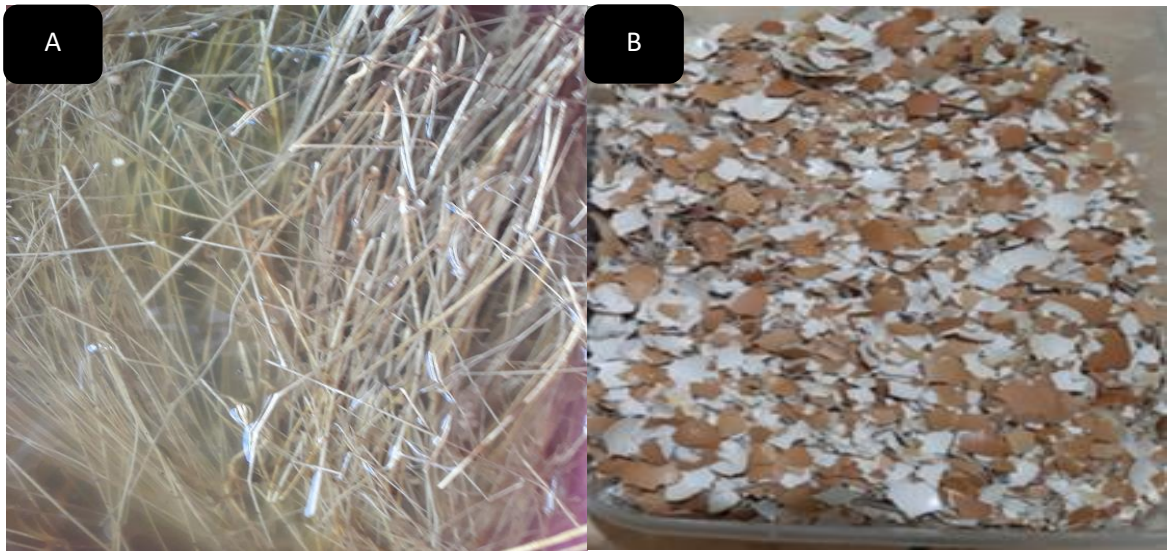

Figure 3.3 (A) Flax fiber retting and soaking process and (B) Eggshell particles

3.2.1 Preparations of Flax fiber and Chemical treatments

The flax fiber plant when reached maturity, was collected and extracted from the flax seed using the ripple process. The longer and higher-quality stem that was collected from the field was soaked in water for 15 days in a tank to begin the retting process as shown in Figure 3.3 (a) above.

This technique separates cellulose fibers from non-fiber tissues after being mechanically extracted. The flax fiber was then thoroughly cleaned for three hours in a caustic soda (5% NaOH) solution to get rid of any remnant red oil after the extraction process as shown in Figure 3.4 below, and finally washed in distilled water. Finally, The flax was allowed to dry on the field in the sun after being taken out of the container, and it was extracted as a short fiber (~2 mm). The chemical reaction is seen as Fiber-OH+N_2OH ⟹ Fiber-O-Na^++H_2O.

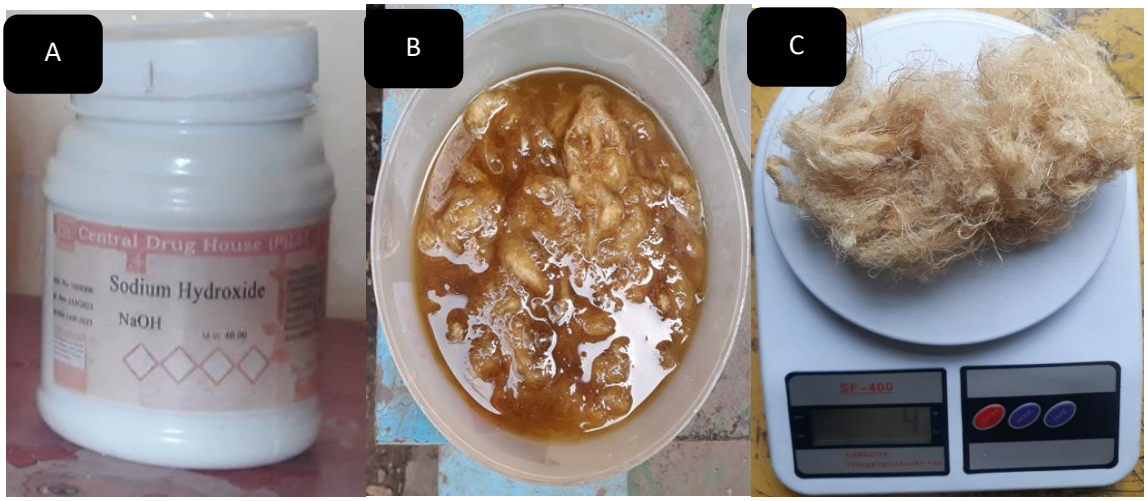

Figure 3.4 (A) NaOH (B) Flax fiber weighting and (C) Alkaline treatments (5% NaOH)

3.2.2 Eggshell particle preparation

The eggshell powder was produced by pulverizing it using a mechanical grinder following a day of sun drying, to get grain size distribution that is about less than 100 μm and that can be sieved in 40 μm, 60 μm to about 100 μm in particle size respectively, the powdered eggshell was sieved through sieve numbers 100, 60 and 40. As shown in Figure 3.5 below. To fill the resin, the eggshell powder was added at weights of 6%,11%, and 21%. The mixture is then adjusted to meet the weight of the fibers.

Figure 3.5 (A)&(B) sieve numbers 100,60, and 40 (C) eggshell powder

3.2.3 Friction Modifier And Binder Materials

Polyester resin, hardener (at the Ratio of 10:1), Al_2O_3, and MWCNTs were also provided by local importers as shown in Figure 3.6 below and the natural-based hybrid nanocomposite was mixed uniformly by using a mechanical stirrer at 1000rpm.

Figure 3.6 (A) polyester resin & hardener,(B) Al_2O_3, and (C)MWCNTs

3.2.4 Preparation of Mold

Steel was the material that was used to create the mold. Base and upper plates make up the mold. Four RHS steel pieces were welded as a frame onto a flat sheet of metal that served as the base plate. The base plate's interior is precisely the same size as the required mold To evenly distribute pressure on the samples, a metal sheet and a cylindrical block with four linked wings were mounted to the upper plate, as seen in figure 3.7 below. The dimensions, number of tests, and quantity of test specimens were taken into consideration when designing the mold. Based on that, the dimensions of 200mm *100 mm *50 mm were designed. During the compression and curing process, a load or pressure of 1MPa~10 bar is applied to the specimen through the mold that is distributed using the bar and its four wings.

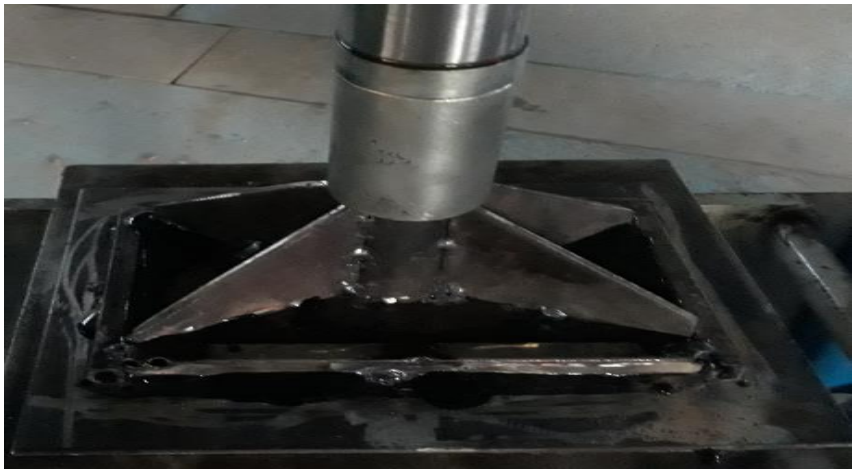

Figure 3.7 Mold setup for composite fabrication

Wax is the releasing agent, which is used to remove the composite from the mold once it has been manufactured. It keeps the resin mixture from adhering to the mold. Figures 3.8 (a)&(b) illustrate the use of wax and aluminum foil in this technique, respectively, for superior surface polish and quality. The favored kind of realizing agent is the wax due to its affordability, accessibility, and simplicity of usage. Aluminum foil also shields the composite from contaminating the mold and its surroundings as shown in Figure 3.8 (b) below. It also makes the removal of the Finished Composite Easier.

Figure 3.8 (a) Wax and (b) Aluminum foil sheets as a releasing agent

3.3 Sample preparation

The particle were mixed and stirred initially for three minutes to create a uniform mixture. The Binder was weighed into a beaker, heated to 70 °C for 20 minutes, and then stirred for another 15 minutes, (the MWCNTs, Al_3O_2, and polyester with EggShell, and Flax Fiber) blended uniformly using a mechanical stirrer set at about 1000 rpm. After that, the fiber material was added and mixed for five minutes. To bake the samples into the mold cavity, the mold is waxed and heated up to 200°C. A uniform mixture of specimens was pressed at 180°C by 1MPa~10 bar of pressure into a formed mold for 20 minutes as shown in Figure 3.9 (a) and (b) below displays the techniques used as well.

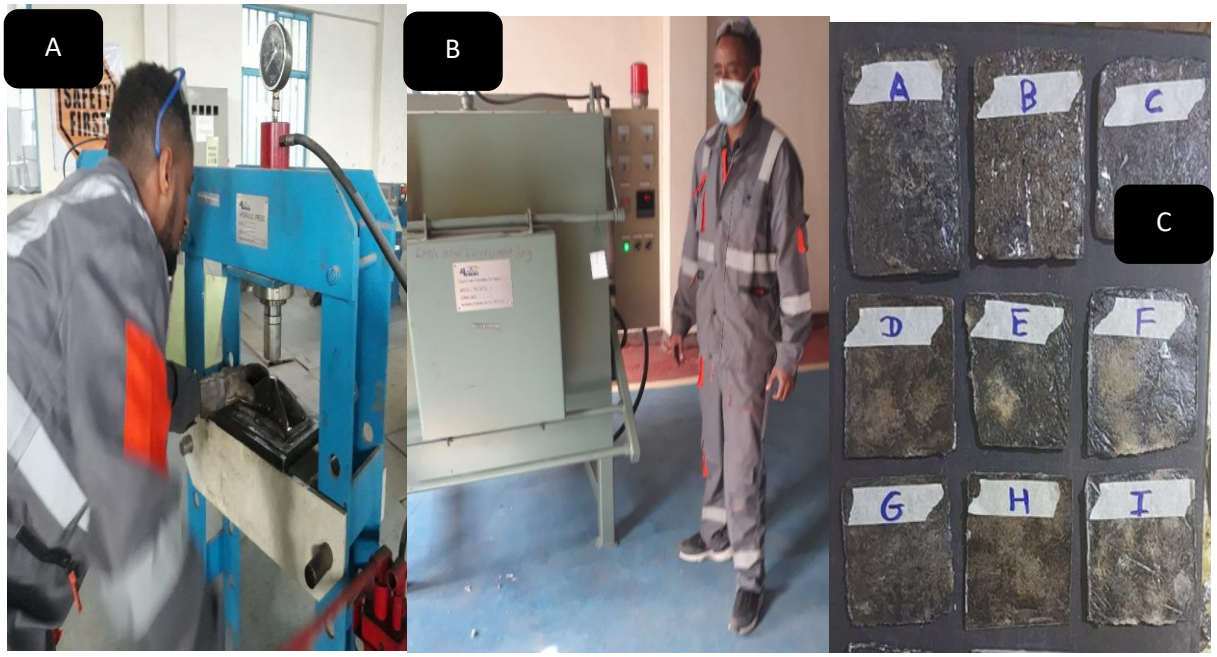

Figure 3.9 (a) Press machine settings (b) curing process (c)Samples of brake pad

Curing was the final step in the sample production process. The curing was carried out in an electric furnace that was set to run from 160 to 200 degrees Celsius for 180 minutes, followed by a 60-minute cooling interval, the heating and cooling that occurred throughout the curing process are displayed in Figure 3.9 (b) above. Since carbon-based additions usually perform significantly in the polymer matrix, the weight fraction of additives (such as CNTs or friction modifiers) in the formulation is minimal. The composite has to be molded and first cured under pressure and heat to produce friction materials. The items listed in Table 3.3 below show utilized materials and equipment used in the experimental study:

Table 3.3 Equipment And Materials Utilized In The Composite's Fabrication

No.	**Materials**	**Supplies**
1	Reinforcement	Flax Fiber, Eggshell
2	Matrix	Epoxy(Polyester) Resin,Hardener
3	Friction modifiers	MWCNTs, Al_2O_3,
4	Others	Aluminum foil, NaOH
5	Equipment	Mold, Wire Brush, Pedestal Grinder, Cutoff machine, Hydraulic Press and Electric Furnace, mechanical stirrer e.t.c

Figure 3.10 Supplies, equipment, and sample preparation

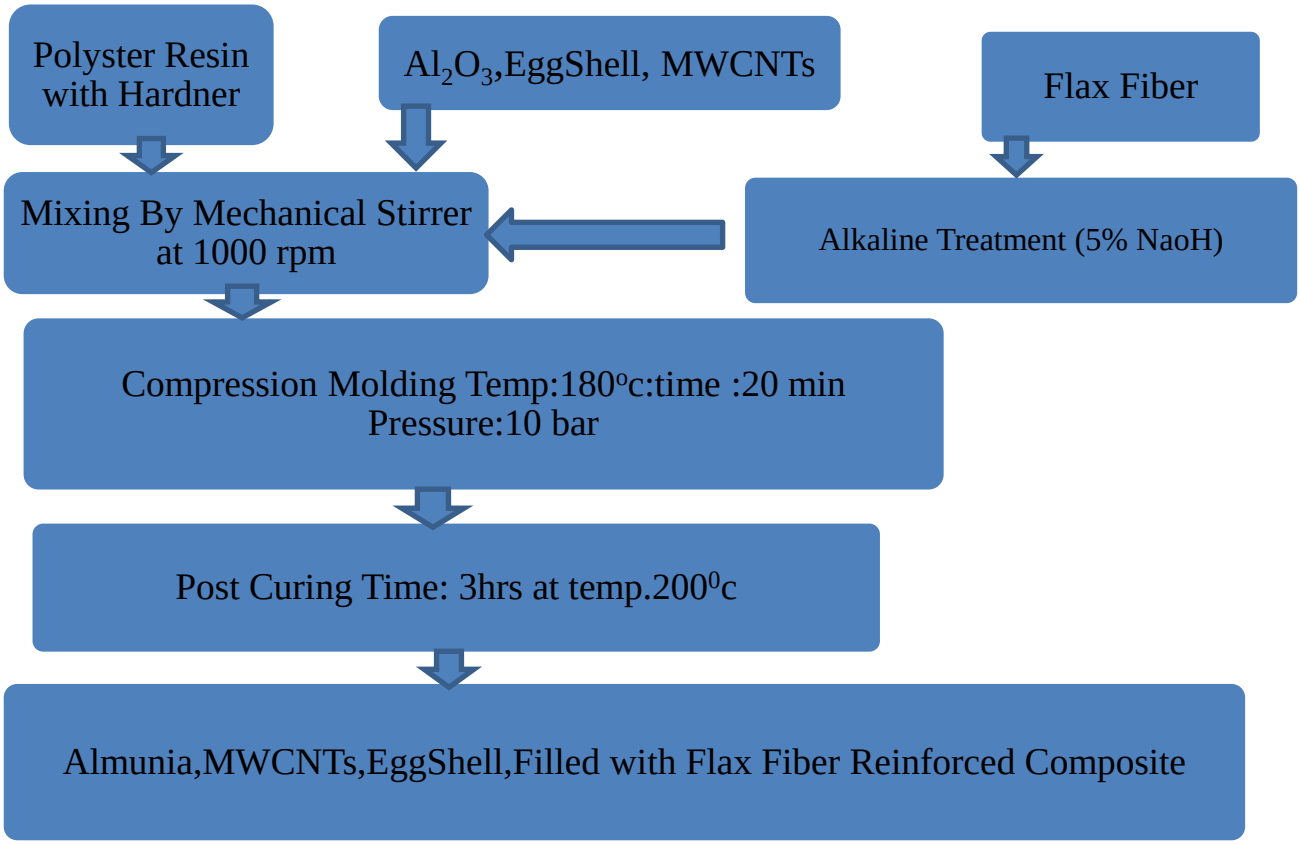

Figure 3.11 Fabrication route of the flax fiber-eggshell-filled composite

3.4 Experimental Procedures

Experimental Procedures will include discussions of the methods used to process the experimental analysis. Following the above-described information, the hybrid natural fibers nanomaterial particle reinforced composite is tested for its mechanical and physical qualities in compliance with ASTM standards.

3.4.1 Hardness testing

A solid's hardness measures how resistant it is to a variety of long-term fatigue when compression or indentation forces are applied. Measurements are made about the indenter tip penetration depth (1/8' ball indenter was utilized with an applied load of 60 kg/mm). Rockwell Hardness testing machine by ASTM D 785 std., the sample size of 25mm*25mm*6mm was prepared for different compositions. Rockwell hardness tests were performed to find out how the particle volume fraction affected the matrix hardness, Initially, the specimen surface was polished to a smooth finish. Tests were performed at a different place for each specimen, As per the Rockwell scale HRH test standard, Fast testing times and a clear presentation of the Rockwell hardness number are two benefits of the Rockwell hardness method [75].

Figure 3.12 Digital Rockwell Hardness tester Beijing United Test CO., LTD.,

Figure 3 13 (A) Hardness test for commercial brake pad and (B) produced brake pad sample

3.4.2 Impact testing

Using the ASTM D 256 standard, the Charpy test was performed at room temperature to ascertain the impact resistance of the created hybrid nanocomposite. From the sample, a geometric size of 64.5 x 12.5 x 5 mm was carved. Every sample had a 2 mm deep mark in the middle, across from the impact area. To evaluate the composite's fracture toughness, an impact test is conducted. The composition of the component materials has a significant impact on the impact qualities of the composite material and is directly connected to its overall toughness. Equation 7 below was utilized to calculate the energy absorption based on the average value obtained, which was 6.7 m/s for the testing equipment. [75].

$$IS= \frac{AE}{WT} \qquad (7)$$

Where: W- is the remaining width at the notch (m),

T -is the specimen thickness (m),

AE- is absorbed energy (Joule), and

IS- is impact strength (KJ/m^2).

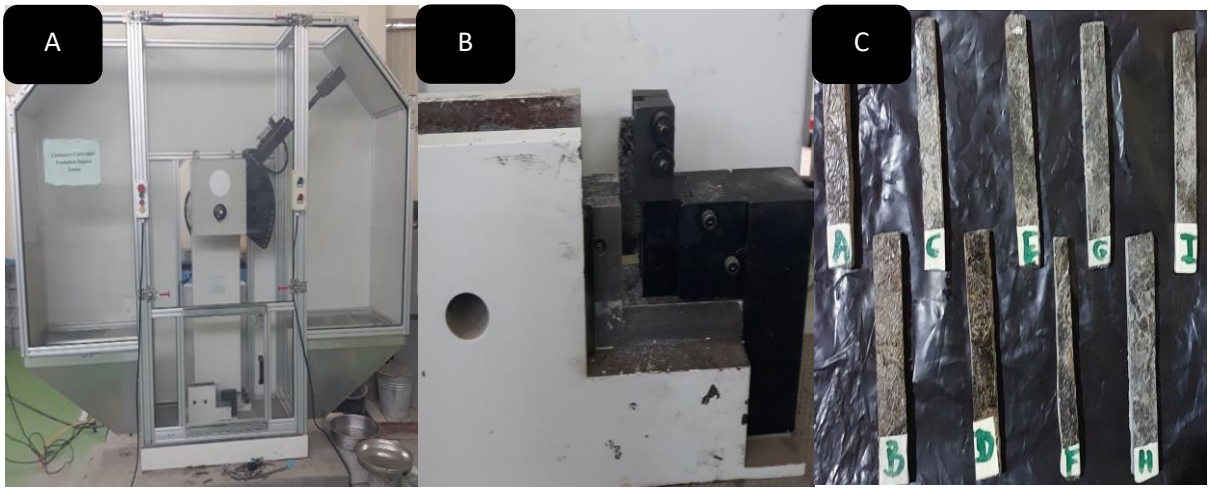

Figure 3.14 (a) Impact testing system (b) Mounting samples (c) samples for Impact test

3.4.3 Wear rate testing

Using the pin-on-disc technique, the specific wear rate and coefficient of friction were determined at room temperature and under dry circumstances. The pressure actuator moved the sample that was secured in the holder horizontally until it came into contact with the revolving disk. A sample with a geometric dimension of 4 mm by 12 mm thickness was cut, and the wear characteristics of a composite were measured as a function of volume fractions at different speeds of 400 rpm and 600 rpm using a pin-on-disk wear testing equipment by ASTM G-99 standards. To weigh the sample brake pads, a digital electronic balance with an accuracy of 0.01 g was utilized. Sample wear loss is measured as the difference between the sample's starting weight and final weight. The friction coefficient's stability and a convincing SWR were obtained over long distances. The potential of the wear mechanisms is examined in light of the studied wear properties [76].

It is predicted that SWR will be more accurate than volumetric wear because it was calculated by dividing the wear volume by the contact force and the sample sliding distance. Rajan et al. found that the formula for calculating SWR is mathematically shown in Equation 8 [10].

$$SWR=\frac{\Delta V}{Ld} \quad \ldots\ldots\ldots\ldots\ldots\ldots(8)$$

Where: SWR stands for specific wear rate.

ΔV the material worn volume (mm^3),

d the sliding distance (m), and

L the contact load (N).

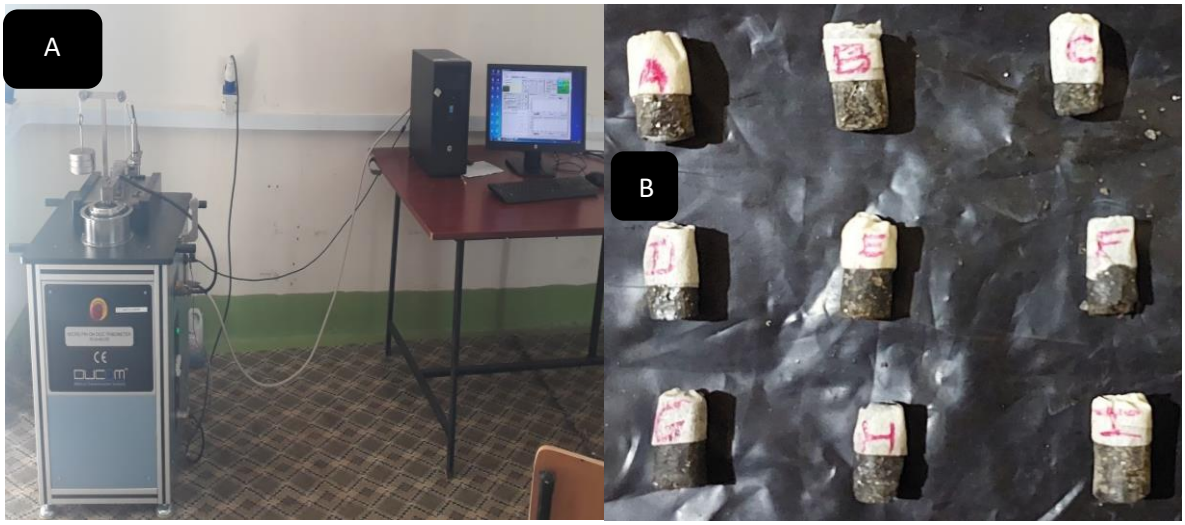

Figure 3.15 (A) Wear test with Micro pin on disk tribometer DUCOM^{TM} (B) testing Samples

3.4.4 Coefficient of Friction Testing

Data acquisition was employed to record the frictional forces that existed between the sample's surface and the disc's surface. To conduct the friction test, the procedure was repeated five times. By dividing the normal force by the friction force, one can find the friction coefficient. This was expressed mathematically as follows in Equation 9 below [10].

$$\mu=\frac{fs}{FN} \quad \text{.....(9)}$$

where: μ=friction coefficient,

fs= frictional force

FN= normal load acting on the specimen in Newton

Equations 9 above were utilized to determine the sample's coefficient of friction, with test parameters of 30 N of friction force and 0.7 m/s disc sliding speed affecting the sample friction material's coefficient of friction. The mass loss is converted into volume loss using the sample density information. [10]

3.4.5 Density results for water absorption samples

Weighing the samples with an electronic scale with 0.01 precision allowed us to determine their mass as shown in Figure 3.16 below. Archimedes' principle was used to measure the density of the composite samples. Table 3.4 below displays the findings for the samples' computed densities for the water absorption testing samples using the Archimedes principle. Density values were in between the range of 1.1225 and 1.3172g/cm^3.

Notice:1ml~1g/cm^3

Table 3 4 samples' measured densities.

Samples	Mass (g)	Volume (cm^3)	Density (g/cm3)
Commercial	7.4057	5	1.4811
SA	4.4951	4	1.1237
SB	2.6344	2	1.3172
SC	4.0679	3.5	1.1622
SD	3.6107	3	1.2035
SE	4.5471	3.5	1.2991
SF	4.4902	4	1.1225
SG	4.6292	4	1.1573
SH	3.4815	3	1.1605
SI	3.7827	3	1.2609

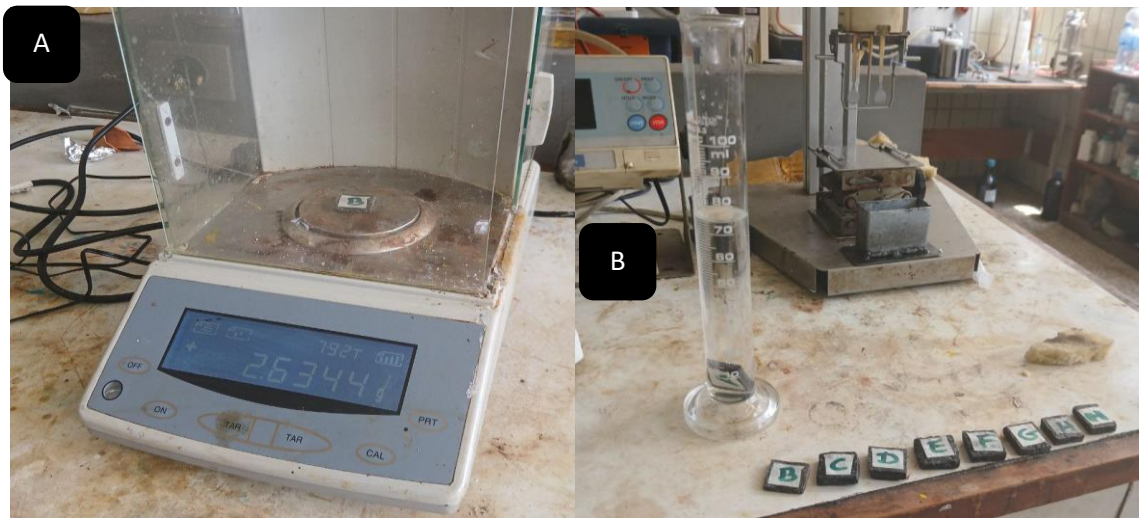

Figure 3.16(A) Weighing water absorption samples and (B) Measuring its densities.

3.4.6 Water and Oil Absorption Testing

The water bath method (ASTM D 570 standard) was used for water absorption investigations. With a size of 50.8mm diameter if circular, or 50.8mm per side if square in shape. The thickness of the specimen must be either 3.175 mm or 6.35 mm. After being weighed to within 0.001 g, the dry specimens were submerged in distilled water. The new weight is noted as W_1. Each sample piece is analyzed. For visualization and discussion, the average of these samples was utilized. Equation. 10 is used to calculate the water absorption percentage [6].

$$P_{WA} = \frac{W_1 - W_o}{W_o} * 100 \ldots\ldots\ldots\ldots\ldots\ldots\ldots\ldots (10)$$

Where: PWA = Percentage of water absorption,

Wo=Initial weight of water sample

W_1=The final weight of the water sample

After being immersed in motor oil, the samples were kept at room temperature for a whole day. The SAE 40 rating is applied to the used car engine oil. A sample is then dried and weighed one more after that. O_1 was the new weight that was noted. The samples from each designed brake pad compute the absorption percentages. For discussions and graphical representations, the recorded samples were used. Equation 11 below may be used to obtain the oil absorption percentage. [6].

$$P_{OA=} \frac{WO_1 - WO_o}{WO_o} * 100 \ldots\ldots\ldots\ldots\ldots\ldots (11)$$

Where: WO_0 = Oil sample beginning weight;

WO_1 = Oil sample end weight;

PO_A = Percentage of oil absorption;

Figure 3.17 (A) Oil absorption test samples and (B) Water absorption test samples

3.4.7 Testing For Microstructural Analysis

The Natural Hybrid of flax fiber and eggshell with MWCNTs and Al3O2 composite morphology was examined using the SEM test. Following wear testing, the sample needed to be polished using various glass papers (abrasive paper), and measurements were collected at 20 µm (X1000), 50 µm (X600), and100 µm (X300) as shown in Figure 3.18 below.

Figure 3.18 SEM analysis Specimens after wear rate test

3.5 Modeling of Natural Fibers Hybrid Nanomaterials for brake pad

The finite element analysis (FEA) method is a numerical method for resolving engineering issues. It's The most effective analytical tool for both simple and complex problems. A finite element model must be developed with the appropriate dimensions, loads, constraints, (element and mesh selection), and other characteristics. An ANSYS model may be built in one of two ways: either by designing in SOLIDWORKS and then importing the file into ANSYS for setup and analysis or by constructing the model using ANSYS's internal drawing capabilities; however, as ANSYS' modeling features are inferior to those of competing CAD applications, we used SOLIDWORKS 2023 and ANSYS 2024 editions for compatibility issues. The next stage was modeling the natural fibers hybrid with MWCNTs and Al3O2 composite for brake pad application by obtaining the necessary data Without the presence of thermal characteristics, then the disc-pad model was subjected to the first analysis was how functions structurally in terms of deformation and Von-Mises stress. Finally, In the same model, the scenario of thermo-elasticity with convection, adiabatic, and heat flux factors included was also examined. Results of the temperature distribution, deformation, stress, and contact pressure predictions are shown. Moreover, a comparison was made between the structural performances of the mechanical and thermomechanical studies as shown in Figure 3.19 below.

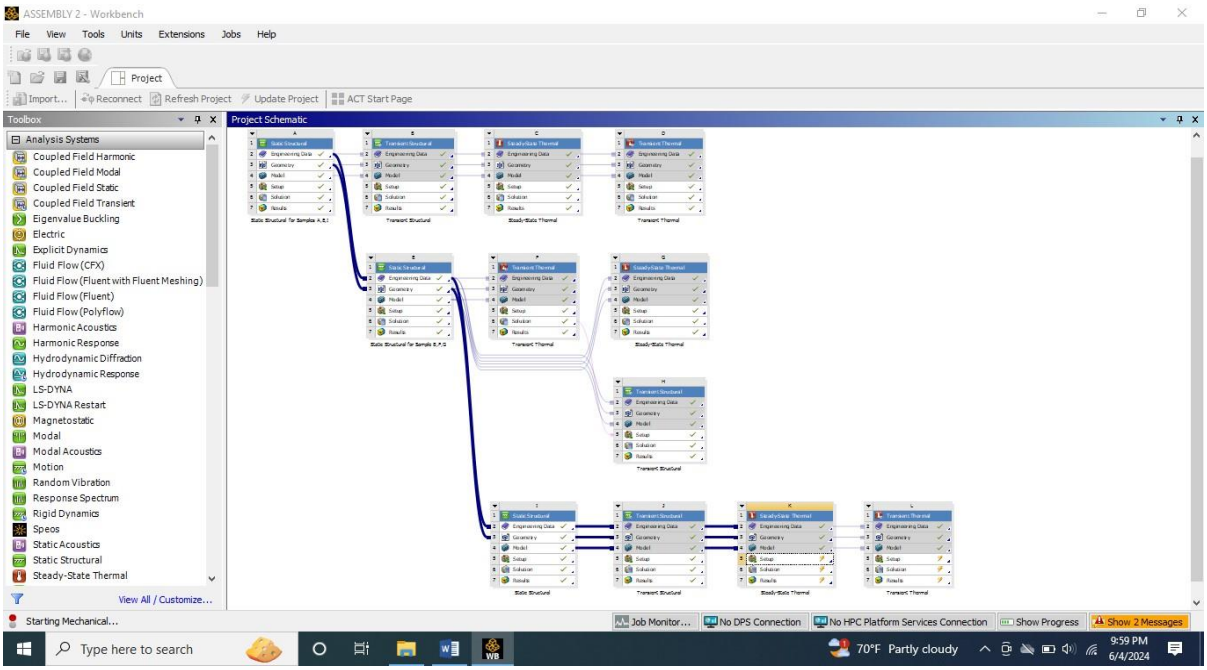

Figure 3.19 ANSYS Workbench's analysis tab

3.5.1 Disk material for brake pad composites

Disc Brake has long been made of gray cast iron because of its strength, durability, wear resistance, heat absorption, thermal conductivity, vibration damping capacity, and reasonable pricing. Throughout this thesis, the compositions of the brake pad materials are designed accordingly to examine variations in braking performance. The FEA material properties for the gray cast iron component are enumerated as shown in Table 3.5 below. (ANSYS 2024 Software version).

Table 3.5 The material properties of gray cast iron used in the FEA (ANSYS 2024)

Disk Component	**Gray Cast Iron**
Mass Density (g/m^3)	7.25
Elastic Modulus (Gpa)	100
Poission Ratio	0.27
Bulk Modulus (Gpa)	72.46
Shear Modulus(Gpa)	39.37
Specific Heat constant pressure($J/Kg^{-1}C^{-1}$)	447
Melting temperature (^oc)	1200
Coefficient of thermal expansion ($1/^oc$)	$1.1*10^{-5}$
Thermal conductivity (λ)$Wm^{-1}K^{-1}$	52

3.5.2 Define Engineering Data

The Engineering Data for representative volume element (RVE) of Natural Hybrid of flax fiber/eggshell with MWCNTs/Al3O2 and polyester resin composites appropriate values are from the experimental results and other Engineering sources as an input to the ANSYS Workbench's analysis tab. Compressive load, Elastic modulus, Poisson's ratio, Density values, and other load conditions are specified as maximum values, Both the load and boundary conditions must be defined to obtain an accurate static structural, transient structural, and transient thermal analysis for the application. A. Belhochine et al., concluded that Shear stresses resulting from friction at this level are the source of this phenomenon in the case of friction, which occurs at the contact surface. Friction conditions encompass the characteristics that impact the quality and flexibility of the generated samples. Friction-related changes might alter the distribution of stress and strain [77].

The input parameters for the FEA techniques are a pressure of 1MPa on both the brake pads, a rotational velocity and a moment of 100 rad/s and 393N-mm respectively on disk brake (Gray Cast Iron), and fixed supports at 5 bolted holes. The disc is tightly restricted in all directions except for rotation at the bolt holes. To allow the pads to move up and down and into contact with the disc surface, the pad remains stationary at the junction in all degrees of freedom other than the typical direction. At the point of contact, the coefficient of friction (μ) is 0.3 for student version software (ANSYS 2024 Software version).

Table 3.6 Design characteristics of the disc and brake pads

Engineering Figures	**Pad**	**Disk**
Volume (mm^3)	17379 mm^3	2.4227e+005 mm^3
Mass (kg)	2.282e-002 kg	1.7564 kg
Nodes	668	32972
Elements	80	16941
Inertia moment Ip1	3.0216 kg·mm^2	3504.9 kg·mm^2
Inertia moment Ip2	14.437 kg·mm^2	3451. kg·mm^2
Inertia moment Ip3	17.364 kg·mm^2	6881.9 kg·mm^2

3.5.3 Mesh Controls For Pads and Disk Assembly

As seen in Figure 3.20 (B) below, a vented disk and two pads comprise a three-dimensional FEA model used in this work. Figure 3.21 depicts the contact zone between the pad and disc, while Table 3.6 above provides information on the mesh qualities. Between disc-pad interfaces, a frictional contact

pair was established. The meshing process separates the complex geometry model into smaller components that can be solved in a case where the model would otherwise be too complex. FEA includes solid modeling as one of its components. Therefore, the only goal of solid modeling is to efficiently and comfortably generate the geometry's mesh. The element type specification comes first, then comes the meshing process. The core concept of FEAs is the analysis of the structure assembly of discrete parts, called elements, connected at a finite number of points, called nodes. As a result, it has 34,308 nodes and 17,101 elements for the assembly model in this thesis. (ANSYS 2024 Software version).

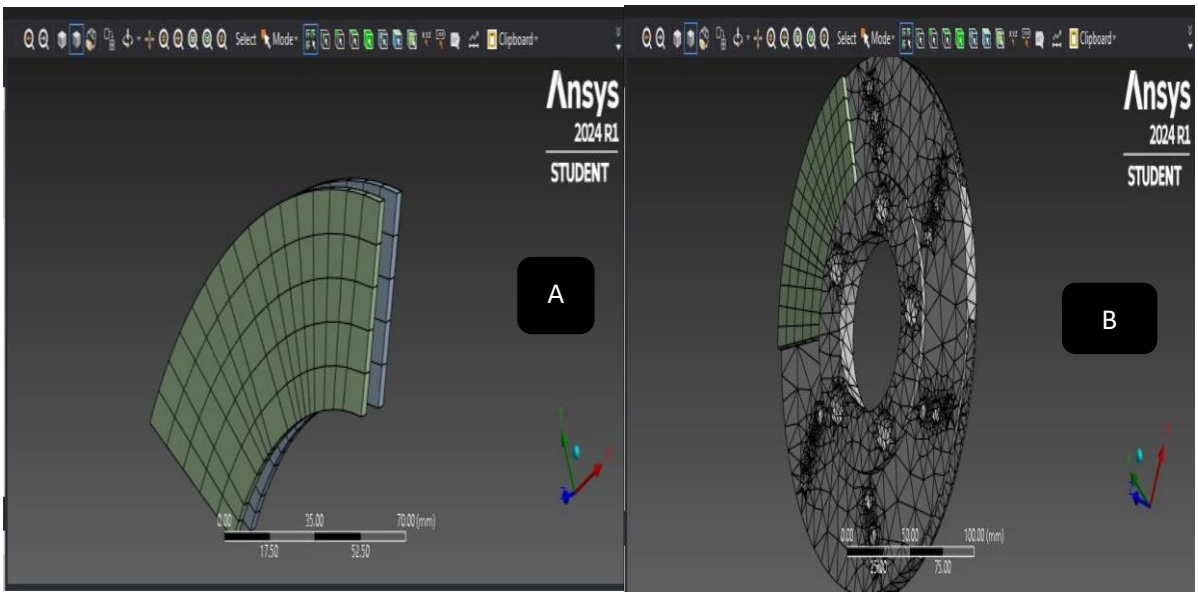

Figure 3.20 (A) Meshing of brake pad and (B) disk brake assembly by ANSYS

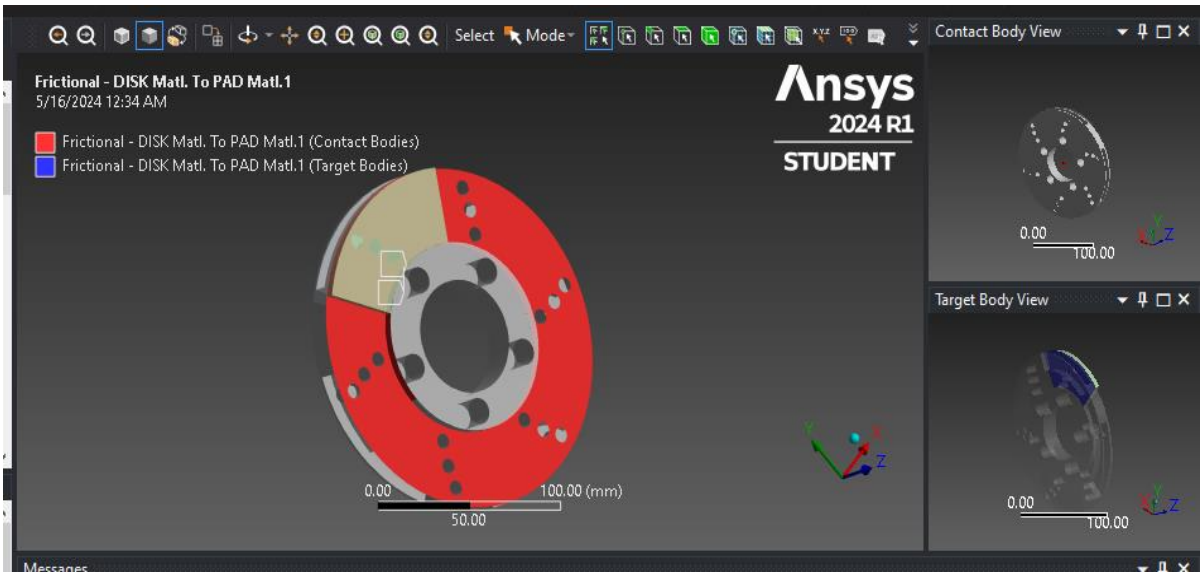

Figure 3.21 Contact zone of the disc and pad

3.5.4 Thermal boundary conditions

Thermal boundary criteria and initial conditions must be established to express the heat transfer in the disc brake model. To determine the contact temperature distribution on the brake's working surface, a mathematical model is used. A transient finite element technique is first utilized to define the temperature fields of the solid rotor with suitable thermal boundary conditions to take into account the impacts of the moving heat source (the brake pad) with relative sliding speed variation. The rate of heat dissipation via friction must be considered when calculating heat generation due to friction. All of this has to do with figuring out how much friction force and how much effort it produces [77]. The heat flux entering the disc from its two sides, as seen in Figure 3.22, defines the thermal loading.The ANSYS workbench module receives the initial and boundary conditions. By selecting the temporary state, the thermal calculation will be performed. The starting temperature is assumed to be 22 ºC, and the max temperature is 1200 ºC the convection coefficient is 9.04e-^{05} W/mm^2 ºC. On the disc and brake pad's non-touching surfaces, convection is available. The disc-to-air radiation is disregarded.

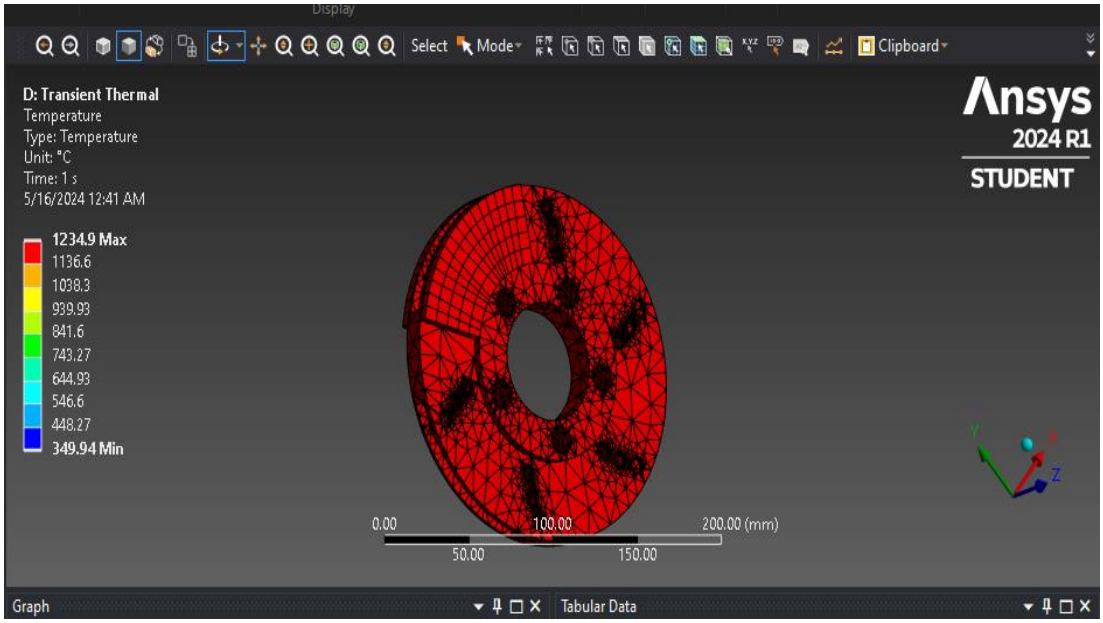

Figure 3.22 Boundary condition for thermal analysis of the pad-disc brake

3.5.5 Simulations of Brake Pad and Disk Assemblies

The braking temperature, which is produced during operation by the friction between the brake pad and disc, has a significant impact on brake performance and is essential for maximizing the wear resistance of automobile brake pads. The following are a few examples of dry contact phenomena that are impacted by brake operating parameters: brake interface temperature, applied pressure, and speed. The way brake pads and a car disc interact is described by the material characteristics of the friction pair at a specific moment in time. The heat equations were formulated using various factors such as

the vehicle velocity, the time the brake was applied, the geometry and dimensions of the brake components, the disk brake rotor materials, and the contact pressure distribution of the pad. The results show that thermal resistance caused by wear particles accumulating in the space between the contact surfaces results in the formation of a heat partition at the point where two sliding components come into contact. The brake lining gets hot due to this condition, which stops the discs from absorbing more heat. As a result, the braking fluid absorbs more heat and is more likely to evaporate [78].

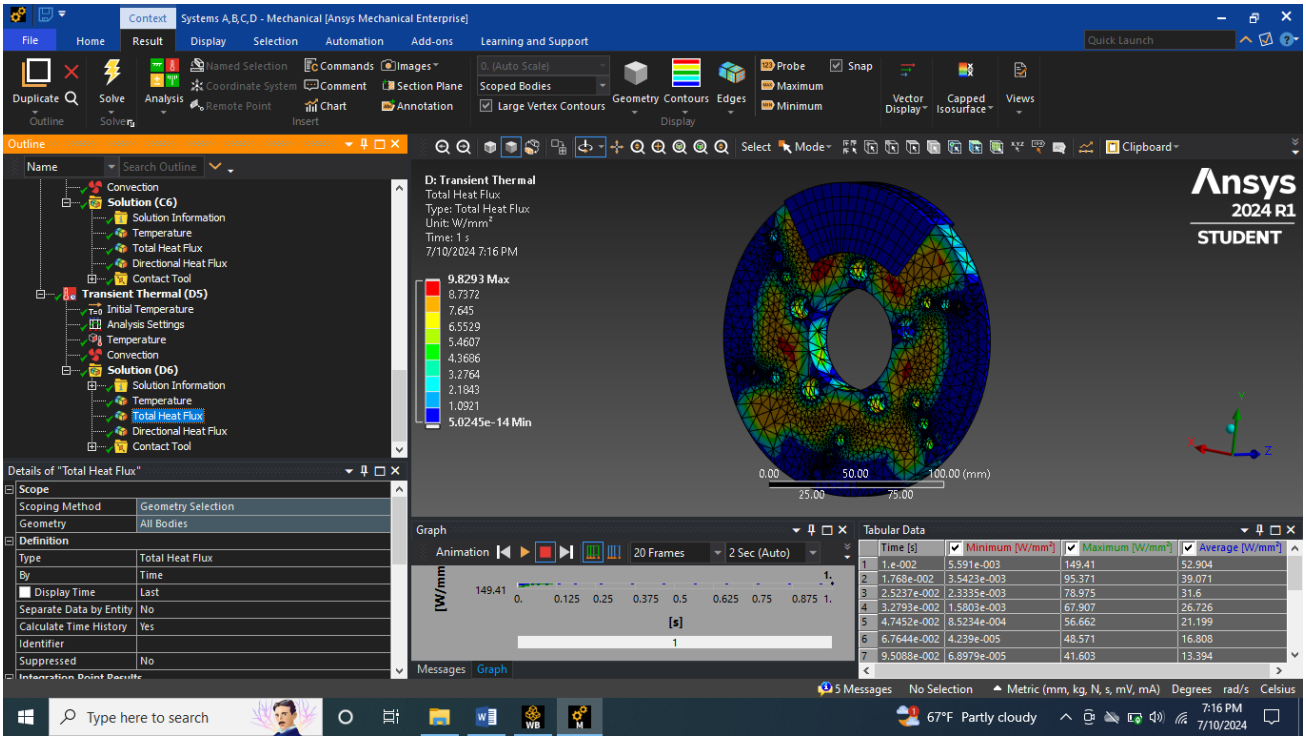

Figure 3 23 Transient thermal (total heat flux) analysis of the pad-disc brake

Chapter Four

4. Result and Discussion

4.1 Experimental results

4.1.1 Hardness results

The commercial brake pad measured hardness value was 76.0 from the commercial brake pad experimental test. The Rockwell Hardness HRH scales for samples tested were tabulated in Table 4.1 below. The maximum result was obtained on specimens SE which is 73.1.

Figure 4.1 Hardness properties of hybrid nanocomposite and commercial brake pad

Samples	Hardness (HRH-Scale) Kg/mm	Density (g/cm^3)
Commercial Pad	75	1.4811
SA	49.8	1.1237
SB	65.0	1.3172
SC	55.0	1.1622
SD	60.4	1.2035
SE	73.1	1.2991
SF	48.5	1.1225
SG	51.4	1.1573
SH	54.4	1.1605
SI	63.1	1.2609

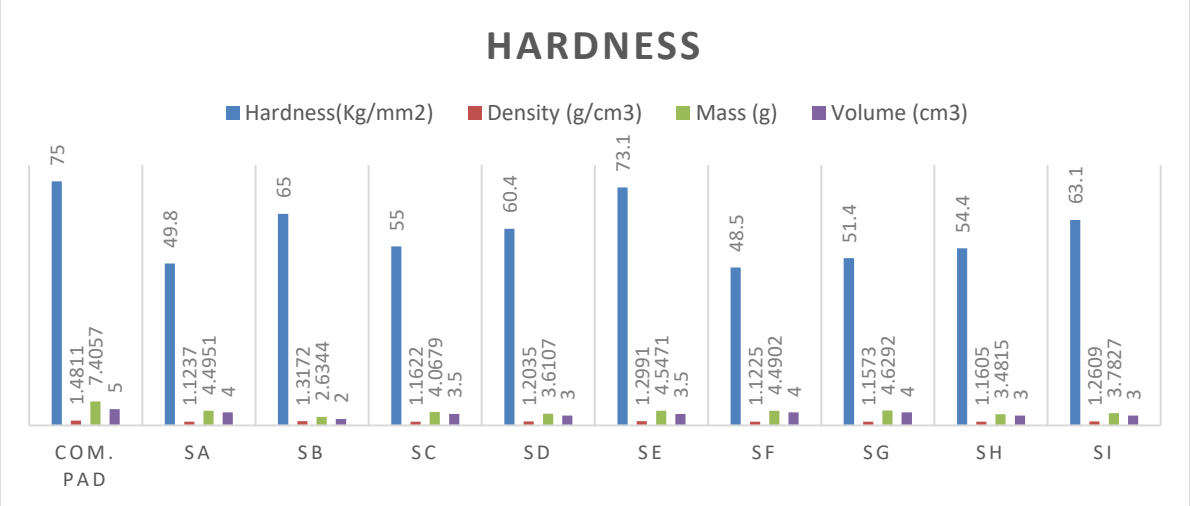

Figure 4.2 Graph of Hardness for samples tested

4.2.2 Impact Test Results

The results of the test indicated that the composite appeared to have an impact strength on hybrid composite sample SE 3.3KJ/mm^2. The good resistance to crack propagation during an impact test was also attributed to the excellent bonding between the matrix and reinforcement.

Table 4.1 Impact strength of the hybrid nano nanocomposite for the samples

Samples	**Impact strength (KJ/mm^2)**	**Area (mm^2)**	**Absorbed energy (KJ)**
Commercial Pad	3.3	62.5	0.20
SA	4.8	62.5	0.30
SB	3.7	62.5	0.23
SC	4.6	62.5	0.28
SD	3.7	62.5	0.23
SE	3.3	62.5	0.20
SF	4.8	62.5	0.30
SG	4.6	62.5	0.28
SH	4.6	62.5	0.28
SI	3.7	62.5	0.23

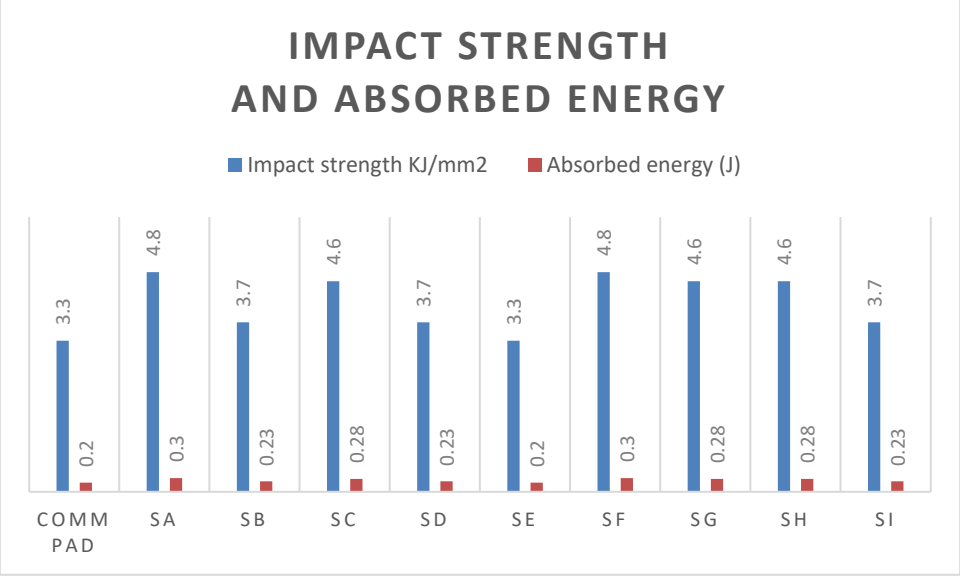

Figure 4.3 Graph of impact strength and absorbed energy for samples tested

4.2.3 Results for Wear Rate and Coefficient of Friction

Processing the data from the pin-on-disk test equipment allowed the wear rate and friction coefficient values to be determined using the previously mentioned calculations. Sample wear loss is measured as the difference between the sample's starting weight and final weight. Table 4.2 and Figure 4.4 below show the mass of the wear before and after and the wear rate in milligrams per minute. The variation in wear and coefficient of friction for newly formulated brake pads were studied.

Table 4.2 shows the mass of the wear before and after and the wear rate in grams per minute.

Sample code	Mass Before (g)	Mass After (g)	Wear loss (g)	Time in (min)	Rate of wear (mg/min)	Specific wear rate (mm^3/Nm)	COF	Density (g/cm3)
SA	0.4361	0.4279	0.0082	30	0.00027	$3.1x10^{-7}$	0.64	1.1237
SB	0.4578	0.4185	0.0393	30	0.00013	$1.4 x10^{-6}$	0.38	1.3172
SC	0.4315	0.4095	0.022	30	0.00073	$8.3x10^{-7}$	0.62	1.1622
SD	0.4947	0.4765	0.0182	30	0.00060	$6.8x10^{-7}$	0.57	1.2035
SE	0.5286	0.5184	0.0102	30	0.00034	$3.8x10^{-7}$	0.62	1.2991
SF	0.4838	0.4612	0.0226	30	0.00075	$8.5x10^{-7}$	0.63	1.1225
SG	0.4554	0.4529	0.0025	30	0.00001	$9.4x10^{-8}$	0.46	1.1573
SH	0.4128	0.3735	0.0393	30	0.00013	$1.4x10^{-6}$	0.38	1.1605
SI	0.4628	0.4624	0.0004	30	0.00001	$1.5x10^{-8}$	0.43	1.2609

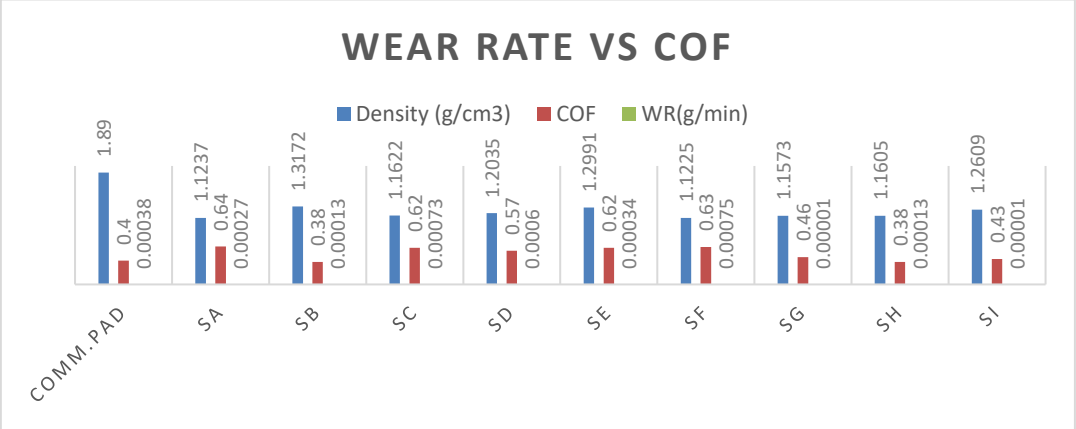

Figure 4.4 Graph of wear rate and COF for samples tested

4.2.4 Water and Oil Absorption

The samples for water and oil were weighed and maintained at ambient temperature for 24 hours in separate containers of water and engine oil, respectively. During the immersion, the pads were removed from both the oil and the water. The difference in mass when they were weighted revealed how much water and oil had been absorbed. Table 4.4 and Figure 4.5 shows the percentage of water and oil absorbed by each sample.

Table 4.3 Water and oil absorption of hybrid nanocomposite and commercial brake pad

Samples	Water (%)	Oil (%)	Density (g/cm^3)
Commercial pad	0.5	0.3	1.4811
SA	0.4	0.2	1.1237
SB	0.2	0.1	1.3172
SC	0.3	0.2	1.1622
SD	0.2	0.1	1.2035
SE	0.1	0.1	1.2991
SF	0.4	0.1	1.1225
SG	0.3	0.2	1.1573
SH	0.3	0.2	1.1605
SI	0.2	0.1	1.2609

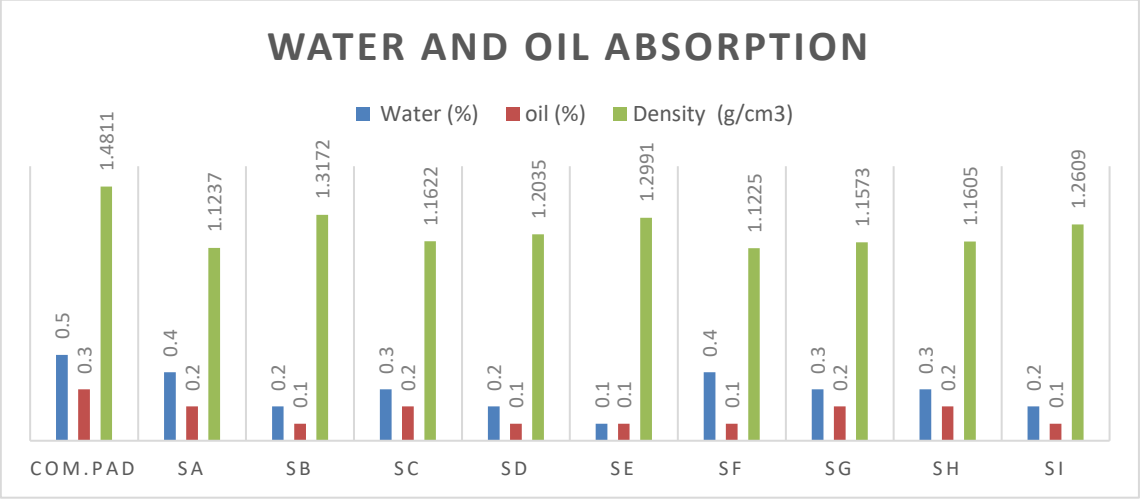

Figure 4.5 Graph of water and oil absorption for samples tested

4.2.5 Surface Morphology

SEM analysis creates a variety of signals at the surface of solid objects by utilizing a focused beam of high-energy electrons, which is used to analyze the microstructure of the samples. Information about the sample, such as its shape, composition, structure, and orientation of material, can be obtained from the signals resulting from interactions between electrons and the sample.

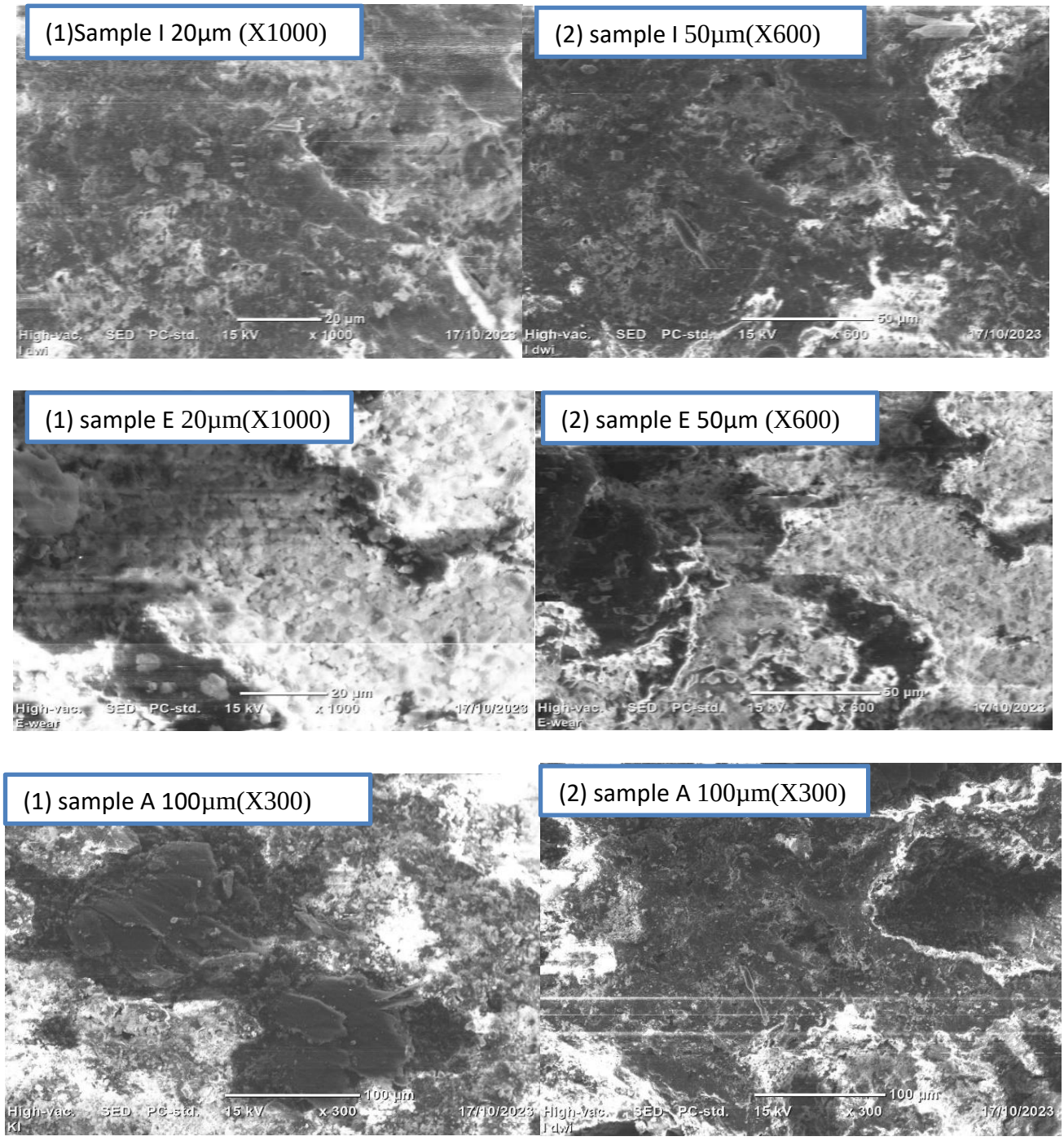

Figure 4.6 SEM samples: (1) 20µm(X1000) (2) 50µm(X600), & (3) 100µm(X300)

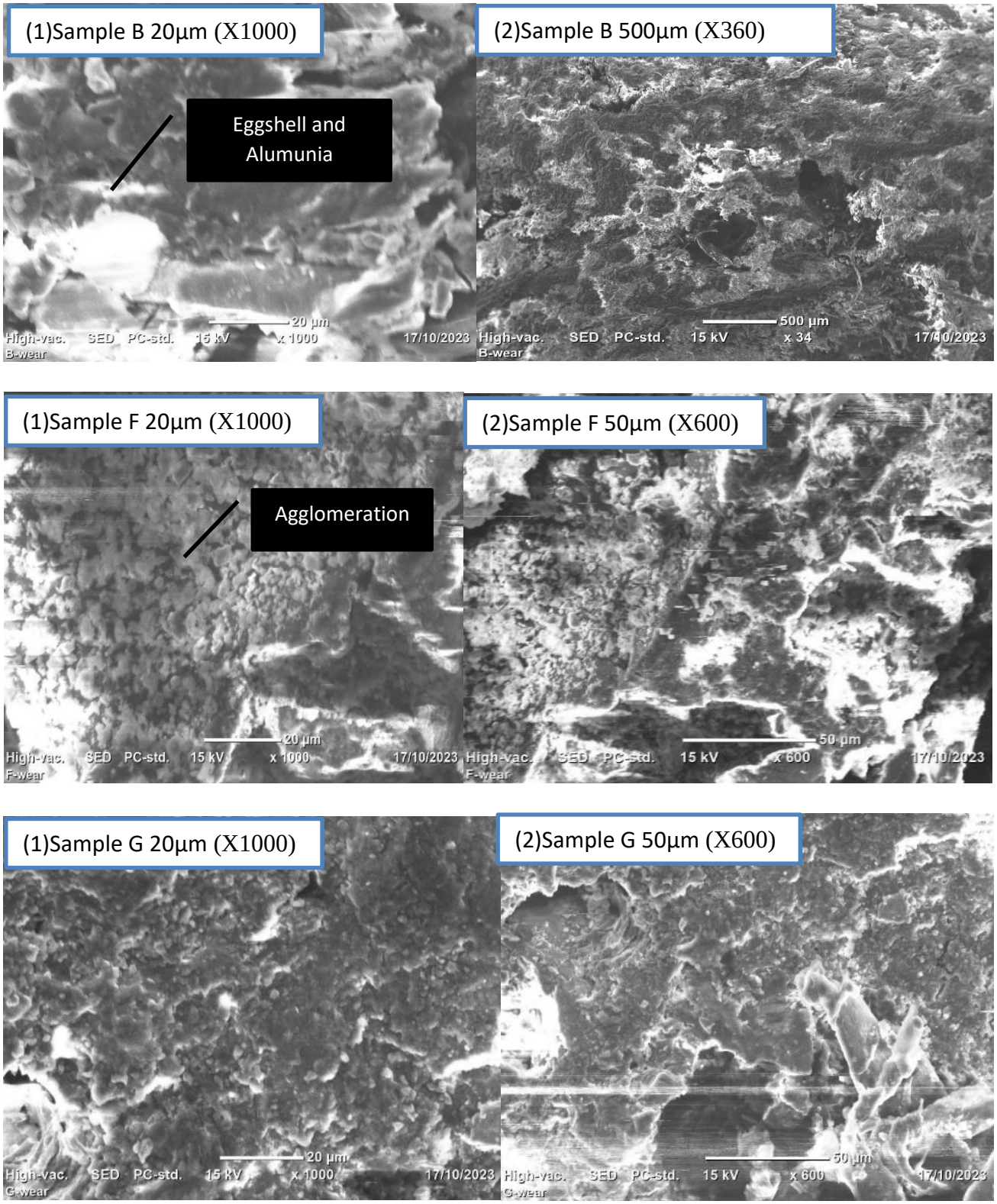

Figure 4.7 SEM samples: (a) 20µm(X1000)&(b) 50µm(X600),

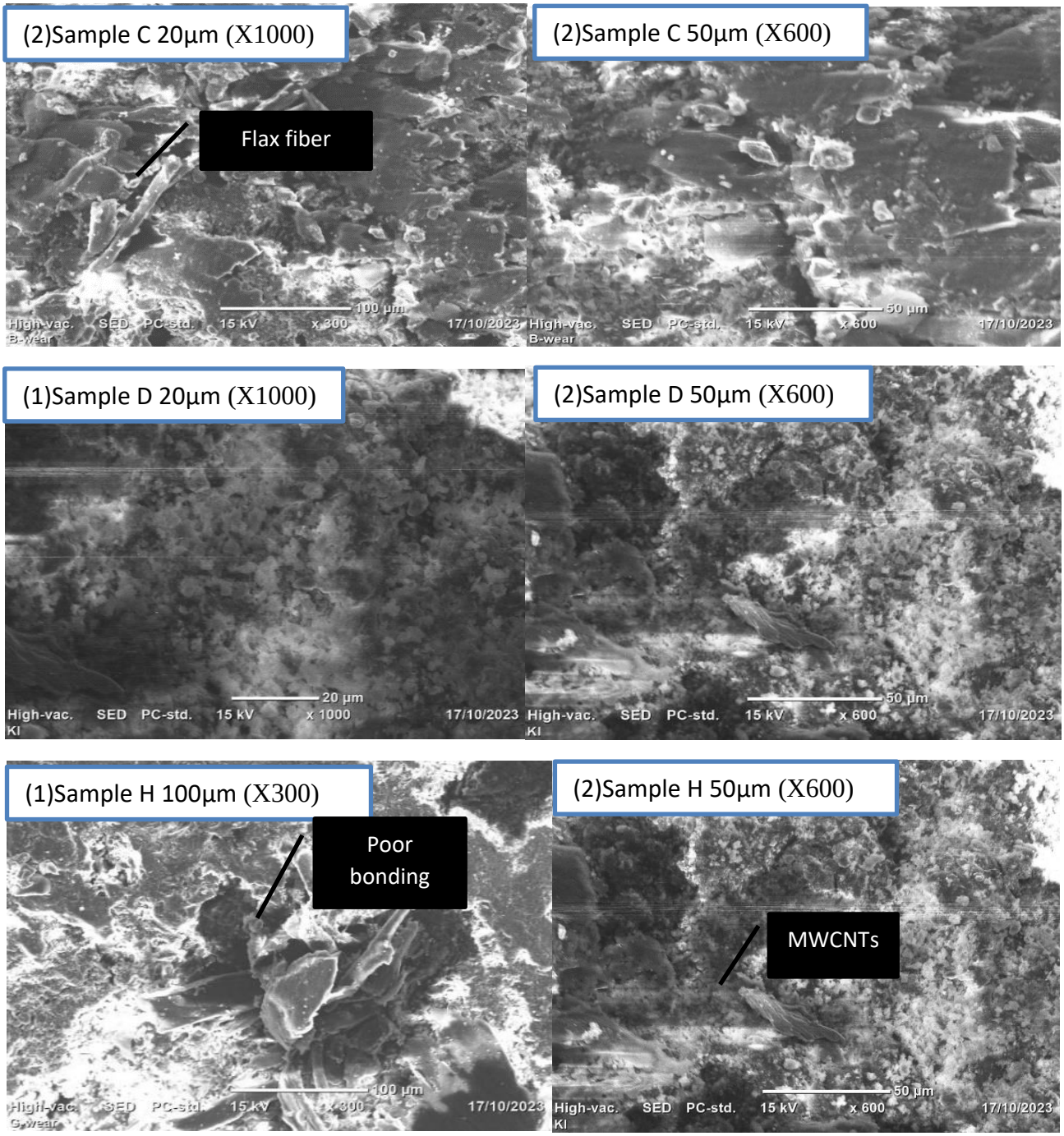

Figure 4.8 SEM samples: 100µm(X300) & (b) 50µm(X600)

4.2.6 Summary of The Surface Morphology

High-resolution images from SEM examination help assess different materials' surface topography, bonding between materials, and corrosion as well as surface fractures, defects, and voids. We performed microstructural investigations on 9 specimens, with a magnification of 20µm (X1000) 50µm (X600), and 100 µm (X300) respectively. The SEM micrograph of the specimens SG, SI, SD, SE, and SA show good bonding between the constituent particles in terms of texture, mixture, and composition; however, there is poor bonding and some micron voids on the surface and a smooth wear

track, which can be attributed to inadequate manufacturing facilities or inadequate fiber treatments with NaOH for samples SF, SC, SB, and SH the result is poor due to uneven distribution of particles and mixing ratios of additive among the constituents.

4.2.7 Result of FEM Analysis

The result is based on four major sections static structural, transient structural, steady-state thermal, and transient thermal. It is observed that a significant distortion is consistently located at the disc's outer radius, or the region that comes into contact with the pad. The largest deformation, 0.00058mm, is projected to occur at braking times t = 1s and beyond, the enormous deformation is situated in the outside radius region as shown in Figure 4.9 (D) in red color. The results are elaborated as shown in Table 4.4 below.

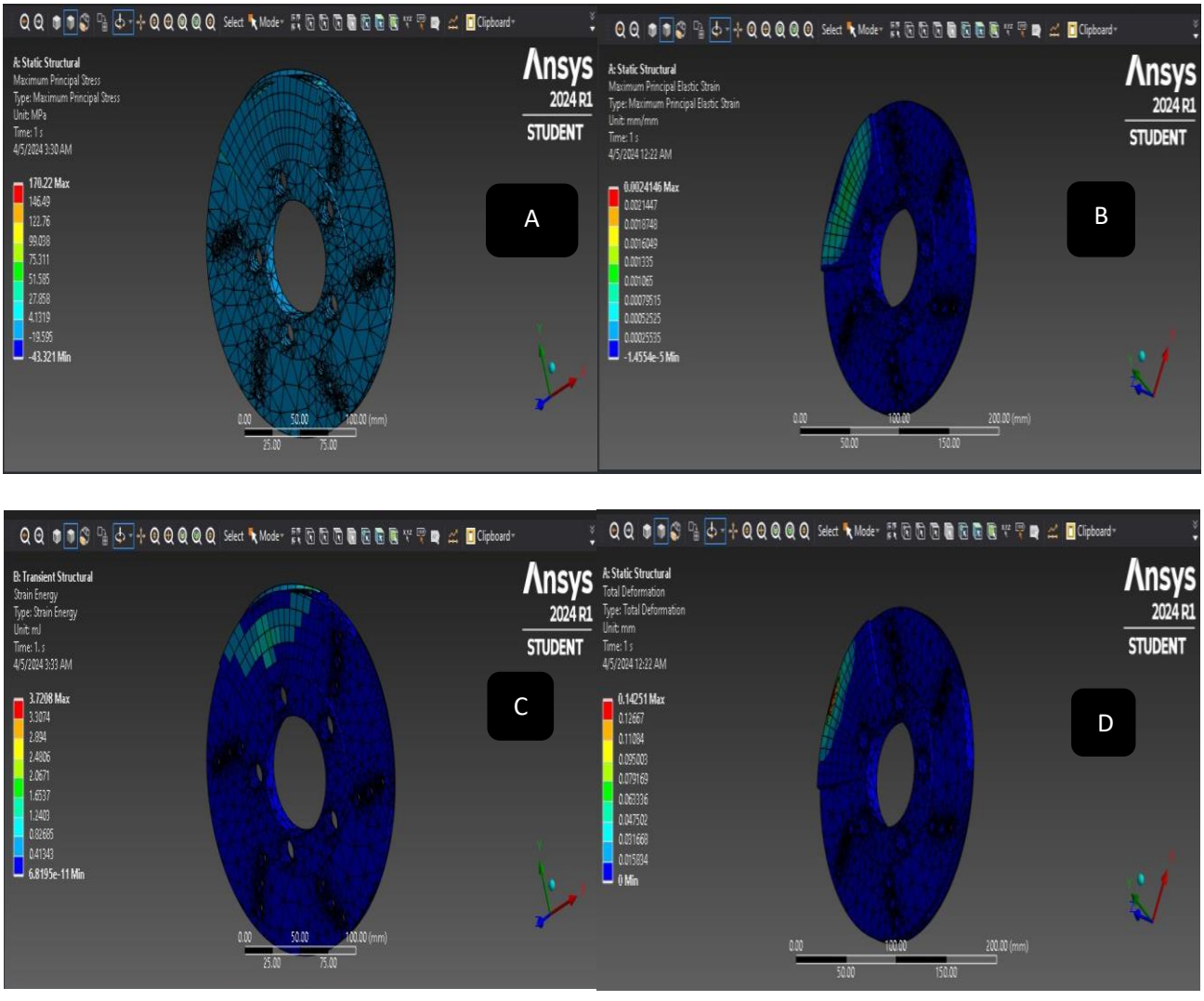

Figure 4.9 (a) maximum principal stress (b) transient structural equivalent elastic strain (c) transient structural strain energy and (d) static structural total deformation (A,E,I)

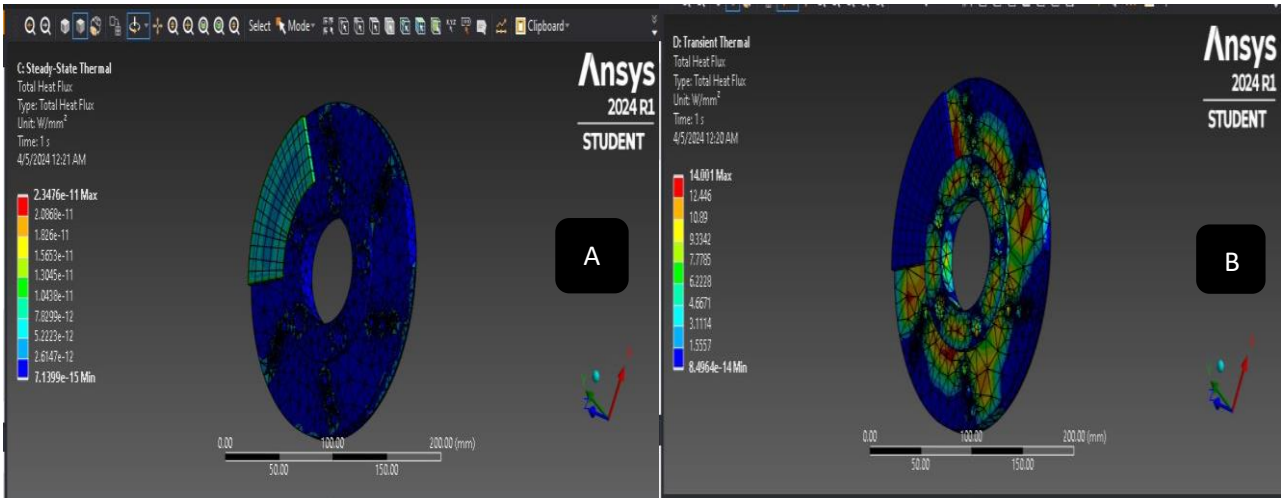

Figure 4.10 (a) Steady-state total heat flux (b) transient thermal total heat flux (A,E,I)

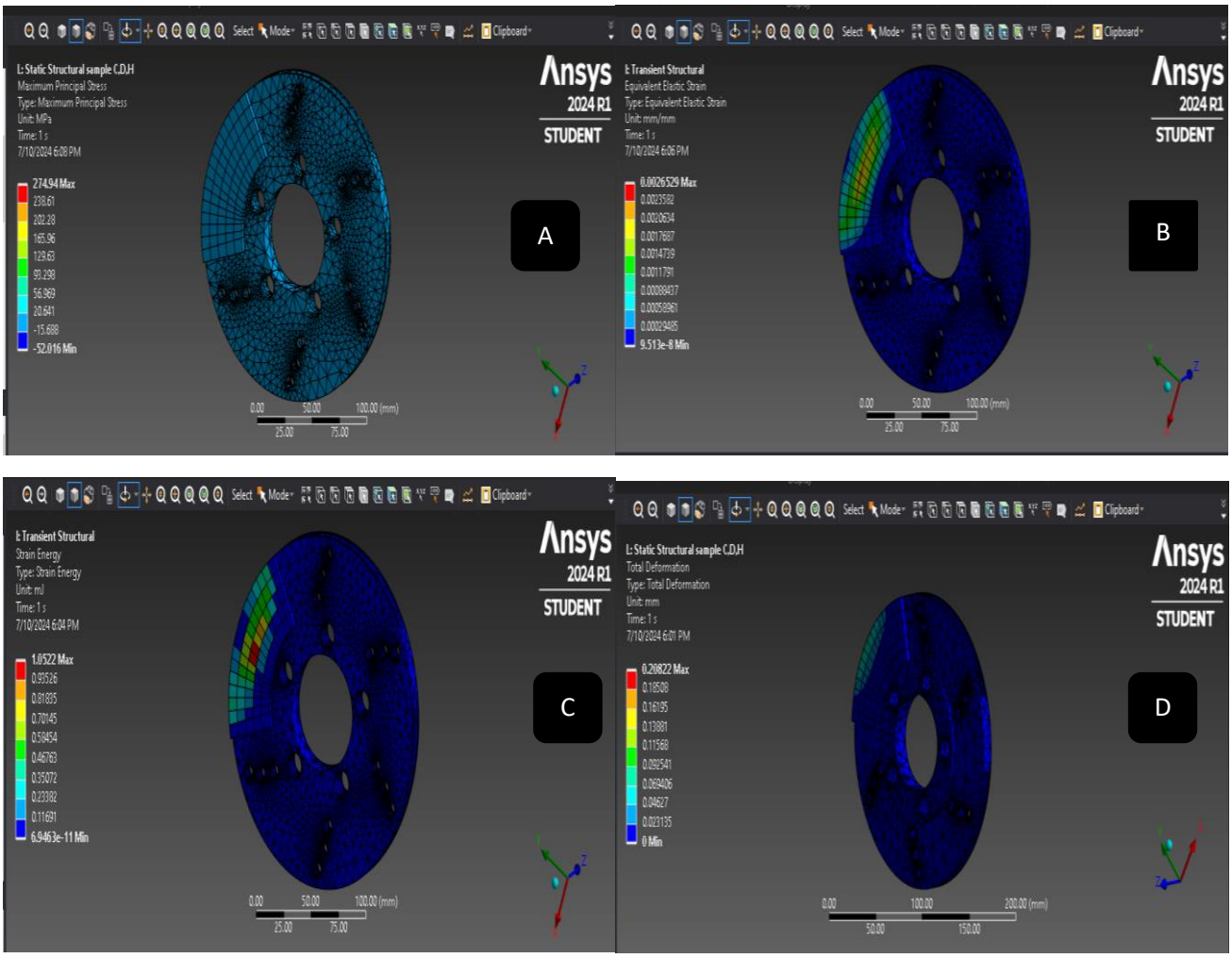

Figure 4. 11 (a) maximum principal stress (b) transient structural equivalent elastic strain (c) transient structural strain energy and (d) static structural total deformation (C,D,H)

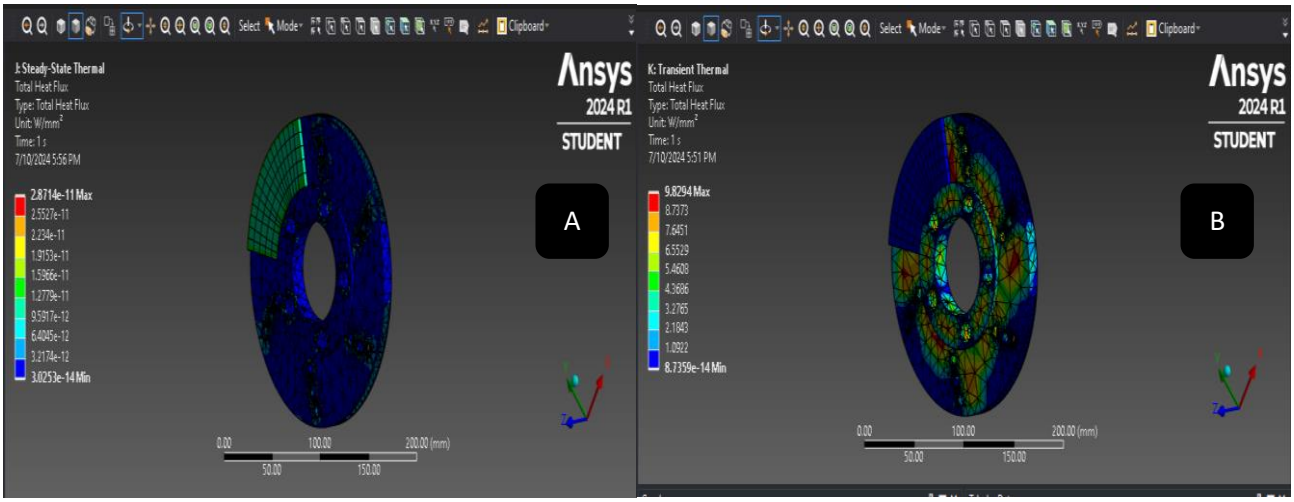

Figure 4. 12 (a) Steady-state total heat flux (b) transient thermal total heat flux (C,D,H)

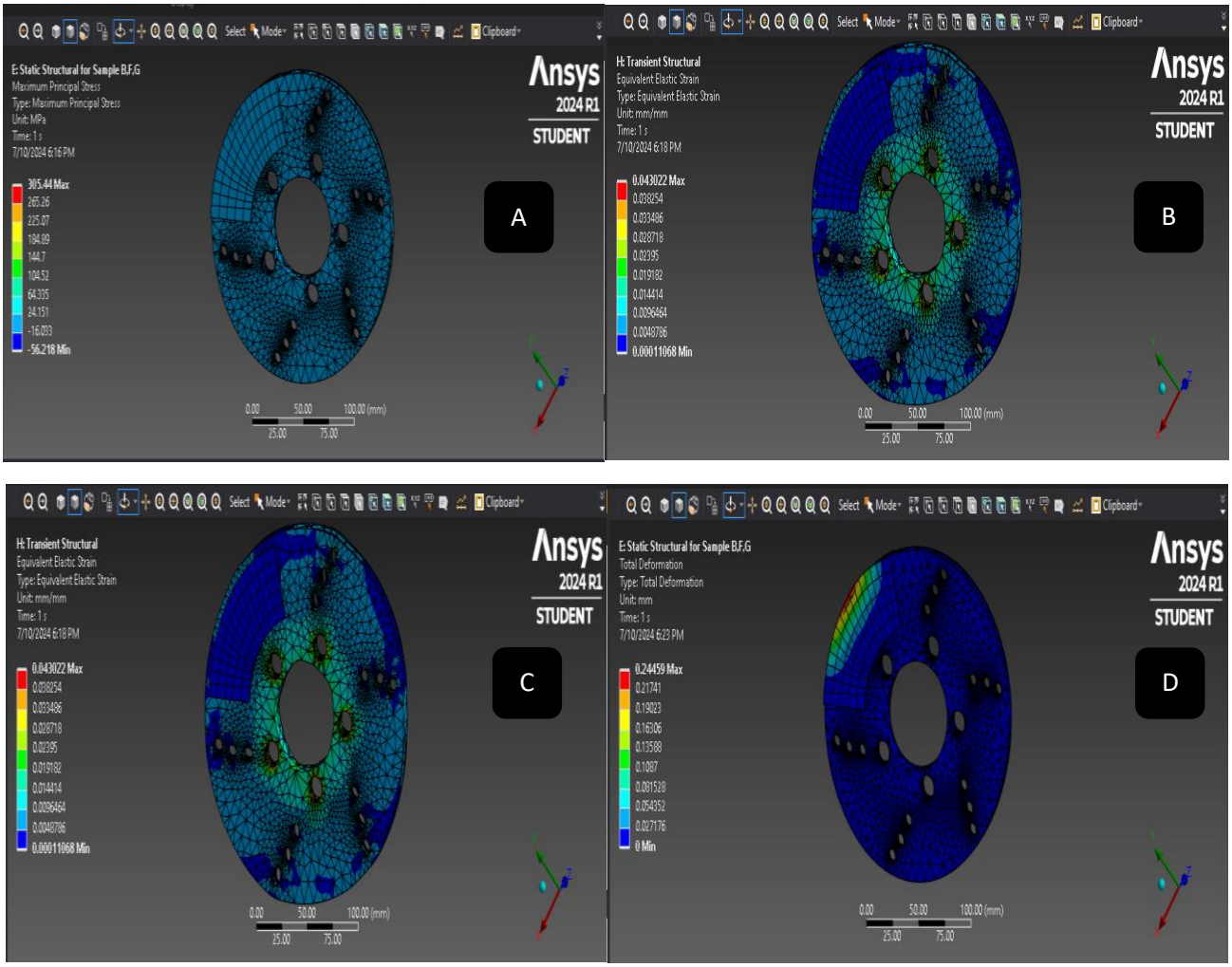

Figure 4. 13 (a) maximum principal stress (b) transient structural equivalent elastic strain (c) transient structural strain energy and (d) static structural total deformation (B,F,G)

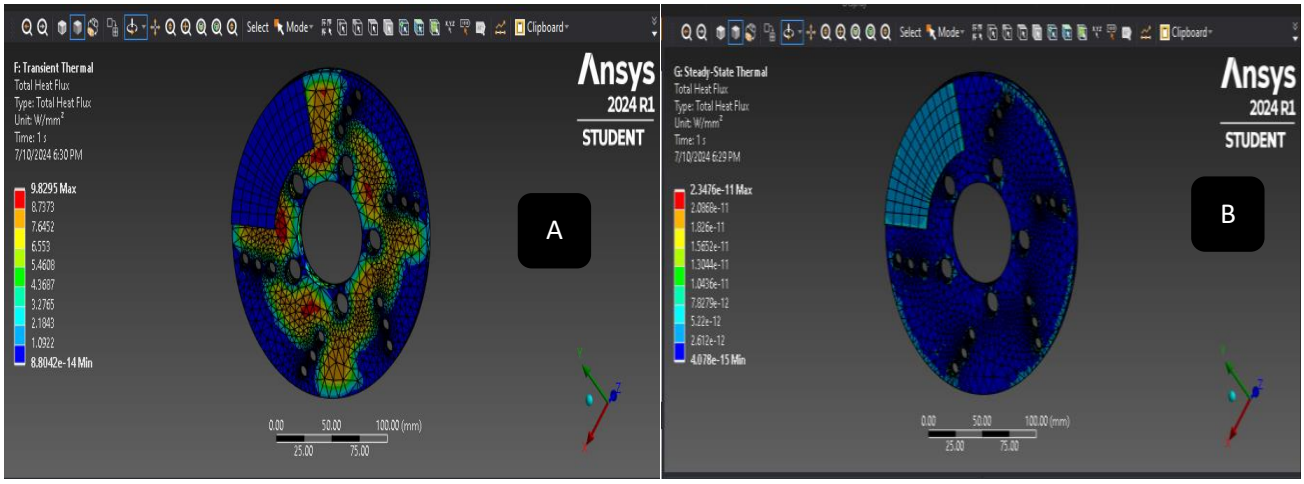

Figure 4. 14 (a) Steady-state total heat flux (b) transient thermal total heat flux (B,F,G)

The comparable equivalent elastic strain is seen to be almost evenly distributed between the pad's leading and trailing sides. The strain value is the only aspect of these strain distributions that seldom changes throughout braking time. The data indicates a progressive increase in strain, which reaches its peak of 3.77 mJ for braking times of 1 second and beyond. It is anticipated that the left side and the pad's outer radius will experience the maximum stress, while the pad's lower radius and the region closest to the groove will experience the lowest stress. In this part, the stress levels and global deformations of the model under study during the braking phase under temperature influence are determined by coupling structural and thermal analysis using ANSYS Multiphysics. The disc and pads are initially heated to 22°C. The disc's entire surface is subjected to the surface convection condition, and the two pads' surfaces are subjected to a convection coefficient (h) of 9.8293 W/mm²°C. Figure 4.11(B) illustrates how the disc and pad surface produces a relatively high-temperature minimum of 349.94°C and maximum of 1234.9 °C during a braking period of 1 second.

Table 4.4 FEM analysis results of the natural-based brake pads for sample SA, SE,&SI

Sample A,E,I	**Sub Analysis**	**Minimum**	**Maximum**	**Average**	**Occurred**
Static Structural	Total deformation (mm)	Null	0.28	5.89e-3	Disk and Pad
	Maximum principal stress (MPa)	-60.49	339.5	2.67	Disk
	Maximum principal elastic strain (mm/mm)	$-3.18e^{-5}$	$3.31e^{-3}$	$4.56e-^{5}$	Pad and Disk
	Strain energy (mJ)	$9.09e^{-11}$	0.97	87.9	Disk and Pad
Transient Structural	Total deformation(mm)	Null	0.56	$1.16e^{-2}$	Disk and Pad
	Equivalent stress (MPa)	$1.32e^{-3}$	645.7	7.98	Disk
	Equivalent elastic strain (mm/mm)	$2.35e^{-8}$	$6.47e^{-3}$	$1.53e^{-4}$	Disk
	Strain energy (mJ)	$2.76e^{-10}$	3.77	347.51	Disk and Pad
Steady-State Thermal	Temperature (^{O}C)	1200	1200	1200	Disk
	Total heat flux (W/mm^2)	$7.06e^{-15}$	$2.34e^{-11}$	$2.22\ e^{-12}$	Disk
	Directional heat flux(W/mm^2)	$-2.15e^{-11}$	$2.15e^{-11}$	$2.78\ e^{-15}$	Disk
	Heat flux on contact tool (W/mm^2)	$-8.02\ e^{-13}$	$1.02\ e^{-12}$	$1\ e^{-13}$	Pad
Transient Thermal	Temperature(^{OC})	349.94	1234.9	1143.8	Disk
	Total heat flux (W/mm^2)	$5.02e^{-14}$	9.8	2	Pad and Disk
	Directional heat flux(W/mm^2)	-8.98	9.08	$7.07e^{-3}$	Disk
	Heat flux on contact tool (W/mm2)	$-8.02\ e^{-13}$	$1.02\ e^{-12}$	$1\ e^{-13}$	Pad

Table 4. 5 FEM analysis results of the natural-based brake pads. for Sample SB, SF,&SG

Sample B, F, G	**Sub Analysis**	**Minimum**	**Maximum**	**Average**	**Occurred**
Static Structural	Total deformation (mm)	Null	0.244	5.25e-3	Disk and Pad
	Maximum principal stress (MPa)	-56.21	305.44	2.41	Disk
	Maximum principal elastic strain (mm/mm)	$-3.17e^{-6}$	$2.97e^{-3}$	$4.03e-^{5}$	Pad and Disk
	Strain energy (mJ)	$1.16e^{-10}$	1.02	76.22	Disk and Pad
Transient Structural	Total deformation (mm)	Null	0.83	0.39	Disk
	Equivalent stress (MPa)	0.37	4301.6	792.63	Pad and Disk
	Equivalent elastic strain (mm/mm)	$1.10e^{-08}$	$4.30e^{-02}$	$8.61e^{-03}$	Pad and Disk
	Strain energy (mJ)	$1.03e^{-02}$	2730.2	$7.98e^{-05}$	Disk
Steady-State Thermal	Temperature (^{O}C)	1200	1200	1200	Disk
	Total heat flux (W/mm^2)	$4.07e^{-15}$	$2.34e^{-11}$	$2.11\ e^{-12}$	Disk
	Directional heat flux(W/mm^2)	$-2.15e^{-11}$	$2.15e^{-11}$	$-5.62\ e^{-16}$	Disk
	Heat flux on contact tool (W/mm^2)	$-3.41\ e^{-12}$	$3.41\ e^{-12}$	$1.01\ e^{-13}$	Pad
Transient Thermal	Temperature(^{OC})	349.94	1234.9	1143.8	Disk
	Total heat flux (W/mm^2)	$8.80e^{-14}$	9.8	2	Pad and Disk
	Directional heat flux(W/mm^2)	-8.98	9.08	$7.07e^{-3}$	Disk
	Heat flux on contact tool (W/mm2)	$-6.01\ e^{-13}$	$1.20\ e^{-12}$	$1.12\ e^{-13}$	Pad

Table 4 6 FEM analysis results of the natural-based brake pads. for Sample SC, SD,&SH

Sample C, D, H	**Sub Analysis**	**Minimum**	**Maximum**	**Average**	**Occurred**
Static Structural	Total deformation (mm)	Null	0.208	4.61e-3	Disk and Pad
	Maximum principal stress (MPa)	-52.00	274.97	2.09	Disk
	Maximum principal elastic strain (mm/mm)	$-1.74e^{-6}$	$2.67e^{-3}$	$3.48e^{-5}$	Disk
	Strain energy (mJ)	$1.23e^{-13}$	1.05	66.44	Disk and Pad
Transient Structural	Total deformation (mm)	1.55	1.83	229.73	Pad
	Equivalent stress (MPa)	7.02e-003	264.29	3.714	Disk
	Equivalent elastic strain (mm/mm)	9.51e-008	2.65e-003	6.35e-05	Disk
	Strain energy (mJ)	$6.94e^{-011}$	1.0522	$7.98e^{-05}$	Disk and pad
Steady-State Thermal	Temperature (^{O}C)	1200	1200	1200	Disk
	Total heat flux (W/mm^2)	$3.02e^{-14}$	$2.87e^{-11}$	$3.42\ e^{-12}$	Disk
	Directional heat flux(W/mm^2)	$-1.95e^{-11}$	$1.83e^{-11}$	$2.31\ e^{-14}$	Disk
	Heat flux on contact tool (W/mm^2)	$-6.01\ e^{-13}$	$1.20\ e^{-12}$	$1.12\ e^{-13}$	Pad
Transient Thermal	Temperature(^{OC})	349.93	1234.9	1143.8	Disk
	Total heat flux (W/mm^2)	$8.73e^{-14}$	9.8	2.06	Pad and Disk
	Directional heat flux(W/mm^2)	-8.67	8.69	$9.43e^{-3}$	Disk
	Heat flux on contact tool (W/mm2)	$-6.01\ e^{-13}$	$1.20\ e^{-12}$	$1.12\ e^{-13}$	Pad

4.2.10 Summary of FEM analysis

Mechanical analysis and thermomechanical analysis were the two methods used in this work to analyze a disc-pad model. To determine its impact on the stress distribution, three-pad designs are simulated. It is clear from the forecast outcomes that:

- The FEM analysis result shows that a total deformation both on static and transient structural analysis predicts maximum and minimum values were recorded for brake pad and disk materials respectively. The largest deformation was 0.00058mm.
- A maximum and minimum values of strain energy on the pad and disk materials occur at 3.77 and 1.02 mJ respectively.
- In terms of thermal stress maximum and minimum values of total and directional heat flux both on steady-state and transient thermal analysis were 2.34e-^{11} and 1.12 e-13 respectively showing that a higher generation of total and directional heat flux occurs on disk materials over time.
- The structure and contact behavior of the disc brake unit are significantly impacted by temperature. The disc-pad model incorporating the temperature effect exhibits significant deformation and elevated contact pressure. Significant deformations happen at the disc's outer radius.
- This concludes that the pad material is worn over disk material in terms of morphological characteristics. Also, maximum and minimum principal stress (339.5 and 274.97MPa) and equivalent elastic stress (4301.6 and 264.29 MPa) occur on disk and pad materials respectively.

Table 4.7 Results that were compared to (Flax fiber and Eggshell) *[79]*, and *[80]*

Property	**Formulation For (Asbestos)**	**Formulation For (PKS)**	**Formulation For Bagasse**	**Formulation For (Flax-Fiber/ Eggshell)**
Hardness Values (HRB)	101	92.2	100.5	110
Relative Density(g/cm^3)	1.89	1.65	1.43	1.45
Coefficient Of Friction	0.30-0.40	0.44	0.42	0.62
Wear Rate (mg/m)	0.00038	0.00044	-	0.00034
Water absorption (%)	0.9	5.03	3.48	0.1
Oil absorption(%)	0.3	0.44	1.11	0.1
Toxicity	Toxic	Non-Toxic	Non-Toxic	Non-Toxic

4.2 Results Discussions

- The commercial brake pad measured a hardness value of 75.0 on the Rockwell Hardness HRH scale. The tested samples showed varying hardness values with the maximum result obtained on specimen SE at 73.1.
- The impact strength decreased with increasing fiber and filler volume, and the good resistance to crack propagation was attributed to the excellent bonding between the matrix and reinforcement. The tested sample E showed 3.3 KJ/mm^2.
- The coefficient of friction (COF) was determined using a pin-on-disk test setup. The results showed that the COF varied across the different specimens, Specimen SE had the highest average COF at 0.62
- The wear rate was measured as the difference in sample weight before and after the test, divided by the test duration. The results showed that the specific wear rate ranged from $1.5x10^{-8}$ to $1.4x10^{-6}$ mm^3/Nm.
- The COF and wear rate results demonstrate the trade-off between these two properties. Specimens with higher COF generally had lower wear rates, and vice versa. The formulation optimization is crucial to achieve the desired balance between friction and wear performance.
- The water absorption of the samples for commercial brake pads had the lowest water absorption and oil absorption of 0.1
- The water absorption results also show a higher amount of absorption relative to oil absorption this may be due to natural fibers having a higher affinity for water.
- The morphology study leads to the finding that, as the amount of flax fiber and eggshell content increased, the density of the generated material or composite began to decrease. Due to the composite's porous behaviors.
- Sample SE has enough mixing sequence and good texture or surface, the compositions are evenly distributed this may be due to better optimization of filler and fiber.
- The FEM analysis result shows that a total deformation both on static and transient structural analysis concludes that the pad material is worn out than disk material in terms of morphological characteristics.
- A maximum and minimum principal stress, equivalent elastic stress, and. Also, strain energy on pad and disk materials occurs respectively.
- Maximum and minimum thermal stress values of total and directional heat flux both on steady-state and transient thermal analysis respectively show that a higher generation of total and directional heat flux occurs on disk materials through time.

Chapter Five

5. Conclusions, Recommendations and Future works

5.1 Conclusion

Brake pads are a vital part of a car's safety system because they allow the friction and force needed for stopping to be generated. The most often utilized materials for brake pads include asbestos, ceramics, and synthetic composites, which release harmful particles into the environment. Natural flax fiber is taken into consideration for this study to promote environmentally friendly materials. The influence of MWCNTs and Al2O3 on the mechanical properties of flax with eggshell used as a filler in the composite is investigated using experimental research methods. Brake pad development included filler material preparation, compression molding, heat treatment, mechanical and tribological testing, and Taguchi Analysis (TA) optimization. Compression molding technique is used to fabricate composites, Experimental evaluation of the wear and impact load is conducted, finite element modeling is conducted to evaluate the mechanical, tribological, and thermal performance of the hybrid nanocomposite, and the results are contrasted with those of other previously researched natural fiber and shell composite materials obtained from the literature and commercially available brake pad materials. According to the findings, the flax fiber and eggshell polyester resin composite with MWCNTs and alumina implanted exhibits superior mechanical qualities than the other natural brake pad composite material. Finally, the result shows that sample (SE) with the composition of flax fiber 6%, Al_2O_3 8%, MWCNTs 3%, Eggshell 21%, and polyester Resin 62% performs well among the remaining samples in terms of friction, impact resistance, and low absorption capabilities. The results demonstrate the potential of this sustainable material to meet the demanding requirements of modern brake systems.

The well-dispersed Flax fiber, eggshell, and alumina particles on the polyester resin of sample SE created a larger contact surface. Consequently, the composite's surface hardness rose, reducing the specific wear rate of the brake linings and raising the coefficient of friction. The ES particles' existence, especially in sample SE, which produced the hardest sample among the others, was the cause of the composite's increased hardness. Three samples were created for the comparison of (flax fiber, eggshell, MWCNTs, and Al_2O_3) reinforced with polyester resin or epoxy composite in detail with variable fractions using the compression molding technique.

5.2 Recommendation

Further, tests such as fatigue, corrosion resistance, and thermal conductivity, are necessary to fully characterize the Natural fibers hybrid nanocomposite materials for automotive brake pads. Despite this, we attempt to examine steady-state, transient, and static structural, as well as thermal stress analysis using FEA methodologies. There are also unanticipated increases in demand for high-performing materials for brake pads. Because of this, composite materials are desirable for use in the fabrication of brake pads due to their high strength, high specific stiffness, low wear rate, and higher coefficient of friction. They are also reasonably priced and ecologically safe.

5.3 Future Work

Flax fiber and Eggshells used as friction material (reinforcements and fillers) outperform other organic materials in terms of performance. Given these circumstances and the fact that everyone has a responsibility to maintain the environment, egg shells, and flax fiber may be utilized as environmentally beneficial substitute materials in the future. In contrast to alternative possible natural materials. Finally, fade recovery analysis, vibration analysis, and thermal conductivity of material need to be addressed for further investigation, and also changing the matrix material could give better results.

Reference

[1] A.P.Irawan, "Overview of the Important Factors Influencing the Performance of Eco-Friendly Brake Pads," *Polymers 2022,14,1180,* 2022.

[2] A. Chinedum Ogonna Mgbemena, "Production of low wear friction lining material from agro-industrial wastes," *Journal of Engineering and Applied Science,* vol. 69, no. 74, pp. 1-17, 2022.

[3] S. Kumaran, "New developments in carbon-based nanomaterials for automotive brake pad applications and future challenges," *journal of nanomaterials,* pp. 1-2, 2021.

[4] G.C.Giovanna, "Ecological Transition in the Field of Brake Pad Manufacturing:An Overview of the Potential Green Constituents," *sustainability,* vol. 14, no. 05, p. 08, 2022.

[5] Z.U. Elakhame, "development and production of brake pads from Palm Kernel Shell composites," *international journal of scientific and engineering research,* vol. 5, no. 10, p. 735, october 2014.

[6] E. I. Oluwafemi, "Development And Study of Tribological Performance of Biobased Hybrid Nanocomposites for Brake Pad Application," *International Journal of Mechanical and Production,* vol. 11, no. 2, p. 89–106, April 2021.

[7] F. Elhilali,, "Towards the development of an optimized numerical model of the brake system pad with natural material," *Materials Today: Proceedings,* vol. 45, p. 5419–5425, 2021.

[8] S. Pujari, "Experimental investigations on wear properties of palm kernel reinforced composites for brake pad applications," *Defence Technology,* vol. 15, no. 3, p. 295–299, 2019.

[9] S.S Lawal, "A Review of the compostions,processing,mateerials and properties of brake bad production," in *International Conference on Engineering for sustainable World,* 2019.

[10] S.Sunardi, "Optimization of eggshell particles to produce eco-friendly green fillers with bamboo reinforcement in organic friction materials," *Reviews on Advanced Materials Science,* vol. 62, pp. 01-11, 2023.

[11] C.Cristescu, "Tribological Behavior of Friction Materials of a Disk-Brake Pad Braking System Affected by Structural Changes—A Review," *Materials,* vol. 15, no. 14, pp. 45-47, 2022.

[12] O.Nosko, "Emission of 1.3–10 nm airborne particles from brake materials," *Aerosol Science and Technology,* vol. 51, no. 1, p. 91–96, 2017.

[13] W.Österle, "Functionality of conventional brake friction materials," *wear,* vol. 271, no. 9-10, pp. 2198-2207, 2011.

[14] Q. Che, "Switching brake materials to extremely wear-resistant self-lubrication materials via tuning interface nanostructures," *ACS Applied Materials and Interfaces,* vol. 10, no. 22, p. 19173–19181, 2018.

[15] M. Bashir, "Friction and wear behavior of disc brake pad material using banana peel powder," *International Journal of Research in Engineering and Technology*, vol. 4, no. 2, p. 650–659, 2015.

[16] N. Shandilya, "A Review on the Study of the Generation of (Nano)particles Aerosols during the Mechanical Solicitation of Materials," *Journal of Nanomaterials*, vol. 16, no. 16, 2014.

[17] P. Ostermeyer, "Experimental investigations of the topography dynamics in brake pads," *SAE International Journal of Passenger Cars - Mechanical Systems*, vol. 6, no. 3, p. 1398–1407, 2013.

[18] P. Purohit R., "Social environmental and ethical impacts of nanotechnology," in *Materials Today: Proceedings*, 2017.

[19] M. K. Venkatesh S., "Scoping review of brake friction material for automotive.," *Materials Today Procsedings*, vol. 16, p. 927–933, 2019.

[20] D. J.Sureshbabu, "Physical Properties and Behavior of Flax Fiber Reinforced Epoxy Composites with Tio2 filler Addition," *Annals of R.S.C.B.*, vol. 25, no. 4, pp. 14762 - 14780, 2021.

[21] E.I.Oluwafemi, "Effects Of Fiber, Fillers, and Binders on Automobile Brake Pad Performance," *International Journal of Mechanical Engineering and Technology (IJMET)*, vol. 10, no. 06, pp. 135-150, June 2019.

[22] A. Atmakuri, "Analysis of Mechanical and Wettability Properties of Natural Fiber-Reinforced Epoxy Hybrid Composites," *Polymers*, vol. 12, pp. 27-28, 2020.

[23] A. T. Singh, "An Overview of Processing and Properties of CU/CNT Nano Composites," in *Materials Today: Proceedings*, 2017.

[24] M. P. Hirematha, "Investigation on Effect of Egg Shell Powder on Mechanical Properties of GFRP Composites," *Materials Today: Proceedings 5*, p. 3014–3018, 2018.

[25] E.I. Oluwafemi, "Biomass-based composites for brake bads: A review," vol. 10, no. 03, pp. 920-943, March 2019.

[26] S.Ray, "Analysis and prediction of abrasion wear properties of glass/epoxy composites filled with eggshell powder. Proceedings of the Institution of Mechanical Engineers," *Part E: Journal of Process Mechanical Engineering*, 2022.

[27] B. M. I.Oladele, "Mechanical and wear behaviour of pulverised poultry eggshell/sisal fiber hybrid reinforced epoxy composites.," *Materials Research Express*, vol. 7, 2020.

[28] D.V. Lucio, "Effect of eggshell particle size in thermal and thermomechanical properties of PP/eggshell Composites.," *International Journal of Engineering Sciences and Research Technology*, vol. 7, no. 4, p. 82–88, 2018.

[29] S.Petrasek, "Polymeric particle composites based on filler from Hen-egg-shell," *Engineering for Rural development,* vol. 24, 26 May 2017.

[30] A. Edokpia, "Evaluation of the properties of ecofriendly brake pad using egg shell particles," *Gum Arabic , Elsevier,* 2014.

[31] R. H. Mohammed, "Expiermental Investigation of Some Properties of Epoxy Reinforced By Egg Shell Particles," *International Journal of Mechanical Engineering and Technology (IJMET),* vol. 10, no. 1, p. 152–163, January 2019.

[32] S. A.Samuel, "Egg Shell As A Fine Aggregate In Concrete For Sustainable Construction: Engineering Environmental Science," *Materials Science International Journal of Scientific & Technology Research,* 2015.

[33] G. S.Manoharan, "Synergistic effect of red mud-iron sulfide particles on fade-recovery characteristics of non-asbestos organic brake friction composites.," *Material Research Express,* vol. 6, pp. 105-311, 2019.

[34] H.Mohammed, "Effects of Waste Eggshells addition on Microstructures, Mechanical and Tribological Properties of Green Metal Matrix Composite," *Scintific Engineering Composite Material,* vol. 26, p. 423–434, 2019.

[35] S. Kumar, "Synthesis and characterization of ball-milled eggshell and Al2O3 reinforcd hybrid green composite material," *Journal of Metals, Materials and Minerals,* vol. 30, no. 2, pp. 67-75, 2020.

[36] P.Ghosh, "Performance assessment of hybrid fibrous fillers on the tribological and thermo-mechanical behaviors of elastomer modified phenolic resin friction composite.," *SN Applied Science,* vol. 2, p. 788, 2020.

[37] K. S.Sathish, "Experimental Investigation of Mechanical and FTIR-analysis of Flax Fiber/Epoxy Composites incorporating SiC, Al2o3 and Graphite," *Romanian Journal of Materials,* vol. 48, no. 4, pp. 476 - 482, 2018.

[38] P.Singh., "Mechanical and Physical Properties of Flax Fiber and its Composites," *Journal of Material Sciences and Engineering,* vol. 11, no. 3, pp. 2-9, 2022.

[39] S.Aiinder, "Flax Fiber Reinforced Polymer Composites: A Review," *International Journal of Research and Analytical Reviews (IJRAR),* vol. 6, no. 1, pp. 828-829, 2019.

[40] Z.Jinchun, "Recent Development of Flax Fibres and Their Reinforced Composites Based on Different Polymeric Matrices," *Materials,* vol. 6, pp. 5171-5198, 2013.

[41] L.Pickering, "A Review of Recent Developments in Natural Fibre Composites and their Mechanica Performance," *Composite Part A: Applied Science Manufacturing,* vol. 83, p. 112, 2016.

[42] J. Inder, “Influence of fiber volume fraction and curing temperature on mechanical properties of jute / PLA green composites,” *Polymeric Composite,* pp. 1-12, 2019.

[43] D. Sood, “"Effect of Fiber Treatment on Flexural Properties of Natural Fiber Reinforced Composites: A Review.",” *Journal of Petrol,* vol. 27, pp. 775-783, 2018.

[44] N.Dhakal, “Effect of water absorption on the mechanical properties of hemp fiber reinforced unsaturated polyester composites,” *Composites Science and Technology,* 2006.

[45] K.Oksman, “High quality flax fiber composites manufactured by the resin transfer moulding process.,” *Journal of Reinforced Plastic Composites,* vol. 20, p. 621–627, 2001.

[46] S.Liang, “comparative study of fatigue behaviour of flax/epoxy and glass/epoxy composites,” *Composite Scince and Technology,* vol. 72, p. 535–543, 2012.

[47] Y.Yuan, “Flax Fibers as Reinforcement in Poly Lactic Acid,” *Intellectual,* vol. 134, p. 547–553, 2011.

[48] S.Sathish., “Experimental Investigation of Mechanical and FTIR-analysis of Flax Fiber/Epoxy Composites incorporating SiC, Al2o3 and Graphite,” *Romanian Journal of Materials,* vol. 48, no. 4, pp. 476 - 482, 2018.

[49] S. Alix, “Study of Water Behaviour of Chemically Treated Flax Fibres Based Composites: A Way to Approach the Hydric Interface.",” *Compitetional Science Techology,* vol. 71, p. 899, 2011.

[50] L. Xue, “chemical treatments of natural fiber for use in natural fiber- reinforced composites:,” *A review Journal Polymeric enivronment,* pp. 25-33, 2007.

[51] S. Saidane, “Assessment of 3D Moisture Diffusion Parameters on Flax/Epoxy Composites,” *Comp Part A: Applied Science Manufacturing,* vol. 80, pp. 53-60, 2016.

[52] U. Huner, “Effect of Water Absorption on the mechanical properties of flax fiber reinforced epoxy composites,” *Advances in Science and Technology Research Journal,* vol. 9, no. 26, p. 1–6, June 2015.

[53] M F.Pucci., “Wetting and swelling property modifications of elementary flax fibres and their effects on the Liquid Composite Moulding process,” *Composite Part A,* p. 2–33, 2017.

[54] E.I. Oluwafemi, “Effects of Fiber, Fillers and Binders on Automobile Braking Pad Performance : Areview,” *International Journal Mechaniacl Engineering Technolology (IJMET),* vol. 10, pp. 625-641, 2019.

[55] M. Ghorbani, “Adsorptive removal of lead (II) ion from water and wastewater media using carbon-based nanomaterials as unique sorbents: a review,” *Journal of Environmental Management,* vol. 254, 2020.

[56] A.Patnaik, “Effect of carbon nanotubes on tribo-performance of brake friction materials,” in *AIP Conference Proceedings*, 2011.

[57] J.Hwang, "Tribological performance of brake friction materials containing carbon nanotubes," *Wear,* vol. 268, pp. 519-525, 2010.

[58] K.J.Lee, "Tribological and mechanical behavior of carbon nanotube containing brake lining materials prepared through sol–gel catalyst dispersion and CVD process.," *Journal of Alloys Composite,* 2009.

[59] J.Gbadeyan, "Tribological behaviors of polymer-based hybrid nanocomposite brake pad," *Journal of Tribology,* vol. 140, no. 3, 2018.

[60] M. Al-bahrania, "The Mechanical Properties of Functionalised MWCNT Infused Epoxy Resin: A Theoretical and Experimental Study," *International Journal of Mechanical & Mechatronics Engineering IJMME-IJENS,* vol. 18, no. 1, February 2018.

[61] E.Kabir, "Environmental impacts of nanomaterials," *Journal of Environmental Management,* vol. 225, p. 261–271, 2018.

[62] A.G.Cattaneo, "Nanotechnology and human health: risks and benefits," *Journal of Applied Toxicology,* vol. 30, no. 8, p. 730–744, 2010.

[63] M.Zhang, "Improved bioleaching of copper and zinc from brake pad waste by low-temperature thermal pretreatment and its mechanisms," *Waste Management,* vol. 87, p. 629–635, 2019.

[64] A.Iijima, "Particle size and composition distribution analysis of automotive brake abrasion dusts for the evaluation of antimony sources of airborne particulate matter," *Atmospheric Environment,* vol. 41, p. 4908–4919, 2007.

[65] J.Mochane, "Recent progress on natural fiber hybrid composites for advanced applications: A review," *Express Polymer Letters,* vol. 13, no. 2, p. 159–198, 2019.

[66] N.Safri, "Impact behaviour of hybrid composites for structural applications: A review.," *Composites Part B: Engineering,* vol. 133, p. 112–121, 2017.

[67] T.Singh, "Optimum design based on fabricated natural fiber reinforced automotive brake friction composites using hybrid CRITIC-MEW approach," *journal of materials research and technology,* vol. 14, pp. 81-92, 1 April 2021.

[68] S. Rajan, "Tribological performance evaluation of epoxy modified phenolic fc reinforced with chemically modified prosopis juliflora bark fibre," *Material Research Express,* vol. 6, 2019.

[69] H.Essabir, "Structural, mechanical and thermal proper ties of bio-based hybrid composites from waste coir residues: Fibers and shell particles," *Mechanics of Materials,* vol. 93, p. 134–144, 2016.

[70] V.S.Srinivasan, "Evaluation of mechanical and thermal properties of banana–flax based natural fibre composite," *Material Design,* vol. 60, p. 620–627, August 2014.

[71] C. D.Egeonu, “production of eco-friendly brake pad using raw materials sourced locally in nsukka,” *journal of energy technologies and policy,* vol. 5, no. 11, pp. 2224-3232, 2015.

[72] M.Assarar, “Influence of water ageing on mechanical properties and damage events of two reinforced composite materials: Flax-fibers and glass-fibers,” *Material Design,* vol. 32, p. 788–795, 2011.

[73] R.Pundir, “Application of Taguchi method for optimizing the process parameters for the removal of copper and nickel by growing Aspergillus sp,” *Water Resources Industry,,* vol. 20, p. 83–92., 2018.

[74] Yilma, “Taguchi method optimization of water absorption behavior by wheat straw-basalt hybrid brake pad composite.,” *Journal of Composites Sciences,* vol. 7, no. 2, 2023.

[75] S. Binoj, “Comprehensive characterization of industrially discarded fruit fiber, Tamarindus Indica L. as a potential eco-friendly bio-reinforcement for polymer composite,” *Journal of Cleaner Production,* vol. 142, no. 3, pp. 1321-1331, 2017.

[76] P.M.Kumar, “development and study of tribological properties of bio composite for brake pad,” *IJMPERD,* vol. 7, no. 6, p. 266, december 2017.

[77] A. Belhocine, “Finite Element Analysis of Automotive Disc Brake and Pad in Frictional Model Contact,” *International Journal of Advanced Design and Manufacturing Technology,* vol. 7, no. 4, December 2014.

[78] O.OgbeIde, “Modelling Of Automobile Brake Pad Wear,” *IRE Journals,* vol. 3, no. 4, 2019.

[79] B. Katsina, “Development of automobile brake lining using pulverized cow hooves,” *Leonardo journal of scince,* vol. 28, pp. 95-108, 2016.

[80] S. Yawas, “Morphology and properties of perwinkle shell asbestos free brake pad,” *Journal of King Saudi University-Engineering Siences,* vol. 28, pp. 103-109, 2016.

[81] K. Mausam, ““Calculating stress,temperature in brake pad using ANSYS composite materials”,” in *Materials Today: Proceedings,* 2021.

Appendix

The Archard formula using Equation 1 is used to determine the pad's wearing strain. [81]

S = C ∗ D ∗ L, ---------- 1

Equation 2 below was used to compare the participants' total $\sum CO_{add}$ emissions.

$\sum CO_{add}=\sum_{i=1}^{n} m(i) * R_t(i)$ ----------2

The composite density at various reinforcement volume percentage fractions was done using Equation 4 below

$\rho c = \rho r Vr + \rho m Vm$…….(3)

The weight % fraction of the matrix (Wm) and reinforcing particles (Wr) is defined by equation 5 below.

$Wr=\rho r \rho c * Vr$; $Wm=\rho m \rho c * Vm$……..(4)

equation 6 defines the volume percentage of the matrix and reinforcing particle

% Vrf =VrVC; % Vmf =VmVC ……..(5)

Equation 7 specifies the volume of the composite for a system consisting of reinforcement particles and matrix. $VC = Vr + Vm = 1$ ……(6)

Energy Absorption using the following Equation 4 below.

IS= $\frac{AE}{WT}$…….(7)

The wear rate is calculated by Equation 5 below

SWR=$\frac{\Delta V}{Ld}$……..(8)

The coefficient of friction is calculated by Equation 6 below

μ=$\frac{M}{Y.N}$----------(9)

water absorption is calculated by Equation 11 below

P_{WA} =$\frac{W_1-W_o}{W_o}$*100----------(10)

oil absorption is calculated by equation 12 below

$P_{OA=}$ $\frac{WO_1-WO_o}{WO_o}$*100----------(11)

Impact Test Pieces Testing Report			
Standard	**ASTM D-256**	**Batch Number**	**1**
Type	**V**	**Deep [mm]**	**2**
Sn	**Area**		**Energy**
	[mm^2]		**[KJ]**
ELA-001-IMP	62.5		4.8
ELA-002-IMP	62.5		3.7
ELA-003-IMP	62.5		4.6
ELA-004-IMP	62.5		3.7
ELA-005-IMP	62.5		3.3
ELA-006-IMP	62.5		4.8
ELA-007-IMP	62.5		4.6
ELA-008-IMP	62.5		4.6
ELA-009-IMP	62.5		3.7
Max Value			4.8
Min Value			3.3
Mean Value			4.43
Standard Deviation			0.55

Graphical results for Wear rate and Coefficient of Friction.The graphs of friction and wear test results of brake pad samples are shown in the Figures below respectively.

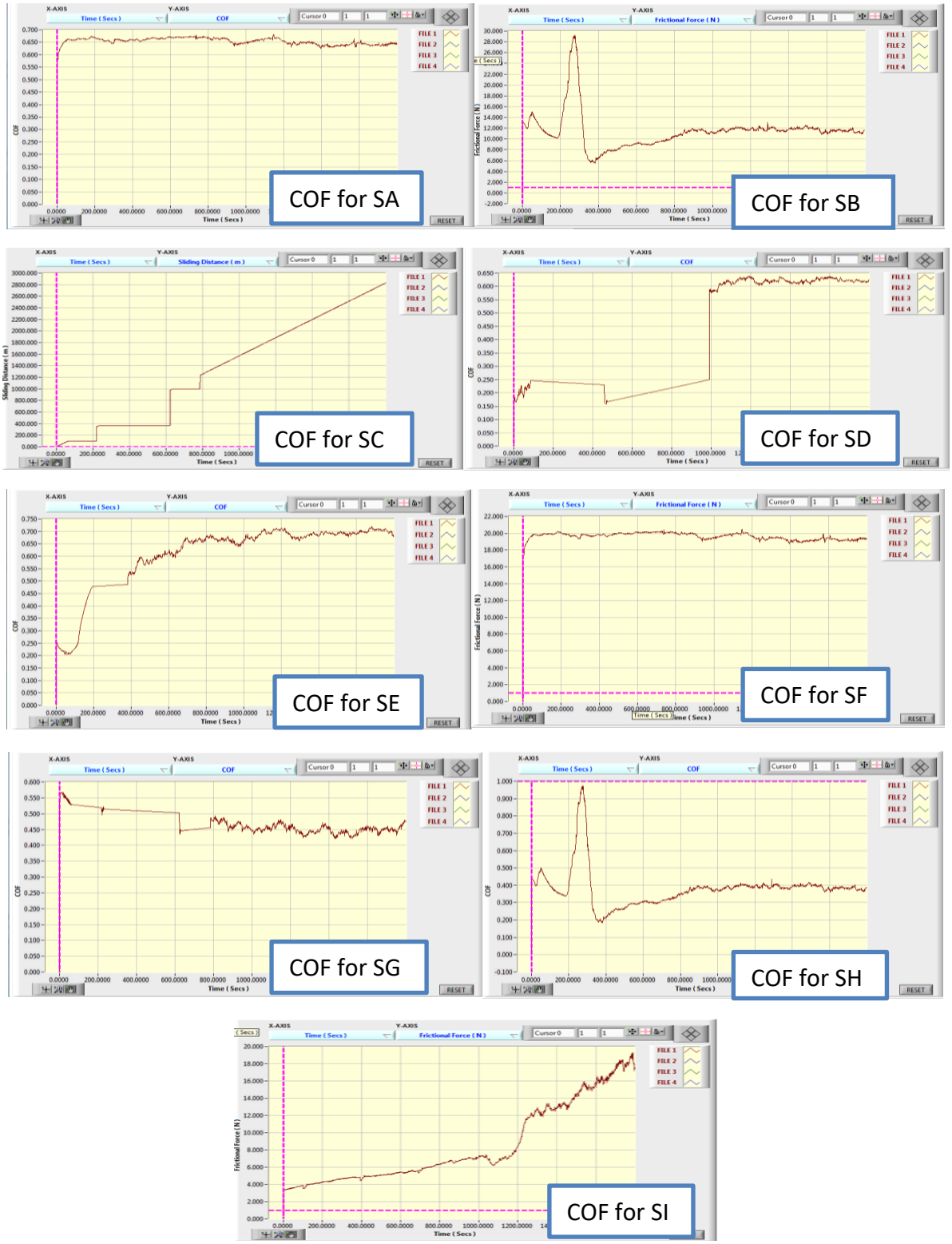

Experimental result Graphs of COF for all nine Specimens

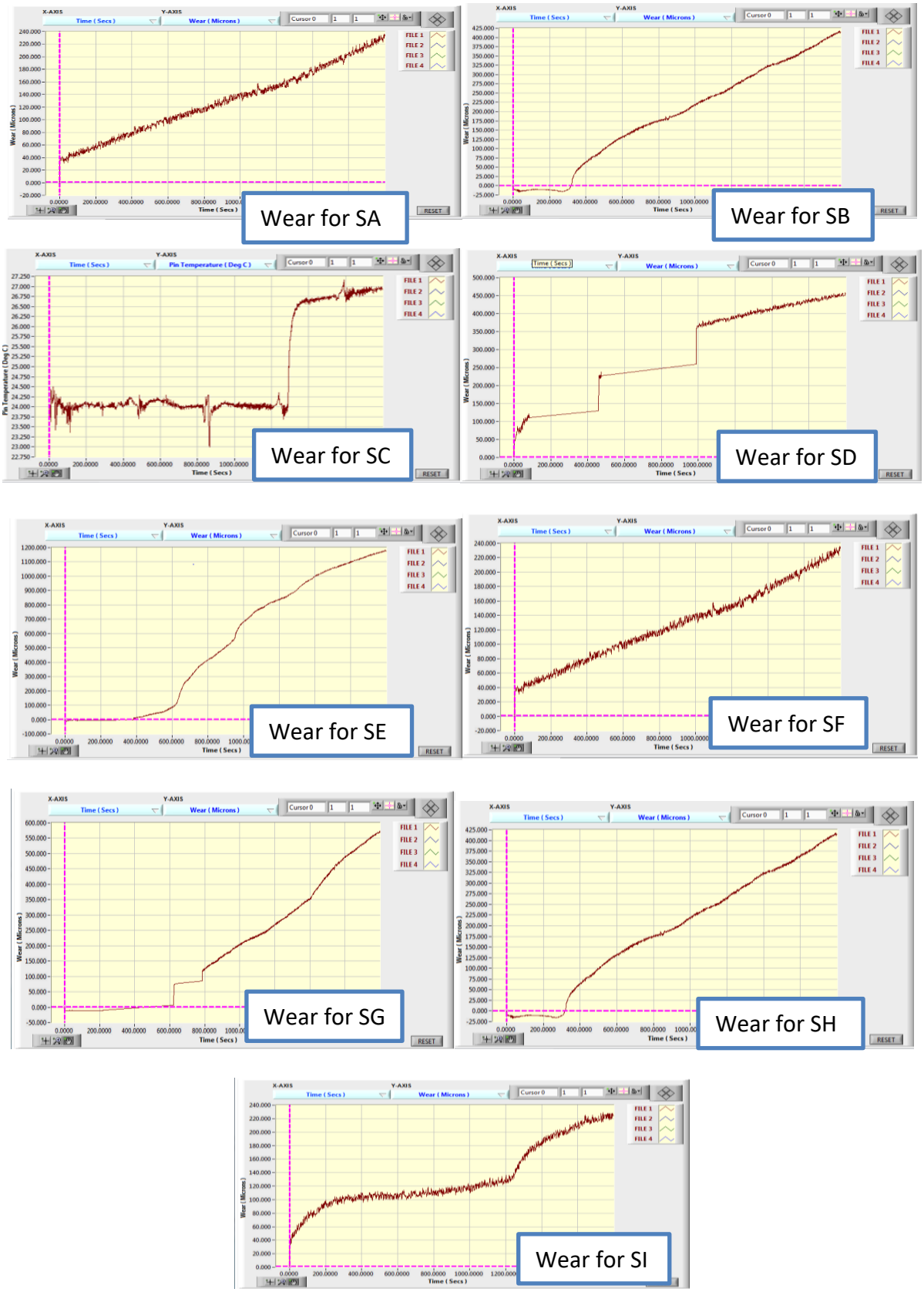

Experimental result Graphs of Wear Rate for all nine Specimens

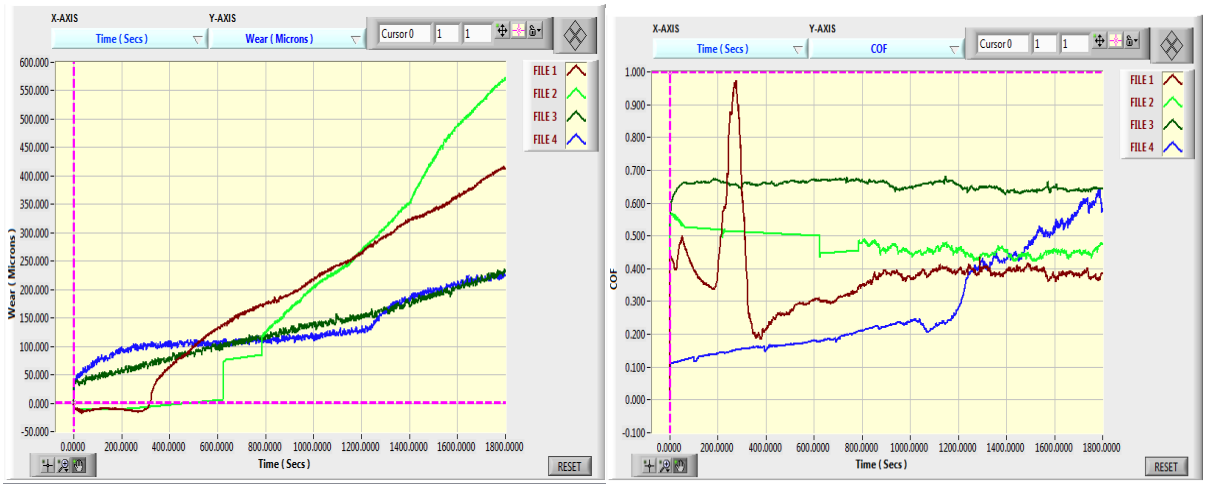

Comparisons Of Wear Rate Vs Coefficient Of Friction

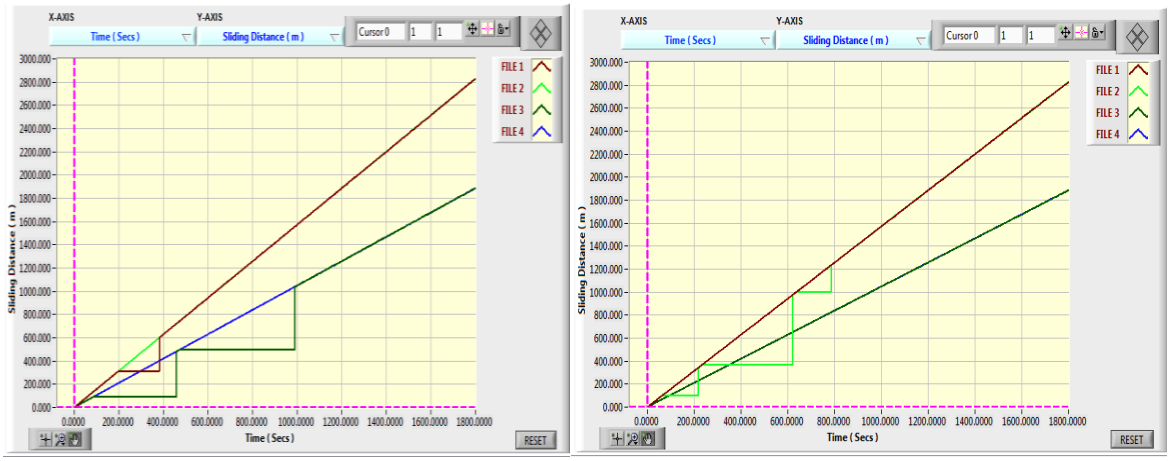

Comparisons Of Sliding Distance Vs Time

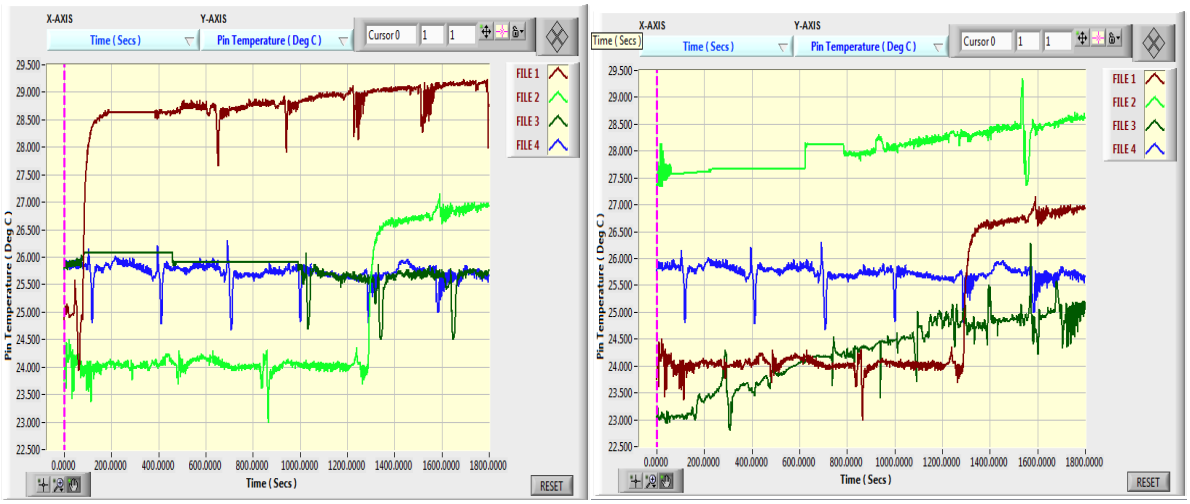

Comparisons Of Pin Temperature Vs Time